/
Article / Book Information

( )	
Title(English)	RGB Multi-Channel Representation for Quantum Images and Its Application to Color Image Watermarking
( )	
Author(English)	Bo Sun
( )	: ( ), : , : 9321 , :2013 9 25 , : , : , , , ,
Citation(English)	Degree:Doctor (Engineering), Conferring organization: Tokyo Institute of Technology, Report number: 9321 , Conferred date:2013/9/25, Degree Type:Course doctor, Examiner:,,,,
( )	
Type(English)	Doctoral Thesis

RGB Multi-Channel Representation for Quantum Images and Its Application to Color Image Watermarking

孫 博

(10D53156)

Supervisor: Prof. Kaoru Hirota

Doctoral Thesis

Tokyo Institute of Technology
東京工業大学
Interdisciplinary Graduate School of Science and Engineering
大学院総合理工学研究科
Department of Computational Intelligence and Systems science
知能システム科学専攻

June 2013

Abstract

Quantum image processing is a new and exciting subdiscipline of quantum computation that aims to extend classical image processing applications on a quantum computer. The research starts with a proposal of a representation of images on a quantum computer, named Multi-Channel Representation for Quantum Images (MCQI). This representation encodes the positions and their corresponding colors in the images as a normalized quantum state. For an n by n sized image, $2n$ qubits and 3 qubits are used to carry the position and color respectively. The preparation procedure of a quantum image is discussed by the multi-channel polynomial preparation, which turns the initial quantum states to the MCQI quantum states. The image retrieval procedure by quantum measurement is proposed which converts the quantum states to classical images. Furthermore, based on MCQI, some categories of possible processing transformations are suggested.

By considering the structure of MCQI representation, the Channel of Interest (CoI), the Channel Swapping (CS), the Color Space Transformation (CST), and Alpha Blending (αB) quantum image processing operators are discussed using unitary transformations with low complexity. All the 4 operators are used to process the information about color in the images. Their complexity are analyzed in terms of the number of basic quantum gates which are needed to build the transformations, and they can be built by 9, 3, 287, 28 basic quantum gates, respectively. Some strategies for designing new transformations from known ones are proposed as well. These strategies can be used to design further algorithms for image processing.

Based on the MCQI representation and the four image processing operators, a quantum measurement based double-key double-domain watermarking strategy for multi-channel quantum images (MC-WaQI) is developed. In these application, a revised of the original MCQI representation and some restricted versions of the transformations are considered.

The research provides the foundation to design other quantum image processing algorithms and can be extend to the following areas:

- MCQI representation can be used to build quantum image database,

- new frequency operations on quantum images based on quantum Fourier quantum discrete cosine, and quantum wavelet transformations,

- building the special effect on color quantum movie,

- image data transmission by quantum communication.

The works in this thesis and its future perspectives will provide the foundation for exploring new ways of processing structured data and their applications using quantum computing framework.

Acknowledgements

Firstly, I would like to express my sincere gratitude to my supervisor, Professor Kaoru Hirota, for accepting me in his laboratory and for guiding me during all of these three years that I studied at Tokyo Institute of Technology. And I really learned a lot from his encouragement, guidance, and inspiration.

I would also like to thank Dr. Fangyan Dong, assistant professor at Hirota Laboratory; she has been a valuable source of advices and support, always pushing me to give my best.

Next, I am forever indebted to the Chinese Government and people for not only shouldering the huge burden of sponsoring my programme over the past three years but for also being friendly and accommodating hosts for me and my family.

Special thanks to Phuc Quang Le, Abdullahi Mohammad Iliyasu, Fei Yan, Adrian Jesus Garcia Sanchez, members Quantum Computation Group at Hirota Laboratory, Tokyo Institute of Technology. I greatly appreciate your collaboration on my research and our numerous enjoyable discussions in such a wide range of topics during the three years.

Many gratefulness go to my colleagues and friends who have helped me in so many ways, Fangming Zhao, Gang Niu, Chen Chen, Qingzhu Wang, Zhengxun Song, Liang Yang, Jingyang Zhao, Yongkang Tang, Martin Leonard Tangel, Chastine Fatichah, and all other Hirota Laboratory members. Your kindness, patience, and valuable advices are the things which I never forget.

Finally, I dedicate the greatest grateful to my family. Their unconditional love and permanent support always motivate and drive me to become a better person. Thank you Mom for your care and generous heart. Thank you Dad for your sacrifice, advices, and especially the freedom you have always given me. Thank you my wife for loving, encouraging, and always being there for me.

Contents

List of Figures

List of Tables

Chapter 1

Introduction

1.1 Motivation

In 1982, Feynman proposed a novel computation model, named quantum computers. [11] Based on principles of quantum mechanics, the quantum computation is more powerful than classical ones. Quantum computation offers a new perspective in terms of high performance computing with algorithms [38][26]. Hence, in order to solve inefficient tasks on classical computers that maybe overcome by exploiting the power of the quantum computation, many researchers are involved in this exciting field. Two famous quantum algorithm are Shor's polynomial time algorithm for the integer factoring problem [44] and Grover's database search algorithm [15] which has been proved much powerful than the classical ones. Image processing and analysis on classical computers have been studied extensively. On quantum computers [9] [42] [6] [35], however, the research on images has faced fundamental difficulties because the field is still in its infancy. To start with, what is the data structure of quantum image or how to represent images on quantum computers? Secondly, what should we do to prepare and process the quantum images on quantum computers? Thirdly, should we be capable of performing some basic image processing tasks and realizing some high level applications using quantum computation algorithms?

Quantum information processing [30] [24] [7] is focused on information whose physical representation is confined within the realm of quantum mechanics. Therein, the information carrying medium (the qubit) and manipulations of such states are dictated by

the quantum mechanical properties inherent to the medium, hence, giving birth to the quantum computing paradigm. Some of these properties such as entanglement, superposition and so on have no classical (conventional or non-quantum) analogues, and are harnessed for various purposes such as unconditionally secure transmission of information, and speeding up certain classical computations [46]. In fact, physical implementations of the qubit and gates to manipulate it are available from different approaches.

In quantum circuit models of computation, designing such circuits is necessary to realize and analyze any quantum algorithm. It is well known that any unitary operation or quantum algorithm can be decomposed into a circuit consisting a succession of basic unitary gates that act on one or two qubits only. Many elementary gates including single qubit gates, controlled-NOT or CNOT and Toffoli gates for quantum computation was proposed in the previous research. Physical implementations of the qubit and these gates are available from many approaches.

In order to process image using quantum computing, the first step in quantum image processing field involves proposals on representations to capture and store the image on quantum computers. Many proposals on quantum image representations are also proposed. In [5], the images are two-dimensional arrays of qubits, called the qubit lattice. In Real Ket [51], the images are quantum states having grey levels as coefficients of the states. The quantum lattice is proposed in [36] which color pixels are stored in quantum system qubit by qubit. A quantum image representation called grid qubit [50] is discussed which the geometric shapes are encoded in quantum states. The image is a normalized quantum state that captures information about the color and position of every point, called FRQI (Flexible Representation of Quantum Images) [27]. A multi-channel representation for quantum images (MCQI) which encodes the R, G, B, and α channels information concurrently by using 3 entangled color qubits is proposed in [48]. Various strategies exploiting the above representation are proposed to process transformations that target the geometric information, GTQI (Geometric Transformation on Quantum Images) [28], and the color information, CTQI (Color Transformation on Quantum Images) [29]. Quantum based related to image processing such as quantum Fourier transform [37],

quantum discrete cosine transform [23] [49], quantum Wavelet transform [12] have also been proposed. In addition, there are some classical image processing operations that can not be applied on quantum images, for example convolution and correlation [31], because all operations in quantum computation must be invertible. The complexity of the preparation of quantum images and the application of quantum transforms to process quantum images, however, have not been studied.

The previous proposed representations treat the image's color information as a single channel (single component). Multi-channel (multi-component) color images, however, are often used in various color spaces, including the standard RGB color model [1] [47] which contains R, G, and B channels (components). Hence, a new representation for quantum images which carries multi-channel information of images maybe requested for further color image processing tasks on quantum computer.

In order to establish the connection between image processing and quantum computation, the thesis starts with a proposal of image representation which captures two fundamental information about images, color and position. In this representation, color information is considered as a multi-channel information, and each channel is separated. After representing a quantum image as a normalized state, various unitary transformations for processing the image's content are proposed. Combining these transformations in a specific way leads to applications of color quantum image quantum image watermarking.

1.2 Outline of the Thesis

The outline of the thesis is shown in Figure 1.1.

In Chapter 2, a multi-channel representation for quantum images (MCQI) which captures information about colors and their corresponding positions in an image into a normalized quantum state is proposed. In this representation, the RGB color information is encoded by 3 entangled qubits (c_1, c_2, and c_3 qubits) and the pixels' positions of a $2^n \times 2^n$ pixels image is represented by $2n$ qubits is proposed.

The preparation procedure for MCQI is indicated by using Hadamard, CNOT and controlled rotation operations. As proven by the proposed Multi-Channel Polynomial
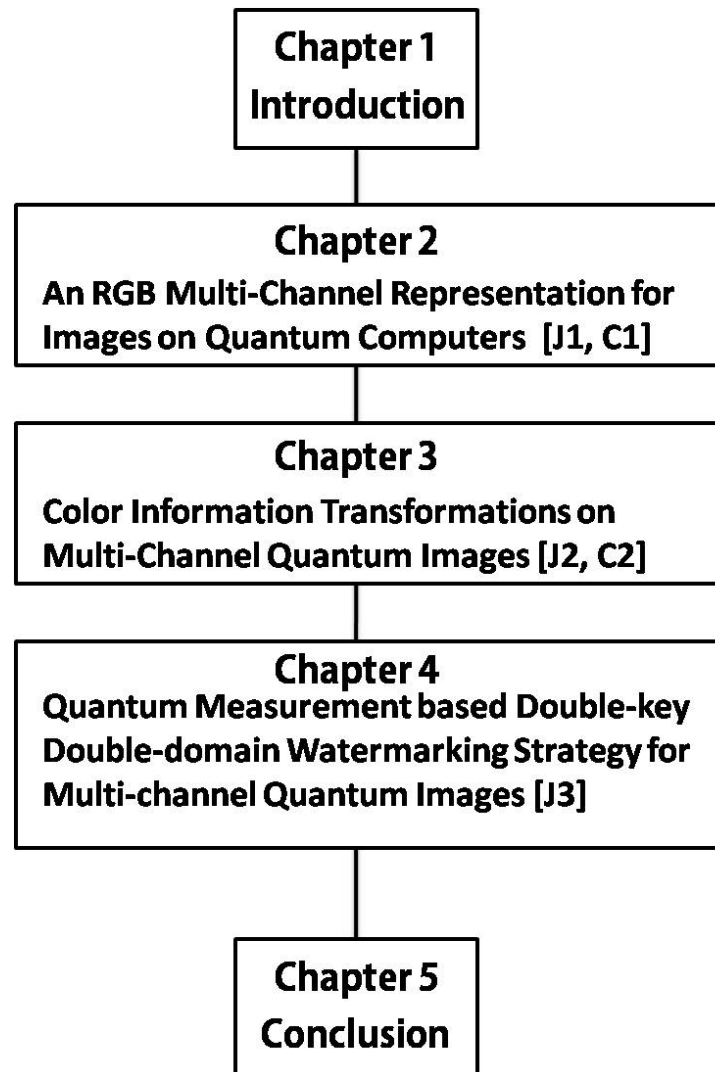
Figure 1.1: *Outline of thesis showing related publications that were realized from each chapter.*

Preparation Theorem, the total number of simple operations used in the process is polynomial for the number of qubits that are used to encode all positions in an image. The measurement based method is used to retrieve the image stored in the quantum states.

In chapter 3, 4 color transformation operators are proposed using basic quantum gates; NOT, CNOT, Toffoli, Rotation, and Controlled Rotation gates based on the multi-channel representation for quantum images (MCQI), where the $RGB\alpha$ color information is encoded by 3 entangled qubits (c_1, c_2, and c_3 qubits) and the pixels' positions of a $2^n \times 2^n$ pixels image is represented by $2n$ qubits.

After having some color information operations, a quantum measurement based double-key, double-domain multi-channel watermarking strategy for quantum images is proposed

in chapter 4, which can be used to find the real owner.

Chapter 2

RGB multi-channel representation for images on quantum computers

2.1 Introduction

The first step in quantum image processing field involves proposals on representations to capture and store the image on quantum computers. In [51], the images are two-dimensional arrays of qubits, called the qubit lattice. The quantum lattice is proposed in [36], which color pixels are stored in quantum system qubit by qubit. A quantum image representation called grid qubit [50] is discussed which the geometric shapes are encoded in quantum states. The image is a normalized quantum state that captures information about the color and position of every point, called FRQI (Flexible Representation of Quantum Images) [27], and it has started gaining acceptability as evinced by proposals targeting a wide range of applications that rely on it. Various strategies exploiting the FRQI representation are proposed to process transformations that target the geometric information, GTQI (Geometric Transformation on Quantum Images) [28], and the color information, CTQI (Color Transformation on Quantum Images) [29] using this representation. The possibility of using the restricted versions of these representations to watermark FRQI quantum images is studied in [20].

The FRQI representation treats the image's color information as a single channel (single component). Multi-channel (multi-component) color images, however, are often

used in various color spaces, including the standard RGB color model [2] [45] [22] which contains R, G, and B channels (components). Hence, a new representation for quantum images which carries multi-channel information of images maybe requested for further color image processing tasks on quantum computer.

In this chapter, an RGB multi-channel representation for images on quantum computers (MCQI) where the RGB color information is encoded by 3 entangled qubits (c_1, c_2, and c_3 qubits) and the pixels' positions of a $2^n \times 2^n$ pixels image is represented by $2n$ qubits is proposed. Then the following computational and image processing aspects on MCQI are developed:

- the complexity (the number of simple operations) of the preparation procedure for MCQI,

- MCQI based image processing operations,

- the measurement based image retrieval from quantum to classical.

The preparation procedure for MCQI is indicated by using Hadamard, CNOT and controlled rotation operations. And the total number of simple operations used in the process is polynomial for the number of qubits that are used to encode all positions in an image. Considering the structure of MCQI, color information operations can be separated into two categories, C_I and rC_I. The C_I category focuses on shifting the color information of the whole image (channel of interest and channel swapping are two example operators in this category), and the rC_I category is the restrict version of C_I, which changes the color information at some specific positions, respectively. Each category has its own type of unitary transform which can be designed in various ways to realize different image processing tasks based on MCQI. The measurement based method is used to retrieve the image stored in the quantum states.

Firstly, the property of quantum parallelism is used to encode the color information and their corresponding positions, e.g., only 15 qubits are used to encode a 64×64 pixels' RGB image in MCQI representation, whereas 4096 qubits are requested in qubit lattice [51], grid qubit [50], and quantum lattice [36] representations. Especially, on classical

computer, 12288 bits are requested to encode the same sized RGB image (64×64 pixels). Secondly, as the multi-channel information (R channel, G channel, and B channel) are stored in the first 3 qubits (entangled) (color qubits) simultaneously, the color information operators applying on the whole image (not focussing on some specific position of an image) can be designed by using unitary quantum gates within these 3 qubits irrespective of the position qubits. It means that the complexity of the MCQI-based color information operators are image size independent, namely, $O(1)$, whereas the color information must be shifted pixel by pixel in the case of operators on classical computers. Thirdly, combining with the quantum measurement based key generation procedure, MCQI may be used to design the color image watermarking algorithm.

2.2 Single channel representation for quantum images

2.2.1 Flexible representation of quantum images

We start by introducing the notations used in this thesis which has been used in a wide range of quantum computation literature. The state of a quantum system is described as a vector in a Hilbert space [14] [16] [41] which is called a ket in Dirac or quantum mechanical notation. The ket and its adjoint, bra, notations are defined as follows;

$$
\begin{aligned}
&|u\rangle = [u_0, u_1, ..., u_n]^T, u_i \in \mathcal{C}, \\
&i = 1, 2, ..., n, \\
&\langle u| = |u\rangle^\dagger = [u_0^\dagger, u_1^\dagger, ..., u_n^\dagger].
\end{aligned}
\tag{2.1}
$$

The notation for the tensor or Kronecker product, $\otimes$, is used to express the composition of quantum systems. The tensor product of two matrices A and B is defined as follows;

$$A = \begin{bmatrix} a_{11} & a_{12} & ... & a_{1m} \\ a_{21} & a_{22} & ... & a_{2m} \\ \vdots & \vdots & \ddots & \vdots \\ a_{n1} & a_{n2} & ... & a_{nm} \end{bmatrix},$$

$$B = \begin{bmatrix} b_{11} & b_{12} & ... & b_{1q} \\ b_{21} & b_{22} & ... & b_{2q} \\ \vdots & \vdots & \ddots & \vdots \\ b_{p1} & b_{p2} & ... & b_{pq} \end{bmatrix},$$

$$A \otimes B = \begin{bmatrix} a_{11}B & a_{12}B & ... & a_{1m}B \\ a_{21}B & a_{22}B & ... & a_{2m}B \\ \vdots & \vdots & \ddots & \vdots \\ a_{n1}B & a_{n2}B & ... & a_{nm}B \end{bmatrix},$$

where

$$a_{ij}B = \begin{bmatrix} a_{ij}b_{11} & a_{ij}b_{12} & ... & a_{ij}b_{1q} \\ a_{ij}b_{21} & a_{ij}b_{22} & ... & a_{ij}b_{2q} \\ \vdots & \vdots & \ddots & \vdots \\ a_{ij}b_{p1} & a_{ij}b_{p2} & ... & a_{ij}b_{pq} \end{bmatrix}$$

The short notation for tensor product $|u\rangle \otimes |v\rangle$ of two vectors or two kets, $|u\rangle$ and $|v\rangle$, is $|uv\rangle$ or $|u\rangle|v\rangle$ and we use $A^{\otimes n} = A \otimes A \otimes ... \otimes A$ to denote the tensor product of matrix A for n times.

Inspired by the pixel representation for images in conventional computers, a representation for images on quantum computers capturing information about colors and the corresponding positions, the quantum exible representation of images (FRQI) is proposed in [27]. This proposal integrates information about an image into a quantum state having its formula as

$$I(\theta) = \frac{1}{2^n} \sum_{k=0}^{2^{2n}-1} |c_k\rangle \otimes |k\rangle,$$

$$|c_k\rangle = cos\theta_k|0\rangle + sin\theta_k|1\rangle,$$

$$\theta \in [0, \pi/2], k = 0, 1, ..., 2^{2n} - 1,$$

(2.2)

where $\otimes$ is the tensor product notation, $|0\rangle$, $|1\rangle$ are 2-D computational basis quantum states, $|k\rangle$, $k = 0, 1, ..., 2^{2n} - 1$ are $2^{2n} - 1$-D computational basis quantum state and $\theta = (\theta_0, \theta_1, ..., \theta_{2^{2n}-1})$ is the vector of angles encoding colors. There are two parts in the FRQI representation of an image; $|c_k\rangle$ and $|k\rangle$ which encode information about the colors and their corresponding positions in the image, respectively.

For the 2-D images, the position information $|k\rangle$ includes two parts, the vertical and horizontal co-ordinates. In 2n-qubit systems for preparing quantum images, or 2n-qubit images, the vector $|k\rangle$.

$$|k\rangle = |y\rangle|x\rangle = |y_{n-1}y_{n-2}...y_0\rangle|x_{n-1}x_{n-2}...x_0\rangle$$

The single channel representation form is quite flexible because of the way the positions of colors are encoded into computational basis states. In this way, the presentation of the geometric appearance of colors will affect on the quantum representation of the image. For example, the line by line and block based addressing methods are some of the encoding mechanisms commonly used. The FRQI form is quite flexible because of the way the positions of colors are encoded into computational basis states. In this way, the presentation of the geometric appearance of colors will affect on the quantum representation of the image. For example, the line by line and block based addressing methods are some of the encoding mechanisms commonly used. These mechanisms are shown in Fig 2.2.

The FRQI representation treats the image's color information as a single channel (single component). Multi-channel (multi-component) color images, however, are often used in various color spaces, including the standard RGB color model which contains R, G, and B channels (components). Hence, a new representation for quantum images

θ_0	θ_1	θ_2	θ_3
0000	*0001*	*0010*	*0011*
θ_4	θ_5	θ_6	θ_7
0100	*0101*	*0110*	*0111*
θ_8	θ_9	θ_{10}	θ_{11}
1000	*1001*	*1010*	*1011/*
θ_{12}	θ_{13}	θ_{14}	θ_{15}
1100	*1101*	*1110*	*1111*

θ_0	θ_1	θ_2	θ_3
0000	*0001*	*0100*	*0101*
θ_4	θ_5	θ_6	θ_7
0010	*0011*	*0110*	*0111*
θ_8	θ_9	θ_{10}	θ_{11}
1000	*1001*	*1100*	*1101*
θ_{12}	θ_{13}	θ_{14}	θ_{15}
1010	*1011*	*1110*	*1111*

Figure 2.1: *Two position encoding methods for colors..*

which carries multi-channel information of images maybe requested for further color image processing tasks on quantum computer.

2.3 RGB multi-channel representation for images on quantum computer

2.3.1 RGB color model

RGB color model [40] as one of the most famous multi-channel color models specifies colors into three primary colors (three channels or components) red (R), green (G) and blue (B) and is an additive color model in which red, green, and blue light is added together in various ways to reproduce a broad array of colors. For example red (255,0,0) and green (0,255,0). The amount of each component gives the intensity of an image. If all components are of highest intensity, then the resulting color is white. In RGB color model, one original color image can be constructed by three grayscale value images (channels or components) as shown in Figure 2.2. As the most widely used color space for the sensing, representation, and display of images in electronic systems [40], RGB color model plays very important role in the image processing field.

To process color images on quantum computers, a new representation encoding the information of R, G, B channels should be established, and these multi-channel information
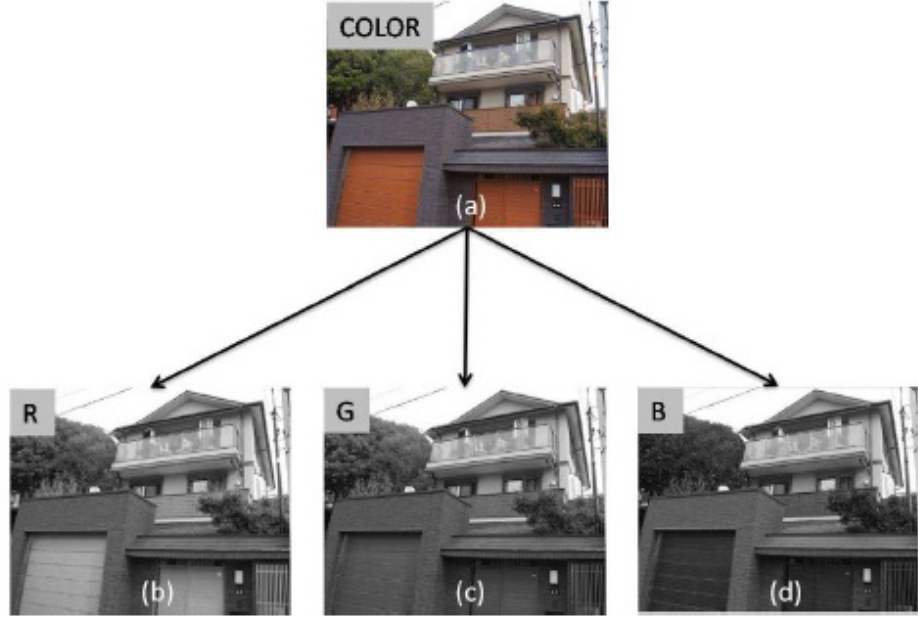
Figure 2.2: *Color image can be constructed by three greyscale value images ((a) The original color image; (b) greyscale image of R channel; (c) greyscale image of G channel; (d) greyscale image of B channel).*

are requested to be stored in quantum states simultaneously. Based on the pixel representation for images on classical computers, the multi-channel representation for quantum image (MCQI) is proposed to capture RGB channels information. This is accomplished by assigning three qubits to encode color information of images. The mathematical expression is presented as

$$|I(\theta)_{mc}\rangle = \frac{1}{2^{n+1}} \sum_{i=0}^{2^{2n}-1} |C_{RGB}^{i}\rangle \otimes |i\rangle. \tag{2.3}$$

The color information $|C_{RGB}^{i}\rangle$ encoding the R, G, B, channels information is defined as

$$
\begin{aligned}
|C_{RGB}^{i}\rangle = {} & \cos\theta_R^i|000\rangle + \cos\theta_G^i|001\rangle + \cos\theta_B^i|010\rangle + \\
& + \sin\theta_R^i|100\rangle + \sin\theta_G^i|101\rangle + \sin\theta_B^i|110\rangle + \\
& + \cos 0|011\rangle + \sin 0|111\rangle,
\end{aligned} \tag{2.4}
$$

where $|000\rangle$, $|001\rangle$, ..., $|111\rangle$ are 8-D computational basis; $\{\theta_R^i, \theta_G^i, \theta_B^i\} \in [0, \pi/2]$ are three angles encoding the colors of the R, G, B, channels of the *ith* pixel, respectively; $\otimes$ is

the tensor product notation; $|i\rangle$ for $i = 0, 1, \ldots, 2^{2n} - 1$ are 2^{2n}-D computational basis states. Specifically, there are two parts in the MCQI quantum image: $|C^i_{RGB}\rangle$ and $|i\rangle$, which encode information about colors and their corresponding positions in the image, respectively. In Eq.(2), the coefficients of $|011\rangle$ and $|111\rangle$ are $\cos 0$ and $\sin 0$. In RGB color images, there are only three channels' information requested to be encoded (6 coefficients are enough), hence, we set the two coefficients be constant ($\cos 0$ and $\sin 0$) to carry no information (these two coefficients are discussed in [48]).

As shown in Figure 2.3, the first 3 qubits (c_1, c_2, and c_3 qubits) are the color qubits, which encode the RGB color information of an image, and the rest $2n$ qubits ($y_{n-1}, y_{n-2}, \ldots, y_0$ and $x_{n-1}, x_{n-2}, \ldots, x_0$) are used to encode the position information (Y-Axis and X-Axis) of pixels of a $2^n \times 2^n$ pixels image as shown in Figure 2.3. A simple 2×2 pixels MCQI image and its quantum state and circuit (upper 3 qubits used for color and lower 2 qubits used for position) are shown in Figure 2.4. Like the FRQI, the MCQI state is also a normalized state, i.e. $\||I(\theta)\rangle\| = 1$ as given by
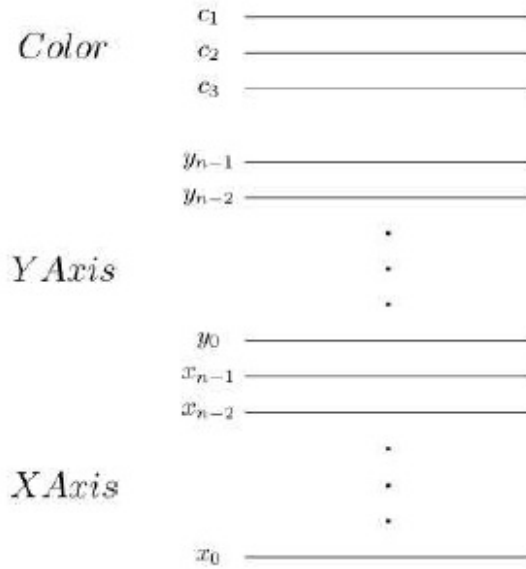
Figure 2.3: *General circuit of MCQI.*

The relationship between the grayscale value of an RGB pixel and the angle value θ^i_X is defined in definition 1.

Definition 1 *The ith pixel's greyscale value G^i_X of MCQI quantum image is encoded by*

14
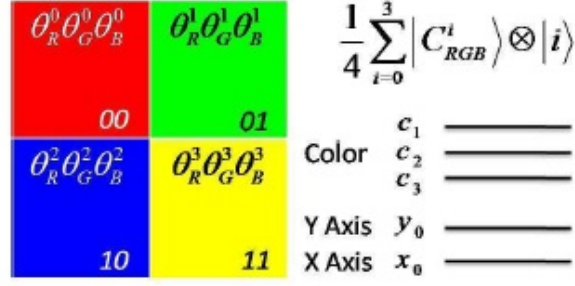
Figure 2.4: *A simple image and its MCQI state.*

the angles θ_R^i, θ_G^i, and θ_B^i defined as

- *Case 1. Values of G_X^i are float (ranging from 0 to 1)*

$$G_X^i = \cos \theta_X^i, \tag{2.5}$$

where, $X \in \{R, G, B\}$.

- *Case 2. Values of G_X^i are 8-bit int (ranging from 0 to 255)*

$$\theta_X^i \in [0, 0.75°) \longrightarrow G_X^i = 0;$$
$$\theta_X^i \in [0.75°, 1.1°) \longrightarrow G_X^i = 1;$$
$$\theta_X^i \in [1.1°, 1.45°) \longrightarrow G_X^i = 2;$$
$$...$$
$$\theta_X^i \in [89.3°, 89.65°) \longrightarrow G_X^i = 254;$$
$$\theta_X^i \in [89.65°, 90°] \longrightarrow G_X^i = 255;$$

$$(2.6)$$

2.3.2 Preparation procedure for MCQI images

Quantum computers are usually initialized in well-prepared states [27]. As a result, the preparation process that transforms quantum computers from the initialized state (assuming $|00\ldots0\rangle$) to the desired quantum image state is necessary. All transforms used in quantum computation are unitary transforms described by unitary matrices. A matrix is said to be unitary if its Hermitian conjugate or its adjoint is the same as its inverse. Quantum mechanics ensures the existence of such unitary transforms for the preparation

process without pointing out explicitly efficient implementation in the sense of using only simple transforms such as Hadamard transform, rotations, etc.

The MCQI polynomial preparation theorem MC-PPT steers a MCQI quantum state from its initialized state to the desired quantum image state, which captures all the information about the image. Based on the results proved in Lemma 1 and Corollary 1, the MC-PPT can be proved.

Lemma 1 *Given 3 vectors of angles* $\theta_X = (\theta_X^0, \theta_X^1, \ldots, \theta_X^{2^{2n}-1})$, $X \in \{R, G, B\}$, *where* $2n$ *is the number of qubits carrying the position information. Assume the initialized state is* $|0\rangle^{\otimes 2n+3}$ *(3 is the number of qubit to encode color information) there is a unitary transformation* $\mathcal{P}$ *that turns the quantum computers to the MCQI state,* $|I_{mc}(\theta)\rangle$ *composed by Hadamard and controlled rotation transformations.*

Proof. There are two steps to achieve the unitary transformation $\mathcal{P}$ as shown in Fig. 5. Hadamard transformations are used in step 1 (step $\mathcal{H}$) and then controlled rotation transformations are used in step 2 (step $\mathcal{R}$) to change from $|H\rangle$ to $|I_{mc}(\theta)\rangle$.

The 2-D identity matrix I and the 2-D Hadamard matrix are shown as

$$I = \begin{pmatrix} 1 & 0 \\ 0 & 1 \end{pmatrix}, \quad H = \frac{1}{\sqrt{2}} \begin{pmatrix} 1 & 1 \\ 1 & -1 \end{pmatrix}.$$

The tensor product of $(2n+2)$ Hadamard matrices is denoted by $H^{\otimes 2n+2}$. Applying the transformation $\mathcal{H} = I \otimes H^{\otimes 2n+2} = I \otimes H^{\otimes 2} \otimes H^{\otimes 2n}$ on $|0\rangle^{\otimes 2n+3} = |0\rangle \otimes |0\rangle^{\otimes 2} \otimes |0\rangle^{\otimes 2n}$ to produce the state $|H\rangle$ given as

$$\begin{aligned} \mathcal{H}(|0\rangle^{\otimes 2n+3}) &= I|0\rangle \otimes \frac{1}{2} \sum_{l=0}^{3} |l\rangle \otimes \frac{1}{2^n} \sum_{i=0}^{2^{2n}-1} |i\rangle \\ &= \frac{1}{2^{n+1}} |0\rangle \otimes \sum_{l=0}^{3} |l\rangle \otimes \sum_{i=0}^{2^{2n}-1} |i\rangle = |H\rangle. \end{aligned} \tag{2.7}$$

Remember, the rotation matrices (the rotations about y axis of Bloch sphere by the angle

2θ) is given as

$$R_y(2\theta) = \begin{pmatrix} \cos\theta & -\sin\theta \\ \sin\theta & \cos\theta \end{pmatrix}, \theta \in \{\theta_R^i, \theta_G^i, \theta_B^i\}. \tag{2.8}$$

Based on the transform Eq.(7), three 8×8 control rotation matrices $\theta_R^i, \theta_G^i, \theta_B^i$ are constructed as

$$R_R^i = I \otimes \sum_{j=1}^{3} |j\rangle\langle j| + R_y(2\theta_R^i) \otimes |0\rangle\langle 0|,$$

$$R_G^i = I \otimes \sum_{j=0,j\neq 1}^{3} |j\rangle\langle j| + R_y(2\theta_G^i) \otimes |1\rangle\langle 1|, \tag{2.9}$$

$$R_B^i = I \otimes \sum_{j=0,j\neq 2}^{3} |j\rangle\langle j| + R_y(2\theta_B^i) \otimes |2\rangle\langle 2|.$$

It is evident that R_R^i, R_G^i, R_B^i are three qubits $(C^2 R_y(2\theta))$ gates as shown in Fig. 2.5. Then we can obtain $R_i' = R_B^i R_G^i R_R^i$, and from R_i', the R_i transform can be constructed with $i = 0, 1, \ldots, 2^{2n} - 1$, as

$$R_i = I^{\otimes 3} \otimes \sum_{j=0,j\neq i}^{2^{2n}-1} |j\rangle\langle j| + R_i' \otimes |i\rangle\langle i|. \tag{2.10}$$

It is clear that R_i is a unitary matrix since $R_i R_i^\dagger = I^{\otimes 2n+3}$. Applying R_k and $R_m R_k$ on $|H\rangle$ gives us

$$R_k(|H\rangle) = \frac{1}{2^{n+1}} \{[I|0\rangle \otimes (I^{\otimes 2} \sum_{l=0}^{3} |l\rangle)] \otimes$$

$$\otimes [(\sum_{j=0,j\neq k}^{2^{2n}-1} |j\rangle\langle j|)(\sum_{i=0}^{2^{2n}-1} |i\rangle)] + \tag{2.11}$$

$$+ [R_k'(|0\rangle \otimes \sum_{l=0}^{3} |l\rangle)] \otimes [(|k\rangle\langle k|)(\sum_{i=0}^{2^{2n}-1} |i\rangle)]\},$$

$$R_m R_k |H\rangle = R_m(R_k|H\rangle)$$

$$= \frac{1}{2^{n+1}} (|0\rangle \otimes \sum_{l=0}^{3} |l\rangle \otimes \sum_{j=0,j\neq k,j\neq m}^{2^{2n}-1} |j\rangle + \tag{2.12}$$

$$+ |C_{RGB}^k\rangle \otimes |k\rangle + |C_{RGB}^m\rangle \otimes |m\rangle),$$

and

$$\mathcal{R}|H\rangle = \left(\prod_{i=0}^{2^{2n}-1} R_i\right)|H\rangle = |I_{mc}(\theta)\rangle. \tag{2.13}$$

Therefore, the unitary transform $\mathcal{P} = \mathcal{RH}$ is the operation turning quantum computer from the initialized state, $|0\rangle^{\otimes 2n+3}$ to the MCQI state $I_{mc}(\theta)$.

In quantum circuit model, a complex transformation is broken down into simple gates, i.e., single qubit and controlled two qubit gates, such as *NOT*, *Hadamard*, and *CNOT* gates [4] [38] as shown in Figure.2.5 and Figure.2.6.

NOT gate $\qquad \alpha|0\rangle + \beta|1\rangle \longrightarrow \boxed{X} \longrightarrow \beta|0\rangle + \alpha|1\rangle$

Hadamard gate $\quad \alpha|0\rangle + \beta|1\rangle \longrightarrow \boxed{H} \longrightarrow \alpha\dfrac{|0\rangle + |1\rangle}{\sqrt{2}} + \beta\dfrac{|0\rangle - |1\rangle}{\sqrt{2}}$
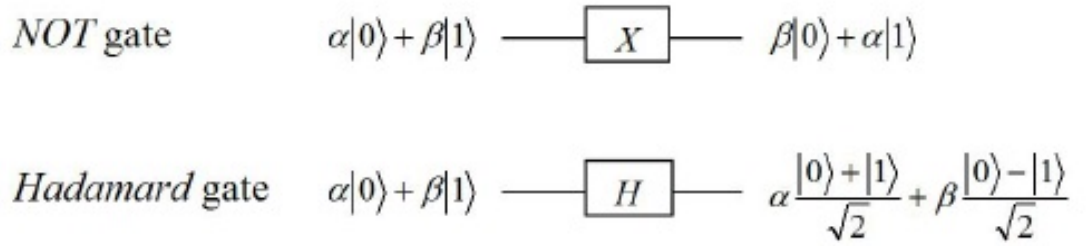
Figure 2.5: *NOT gate and Hadamard gate..*

Gate notation   Matrix representation

Controlled-NOT gate
$$\begin{bmatrix} 1 & 0 & 0 & 0 \\ 0 & 1 & 0 & 0 \\ 0 & 0 & 0 & 1 \\ 0 & 0 & 1 & 0 \end{bmatrix}$$
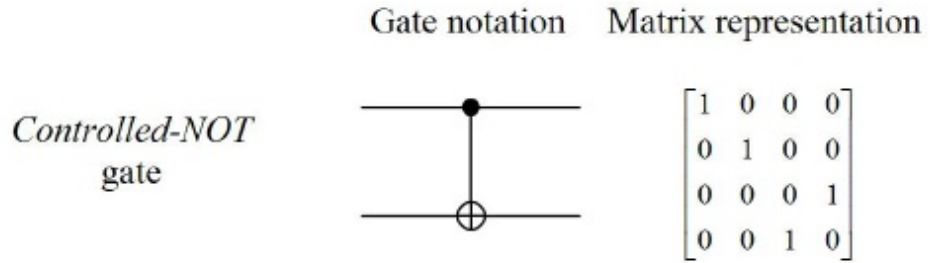
Figure 2.6: *CNOT gate..*

Corollary 1 *The unitary transform $(\mathcal{P})$, described in the Lemma 1, for three given vectors of angles, $\theta_X = (\theta_X^0, \theta_X^1, \dots, \theta_X^{2^{2n}-1})$ $n \in \{0, 1, 2, \dots\}$, $X \in \{R, G, B\}$, can be implemented using the Hadamard, CNOT and $C^{2n+2}(R_y\left(\frac{2\theta_i}{2^{2n}-1}\right))$ gates, where $R_y\left(\frac{2\theta_i}{2^{2n}-1}\right)$ are the rotations about y axis by the angle $\frac{2\theta_i}{2^{2n}-1}, i = 0, 1, \dots, 2^{2n} - 1$.*

Proof. From the proof of Lemma 1, the transform $\mathcal{P}$ is composed of $\mathcal{RH}$. The transform $\mathcal{H}$ can be directly implemented by one 2×2 identity matrix and $(2n+2)$ *Hadamard* gates;

18

and the $\mathcal{R}$ is constructed by $\prod_{i=0}^{2^{2n}-1} R_i$, where $R_i = (I^{\otimes 3} \otimes \sum_{j=0,j\neq i}^{2^{2n}-1} |j\rangle\langle j|) + R_i' \otimes |i\rangle\langle i|$, $R_i' = R_B^i R_G^i R_R^i$, $R_X^i = C^2(R_y(2\theta_X^i))$, $X \in \{R,G,B\}$.

As discussed previously, the first step to implement the unitary transform $\mathcal{P}$ is $\mathcal{H} = I \otimes H^{\otimes 2n+2}$, which contains (2n+2) Hadamard gates, and the second step ($\mathcal{R}$) is constructed by 2^{2n} R_i operations (Eq. (10)). Also, because R_i is constructed by three $C^{2n+2}R_y(2\theta)$ gates, and $C^{2n+2}R_y(2\theta)$ gates can be broken down into $2^{2n+2}-1$ simple operations (or elementary gates) $(R_y(\frac{2\theta_i}{2^{2n+2}-1})$, and $R_y(-\frac{2\theta_i}{2^{2n+2}-1}))$ and $2^{2n+2}-2$ CNOT operations (or gates) [4](an example of $C^2 R_y(2\theta)$ broken down into 3 controlled-rotation gates and 2 CNOT gates is shown in Fig. 6). Hence, in order to prepare MCQI state, $(2n+2)$ Hadamard gates, $3 \times 2^{2n} \times (2^{2n+2}-1)$ Rotation gates $(R_y(\frac{2\theta_i}{2^{2n+2}-1})$, and $R_y(-\frac{2\theta_i}{2^{2n+2}-1}))$, and $3 \times 2^{2n} \times (2^{2n+2}-2)$ CNOT gates are used. Then, the total number of simple operations is computed as follows

$$2(n+1) + 3 \times 2^{2n} \times (2^{2(n+1)} - 1) + 3 \times 2^{2n} \times (2^{2(n+1)} - 2)$$
$$= 24 \times 2^{4n} - 9 \times 2^{2n} + 2n + 2. \tag{2.14}$$

This number is quadratic to the total 2^{2n} angle values. This indicates the efficiency of the preparation process.
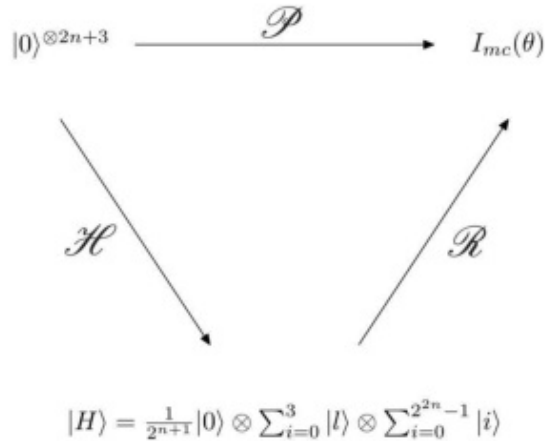
Figure 2.7: *Two steps to achieve P.*

Theorem 1 *(Multi-Channel Polynomial Preparation Theorem) Given three vectors,*
$\theta_X = (\theta_X^0, \theta_X^1, \ldots, \theta_X^{2^{2n}-1}), X \in \{R,G,B\}$ *of angles, there is a unitary transform $\mathcal{P}$ that*
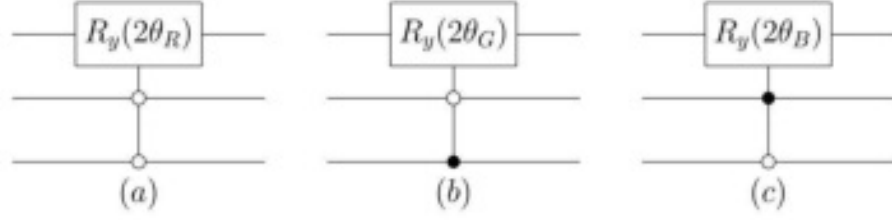
Figure 2.8: *The general quantum circuit of R_R^i, R_G^i, and R_B^i gates..*
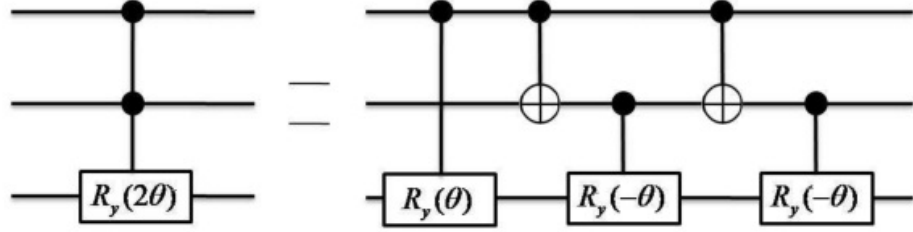
Figure 2.9: *$C^2 R_y(2\theta)$ gates can be built from $C(R_y(\theta))$, $C(R_y(-\theta))$, and CNOT gate.*

turns quantum computers from the initialized state, $|0\rangle^{\otimes 2n+3}$ to the MCQI state

$$I_{mc}(\theta) = \frac{1}{2^{n+1}} \sum_{i=0}^{2^{2n}-1} |C_{RGB}^i\rangle \otimes |i\rangle,$$

composed of polynomial number of simple gates.

Proof. From Lemma 1, two unitary transforms, $\mathcal{H}$ and $\mathcal{R}$, are introduced. The $\mathcal{H}$ is built by 2n+2 Hadamard gates, and from Eq.2.7, after applying it on the initialized quantum state, state $|H\rangle$ is obtained. Then from Eq. 2.11, 2.12 2.13, by applying $\mathcal{R}$ on $|H\rangle$, the MCQI state is realized. From Eq. 2.10, it is clear that $\mathcal{R}$ is constructed by three C^{2n+2} gates, which can be broken down into simple operations proved in Corollary 1. Hence, the unitary transform $\mathcal{P} = \mathcal{RH}$ turns quantum computers from the initialized state to the MCQI state.

2.4 Image processing operations on MCQI quantum images and measurement based quantum image retrieval operation

Representations for images provide the background for image processing algorithms. The algorithms use an image as input to produce another image as output by performing simple operations. Furthermore the output image is analyzed to obtain useful information. This procedure in classical computers can be applied to quantum computers by using unitary transforms as image processing operations.

In classical image processing, basic operators provide fundamental manipulations in various algorithms for processing images. These operators include changes of colors at some positions, geometric transformations, shifting the color information on any channel of interest (CoI operation), etc. These basic operations are important in constructing and understanding the processing algorithms. In quantum image processing, however, the primary manipulations are not obvious since they should be invertible. Meanwhile, some classical operations are not invertible such as convolution operators [31] that means they are physically impossible in quantum computation.

The FRQI and MCQI representations share the same method for position information encoding (the same arrangement for position qubits), and the differences between the two representations are the color qubits (The FRQI uses 1 qubit to encode the color of an image. The MCQI, however, applies 3 qubits to carry the multi-channel color information). These results bring two advantages of MCQI representation:

- all the FRQI based geometric operations G_I (such as two-point swapping, flip and co-ordinate swap, etc) proposed in [28] can be directly extended to the MCQI,

- as the multi-channel information is stored in the three color qubits, the Channel of Interest (CoI) (applying operator only on one channel of interest, such as, R G or B channel) operation and Channel Swapping operation (swapping the grayscale values between two channels) can be realized by simple quantum operations (including

NOT, CNOT, and SWAP gates), both of which cannot be executed using the FRQI representation for images.

As discussed in section 2.2, images are expressed in their MCQI quantum states. Hence, quantum image processing operations can be designed using unitary transforms on those states. These transforms are divided into 3 categories; G_I, C_I and rC_I (restricted version of C_I), applied to MCQI states dealing with only geometric, color channels, and color channels at some specific positions, respectively. The first type of operators (G_I) have been discussed in [28] based on FRQI representation. The second and the third type operators $(C_I$ and $rC_I)$ are focused on the color information of images and applied on color qubits. Each category (the first category G_I on MCQI is same as applying it on the FRQI images and are hence not discussed in this paper.) has its own type of unitary transform. The unitary transforms are in the following forms

$$C_I = U_1 \otimes I^{\otimes 2n}, \tag{2.15}$$

$$rC_I = U_2 \otimes Po + I^{\otimes 3} \otimes \bar{P}o, \tag{2.16}$$

where U_1, U_2 are 1 qubit, 2 qubits, or 3 qubits (1 qubit and 2 qubits gates are elementary gates, and 3 qubits gates can be built by elementary gates, and an example is shown in Fig. 5) transformations (3 color qubits in MCQI), Po and $\bar{P}o$ are matrices regarding eligible and ineligible positions,

$$I = \begin{pmatrix} 1 & 0 \\ 0 & 1 \end{pmatrix}$$

is the identity operator and $2n$ is the number of qubits encoding positions. From the point of quantum circuit modeling, C_I uses a 1 qubit, 2 qubits, or 3 qubits (U_1), while the rC_I category uses an additional control from the position on the gate U_2. These circuits are shown in Figure 2.10 and 2.11, respectively.

In Figure 2.8 and 2.9, P is the quantum circuit for preparation procedure discussed in 2.2.
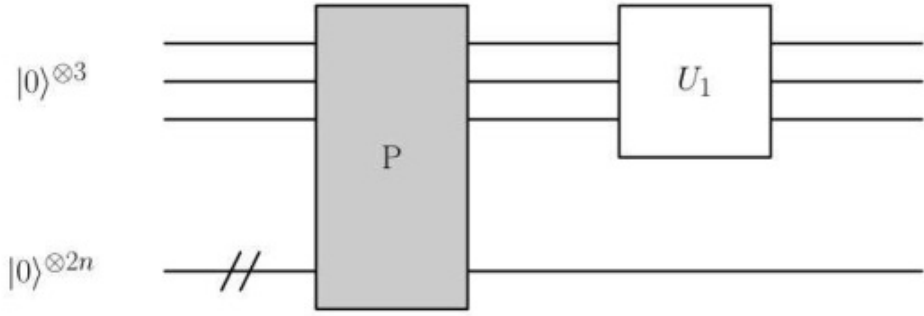
Figure 2.10: *Quantum circuit of C_I operations dealing with color channels by U_1.*
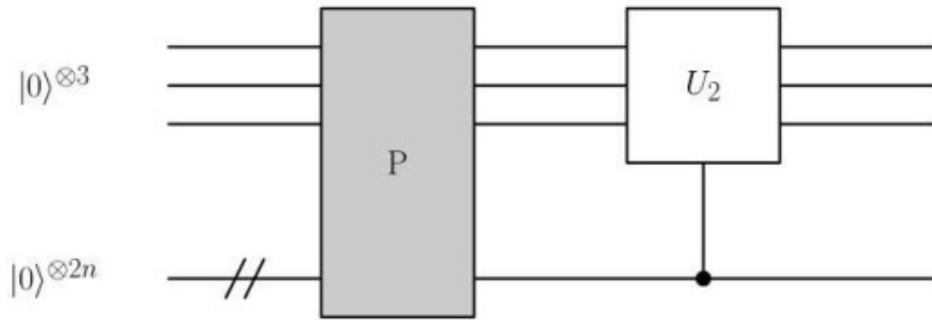
Figure 2.11: *Quantum circuit of rC_I operations dealing with color channels at some positions by U_2.*

2.4.1 Measurement based image retrieval operation

The measurement [53] [18] [8] [52] of the quantum image state produces a probability distribution that is used for the retrieval of the image. A measurement of a quantum state based on the set of basis vectors produces only one result which is one of the basis vectors. In quantum computation, measurements are performed on identical states instead of one state. With only one quantum state, it is impossible to get information from that state. Therefore, a measurement process needs many identical quantum states. For instance, in order to retrieve information about the quantum state

$$|\psi\rangle = \alpha|0\rangle + \beta|1\rangle, \tag{2.17}$$

many identical states, $|\psi\rangle$, are prepared. Each measurement on $|\psi\rangle$ gives either 0 or 1 as result. Many measurements, however, reveal either the result 0, with probability $|\alpha|^2$ or

the result 1, with probability $|\beta|^2$. More complex, the color information of the ith pixel of MCQI image is encoded in the entangled 3 qubits state

$$
\begin{aligned}
|C^i_{RGB}\rangle = {}& \cos\theta^i_R|000\rangle + \cos\theta^i_G|001\rangle + \cos\theta^i_B|010\rangle + \\
& + \sin\theta^i_R|100\rangle + \sin\theta^i_G|101\rangle + \sin\theta^i_B|110\rangle + \\
& + \cos 0|011\rangle + \sin 0|111\rangle.
\end{aligned}
\tag{2.18}
$$

Hence, to retrieve the coefficients, we need to measure this state separately. And Eq. (2.14) can be rewritten as

$$
|C^i_{RGB}\rangle = |C_R\rangle|00\rangle + |C_G\rangle|01\rangle + |C_B\rangle|10\rangle + |C_0\rangle|11\rangle,
\tag{2.19}
$$

where

$$
\begin{aligned}
|C_R\rangle &= \cos\theta^i_R|0\rangle + \sin\theta^i_R|1\rangle, \\
|C_G\rangle &= \cos\theta^i_G|0\rangle + \sin\theta^i_G|1\rangle, \\
|C_B\rangle &= \cos\theta^i_B|0\rangle + \sin\theta^i_B|1\rangle, \\
|C_0\rangle &= \cos 0|0\rangle + \sin 0|1\rangle.
\end{aligned}
\tag{2.20}
$$

Then we can apply the measurement operation on $|C_R\rangle$ (encoding the greyscale value of R channel), $|C_G\rangle$ (encoding the greyscale value of G channel), and $|C_B\rangle$ (encoding the greyscale value of B channel) separately by using 2 control operation from c_2 and c_3 qubits, as shown in Figure 2.12.
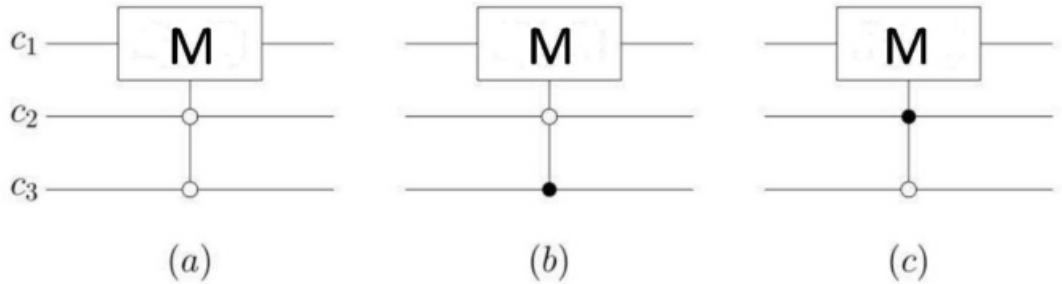
Figure 2.12: *The general quantum circuit of measurement operations ((a) measurement on $|C_R\rangle$, (b) measurement on $|C_G\rangle$, (c) measurement on $|C_B\rangle$)..*

Specifically, each measurement on $|C_X\rangle$ ($X \in \{R, G, B\}$) gives either 0 or 1 as result.

Many measurements reveal either the result 0, with probability $\cos^2 \theta_X^i$ or the result 1, with probability $\sin^2 \theta_X^i$. From this probability, the greyscale value of X channel can be retrieved.

2.5   Experiments on MCQI images

The experiments reported in this section were executed using a laptop computer with Intel Core (TM) i5 Duo 2.40 GHz CPU and 4 GB RAM. The simulations are linear algebra based with complex vectors as quantum states and unitary matrices as unitary transforms using MATLAB. To demonstrate the feasibility of storage and retrieval of quantum images, experiments on storage and retrieval of MCQI images are conducted.
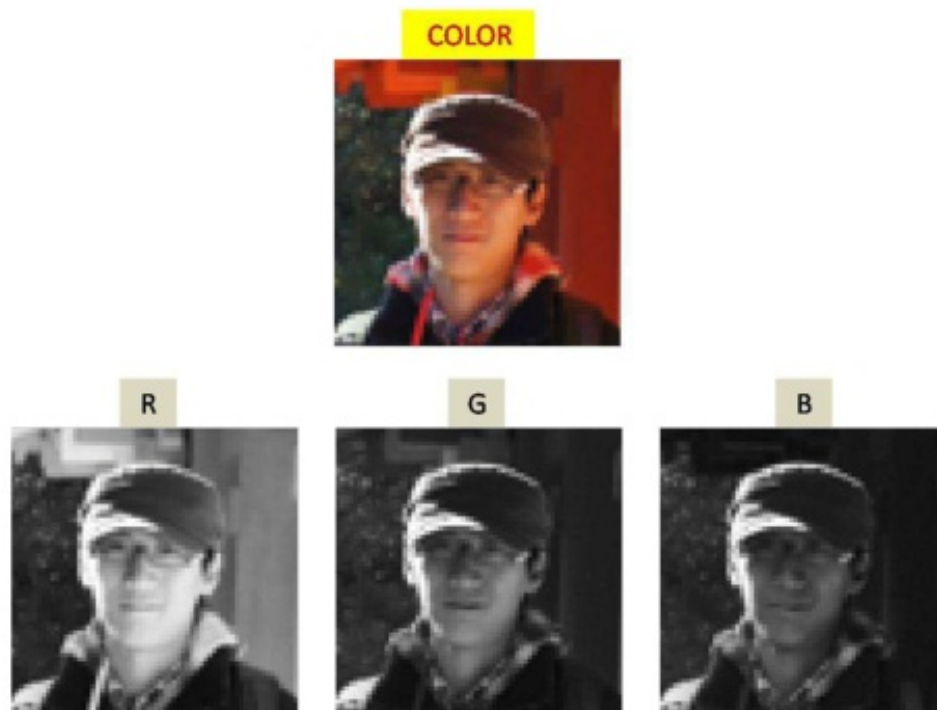
Figure 2.13: *The image used in experiment of storage and retrieval of MCQI quantum images..*

The essential requirements for representing a classical or quantum image are the simplicity and efficiency in the storage and retrieval of the image. The storage of a quantum image is achieved by the preparation process, which is possible using the proposed MC-PPT theorem presented earlier in section 2. A 64×64 colored image is used for this

experiment shown in Figure 2.13. To represent the image on Matlab, a vector of 32768 $(64 \times 64 \times 8)$ real-valued coefficients is stored for the first experiment. Hence, 15 qubits are needed for MCQI representation (3 color qubits and 12 position qubits) which is much lesser than the qubit lattice, grid qubit, and quantum lattice representations (4096 qubits are requested for storing a 64×64 image). From Figure 2.13, the angles encoding the gray levels of each channel (R, G, and B) and corresponding positions are extracted. The measurement operation method introduced in 2.2 is used to image retrieval experiments. To evaluate the quality of the retrieved images, average RGB peak-signal-to-noise ratio (RGB-PSNR) [33] [3] [10] is used. Figure 2.14 shows the relationship between the measurement times of all pixels. Figure 2.14 shows the relationship between the measurement times of all pixels and PSNR. The PSNR of the retrieved images is shown in Table 2.1, and it is defined as

$$PSNR_{RGB} = (PSNR_R + PSNR_G + PSNR_B)/3, \tag{2.21}$$

where

$$PSNR_X = 20log_{10}\left(\frac{255}{\sqrt{MSE}}\right), X \in \{R, G, B\},$$

$$MSE = \frac{1}{mn}\sum_{i=0}^{m-1}\sum_{j=0}^{n-1}[I(i,j) - R(i,j)]^2. \tag{2.22}$$

Here, MSE is mean squared error between the original image $I(i, j)$ and the retrieved image $R(i, j)$. $m \times n$ are the number of pixels of the image.

Let mp denote the number of measurements performed to retrieve the value of a given pixel in an MCQI image. Then, by performing a sufficient number of measurements (i.e. making mp big enough) the corresponding pixel value could be retrieved with arbitrary accuracy. Specifically, if $mp > 200$, the $PSNR > 30dB$, and if $mp > 2000$, the $PSNR > 40dB$. Hence, the total measurement time M can be computed as

$$M = mp \times N, \tag{2.23}$$

where N is the number of pixels of the image. Hence, it is clearly that the complexity of
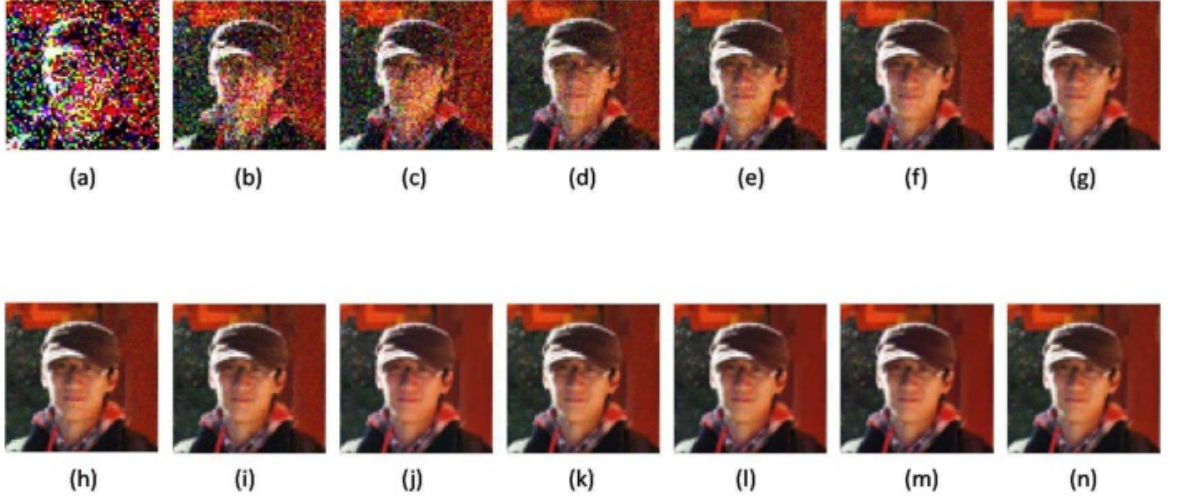
Figure 2.14: *The retrieved images based on measurement ((a)mp = 1; (b)mp = 5; (c)mp = 10; (d)mp = 50; (e)mp = 100; (f)mp = 200; (g)mp = 300; (h)mp = 400; (i)mp = 500; (j)mp = 1000; (k)mp = 2000; (l)mp = 3000; (m)mp = 4000; (n)mp = 5000)..*

the image retrieval procedure (C_r) is $O(N)$. Also, as discussed in 2.2, the total number of simple operations for the preparation procedure is $24 \times 2^{4n} - 9 \times 2^{2n} + 2n + 2$ ($2n$ is the number of position qubit), hence the complexity of preparation procedure (C_p) is $O(N^2)$ ($N = 2^{2n}$). The full algorithmic complexity (C) of the both parts (preparation and retrieval) is shown as

$$C = C_p + C_r = O(N^2) + O(N) = O(N^2). \tag{2.24}$$

From this experiment, it is easy to conclude:

- using the classical of images the proposed MC-PPT procedure allows for the preparation of quantum replicas;

- the multi-channel information (color information) can be retrieved based on measurement;

- the quality of the retrieved image depends on mp (see Table 2.1);

- the number of qubit for encoding $2^n \times 2^n$ pixels image is $2n + 3$.

Table 2.1: *Average RGB PSNRs of the retrieved images.*

Retrieved images	Measurement times, mp	Average RGB PSNR (dB)
Fig.11(a)	1	8.0539
Fig.11(b)	5	15.2072
Fig.11(c)	10	18.1186
Fig.11(d)	50	25.0933
Fig.11(e)	100	28.2195
Fig.11(f)	200	31.1567
Fig.11(g)	300	32.9445
Fig.11(h)	400	34.1605
Fig.11(i)	500	35.1229
Fig.11(j)	1000	38.1565
Fig.11(k)	2000	41.2268
Fig.11(l)	3000	42.9893
Fig.11(m)	4000	44.1213
Fig.11(n)	5000	45.2604

As discussed in 2.2, the compare along side the qubit lattice representation (grid qubit and quantum lattice representations using the same number of qubit with qubit lattice), MCQI quantum image representation uses much less qubits to encode images of the same size, as shown in Figure 2.15.

2.6 Summary of RGB multi-channel representation for images on quantum computer

An RGB multi-channel representation for images (MCQI) is proposed in order to provide a basis for the polynomial preparation process and quantum image processing operations based on unitary operators where the RGB color information is encoded by 3 entangled qubits (c_1, c_2, and c_3 qubits) and the pixels' positions of a $2^n \times 2^n$ pixels image. The MCQI captures image colors and their corresponding positions in a quantum state. After the proposal the MCQI, the following issues are also discussed:

- the complexity (the number of simple operations) of the preparation procedure for MCQI,

- MCQI based image processing operations,
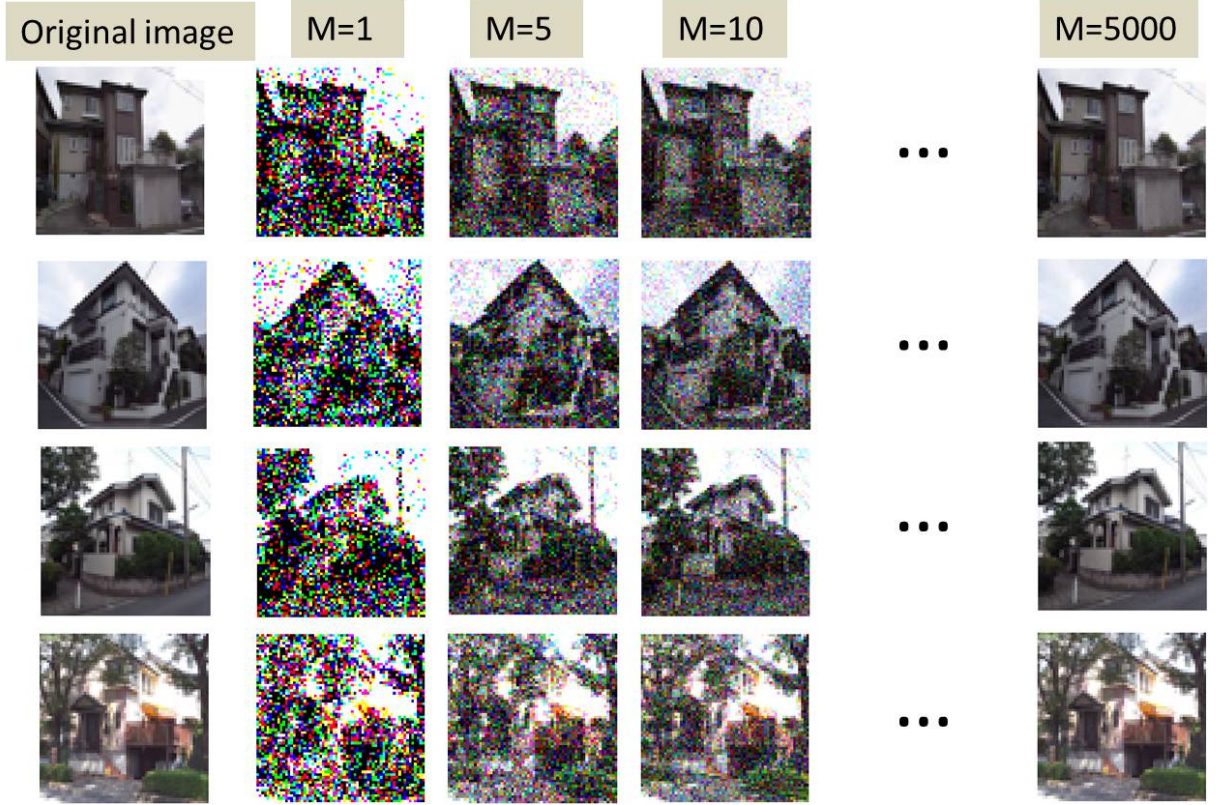
Figure 2.15: *Measurement based image retrieval..*

- the measurement based image retrieval from quantum to classical.

The proposed multi-channel polynomial preparation procedure achieves a unitary preparation process using a polynomial number of simple operators transforming quantum computers from the initial state to MCQI state. Based on MCQI, all the RGB information about the image is stored simultaneously. Firstly, the property of quantum parallelism is used to encode the color information and their corresponding positions, e.g., only 15 qubits are used to encode a 64×64 pixels image in MCQI representation, whereas 4096 qubits are requested in qubit lattice, grid qubit, and quantum lattice representations. Secondly, as the multi-channel information (R channel, G channel, and B channel) are stored in the first 3 qubits (entangled) (color qubits) concurrently, the color information operators applying on the whole image (not focussing on some specific position of an image) can be designed by using unitary quantum gates within these 3 qubits irrespective of the position qubits. It means that the complexity of the MCQI-based color information operators are image size independent, namely, $O(1)$, whereas the color information must
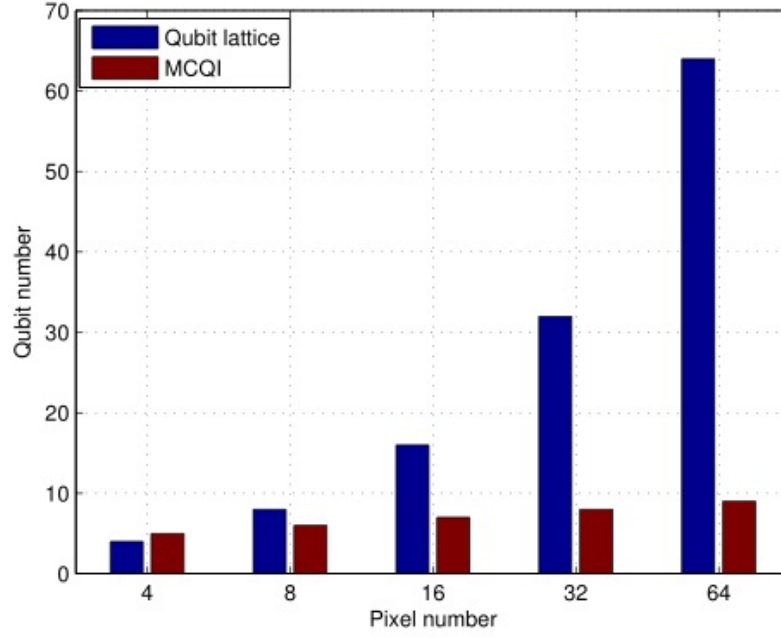
Figure 2.16: *Qubit number using for encoding the images in- formation..*

be shifted pixel by pixel in the case of operators on classical computers. It also points out the design of the quantum circuit using Hadamard gates and controlled rotation gates for the transform. And the Measurement based image retrieval operation is also proposed.

The results of storage and retrieval experiment of MCQI image reveal that the classical images can be stored in normalized quantum states simultaneously by using basic gates; the multi-channel information (color information) can be retrieved based on measurement; and specifically, the number of qubit for encoding a 64×64 pixels image is 15, which proves the efficiency of the proposed MCQI representation for image storage. The measurement experiment is conducted. The results demonstrate that only one time measurement (mp=1) is not sufficient to retrieve the content of an image (RGB PSNR= $8.0539dB$), and if measurement time is $mp > 200$, the RGB PSNR$> 30dB$, also $mp > 2000$, the RGB PSNR$> 40dB$ which prove that the classical information can be retrieved by measurement and the qualities of the retrieved images are depend on measurement times mp.

In the next chapter, the results in this chapter will be extended to understand deeper about unitary transformations on quantum images. As the discussion in section 2.4, the image processing operators are divided into 2 types. The channel information operations

will proposed based on the results obtained in this chapter, and the property of collapse after measurement will also be discussed.

Chapter 3

Color information transformations on Multi-Channel Quantum Images

3.1 Introduction

Representations for images provide the background for image processing algorithms. The algorithms use an image as input to produce another image as output by performing simple operations. Furthermore the output image is analyzed to obtain useful information. This procedure in classical computers can be applied to quantum computers by using unitary transforms as image processing operations.

In classical image processing, basic operators provide fundamental manipulations in various algorithms for processing images. These operators include changes of colors at some positions, geometric transformations, shifting the color information on any channel of interest (CoI operation), etc. These basic operations are important in constructing and understanding the processing algorithms. In quantum image processing, however, the primary manipulations are not obvious since they should be invertible. Meanwhile, some classical operations are not invertible such as convolution operators [31] that means they are physically impossible in quantum computation.

The FRQI and MCQI representations share the same method for position information encoding (the same arrangement for position qubits), and the differences between the two representations are the color qubits (The FRQI uses 1 qubit to encode the color

of an image. The MCQI, however, applies 3 qubits to carry the multi-channel color information). These results bring two advantages of MCQI representation:

- all the FRQI based geometric operations G_I (such as two-point swapping, flip and co-ordinate swap, etc) proposed in [28] can be directly extended to the MCQI,

- as the multi-channel information is stored in the three color qubits, the Channel of Interest (CoI) (applying operator only on one channel of interest, such as, R G or B channel) operation and Channel Swapping operation (swapping the grayscale values between two channels) can be realized by simple quantum operations (including NOT, CNOT, and SWAP gates), both of which cannot be executed using the FRQI representation for images.

The goal of this chapter is to extend the use of quantum circuit models using the basic gates in the NCT library for quantum image representation and processing. In this chapter, 4 color transformation operators are proposed using basic quantum gates; NOT, CNOT, Toffoli, Rotation, and Controlled Rotation gates based on the multi-channel representation for quantum images (MCQI), where the $RGB\alpha$ color information is encoded by 3 entangled qubits (c_1, c_2, and c_3 qubits) and the pixels' positions of a $2^n \times 2^n$ pixels image is represented by $2n$ qubits.

The Channel of Interest is the operator shifting the color information on only one channel (R, G, B, or α channel) by applying C^2-Rotation gates on c_1 qubit (The controlled operations are applied on c_2 and c_3 qubits). The Channel Swapping operator is designed to swap the information between two channels (R and G, R and B, or G and B) which can be realized by CNOT and SWAP (constructed by 3 CNOT gates) gates on c_2 and c_3 qubits (no operation on c_1 qubit). A little bit more complex operator is Color Space Transformation which transforms the color space of an image from RGB to other color spaces such as YIQ, YUV, and XYZ, etc. The CST operator is designed by utilizing the proposed 3×3 steps algorithm combined with two ancilla qubits, which are used for preparing four identical MCQI images concurrently in the quantum state. The final operator proposed in this paper is Alpha (α) Blending which is used for combing the color information of two different images (One is considered as original image and the other

one is background image), and to designed the circuit, a C^2 Rotation gate is applied on ancilla qubit (The controlled operations are on c_2 and c_3 qubits).

The complexity of the proposed 4 operators are low compared with their classical version. Firstly, as the multi-channel information (R channel, G channel, B channel, and α channel) are stored in the 3 color qubits (c_1, c_2, and c_3) (entangled) concurrently, the proposed color information operators applying on the whole image (not focussing on some specific position of an image) can be designed by using unitary quantum gates within these 3 qubits (for CST and αB operators, operations are applied on both the 3 color qubits and ancilla qubits) irrespective of the position qubits. It means that the complexity of the MCQI-based color information operators are image size independent, namely, $O(1)$ for an N-sized image, whereas the color information must be shifted pixel by pixel in the case of operators on classical computers. Secondly, the information of α channel is also stored (or encoded) in the MCQI quantum states, which opens the door to design further α based operations on quantum computer (Only few of them are known as mentioned earlier). Thirdly, all the invertible classical color information transformation of images can be transplant into quantum computer by careful designing and combination of the proposed 4 operators and GTQI [28] operators. Finally, the proposed operators (especially the αB operator) can be applied for designing color version of quantum movie QuMovie [21] and make special visual effects on it (not only the expression of motion as mentioned in [21]).

3.2 Revised multi-channel representation for quantum images

3.2.1 RGBα color model

The RGBα color space which is actually simply a use of the RGB color model, with extra information. The color is RGB, and belong to RGB color space discussed in 2.1, and α represent the α channel [17], [43] which is normally used as an opacity channel.

Specifically, if a pixel has a value of 0 ($T_\alpha = 0$) in its alpha channel, this pixel is full transparent (and, thus, invisible), whereas a value of 255 ($T_\alpha = 255$) in the alpha channel gives a fully opaque pixel (traditional digital images). Values between 0 and 255 make it possible for pixels to show through a background like a glass (translucency). For example, given two images A and B, A is the original image and B is the background image, after α blending (assuming the size ($m \times n$ pixels) of the two images are same), the obtained image D can be defined as

$$D_X(i,j) = (T_\alpha A_X(i,j) + (255 - T_\alpha)B_X(i,j))/255, \tag{3.1}$$

where $A_X(i,j)$, $B_X(i,j)$, and $D_X(i,j)$ are the X channel's grayscale value of pixels of images A, B, and D, respectively, and $X \in \{R, G, B\}$. The T_α is the transparency value (transparency parameter) of α channel. Examples of α blending images are shown in Figure 3.1
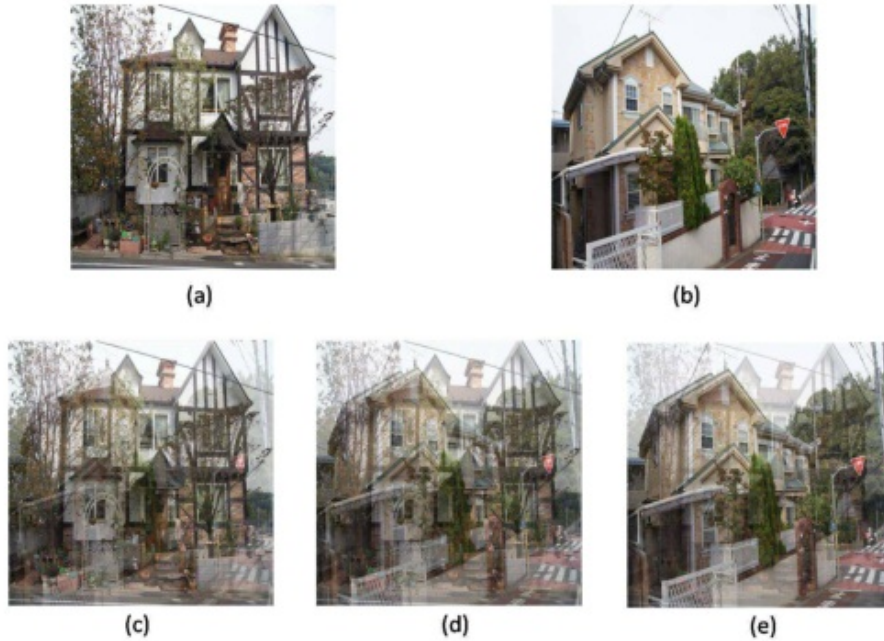
Figure 3.1: *Examples of α blending images ((a) The original image; (b) the back ground image; (c) the blended image with $T_\alpha = 178$); (d) the blended image with $T_\alpha = 128$; (d) the blended image with $T_\alpha = 77$.*

3.2.2 Multi-channel representation for quantum images with α channel

The MCQI has already been discussed in chapter 2. In this section, we revise the MCQI representation to make it include the information of α channel. This is accomplished by assigning 3 qubits ($2^3 = 8$ coefficients)(2 coefficients represent 1 channel/component) to encode the images information of colors. The mathematics expression is presented as

$$|I(\theta)_{mc}\rangle = \frac{1}{2^{n+1}} \sum_{i=0}^{2^{2n}-1} |C_{RGB\alpha}^i\rangle \otimes |i\rangle. \tag{3.2}$$

The color information $|C_{RGB\alpha}^i\rangle$ encoding the R, G, B, and α channels information is defined as

$$\begin{aligned}
|C_{RGB\alpha}^i\rangle = {}& \cos\theta_R^i|000\rangle + \cos\theta_G^i|001\rangle + \cos\theta_B^i|010\rangle + \cos\theta_\alpha^i|011\rangle + \\
& + \sin\theta_R^i|100\rangle + \sin\theta_G^i|101\rangle + \sin\theta_B^i|110\rangle + \sin\theta_\alpha^i|111\rangle,
\end{aligned} \tag{3.3}$$

where $|000\rangle$, $|001\rangle$, ..., $|111\rangle$ are 8-D computational basis; $\{\theta_R^i, \theta_G^i, \theta_B^i, \theta_\alpha^i\} \in [0, \frac{\pi}{2}]$ are four angles encoding the colors of the R, G, B, and α channels of the *ith* pixel, respectively; $\otimes$ is the tensor product notation; $|i\rangle$ for $i = 0, 1, \ldots, 2^{2n} - 1$ are 2^{2n}-D computational basis states. Specifically, there are two parts in the revised MCQI quantum image: $|C_{RGB\alpha}^i\rangle$ and $|i\rangle$, which encode information about colors and their corresponding positions in the image, respectively.

A simple 2×2 size revised MCQI image (4 pixels with color Red (255,0,0), Green (0,255,0), Blue (0,0,255), and Yellow (255,255,0)) and its quantum state and circuit (upper 3 qubits used for color and lower 2 qubits used for position) are shown in Figure 3.2.
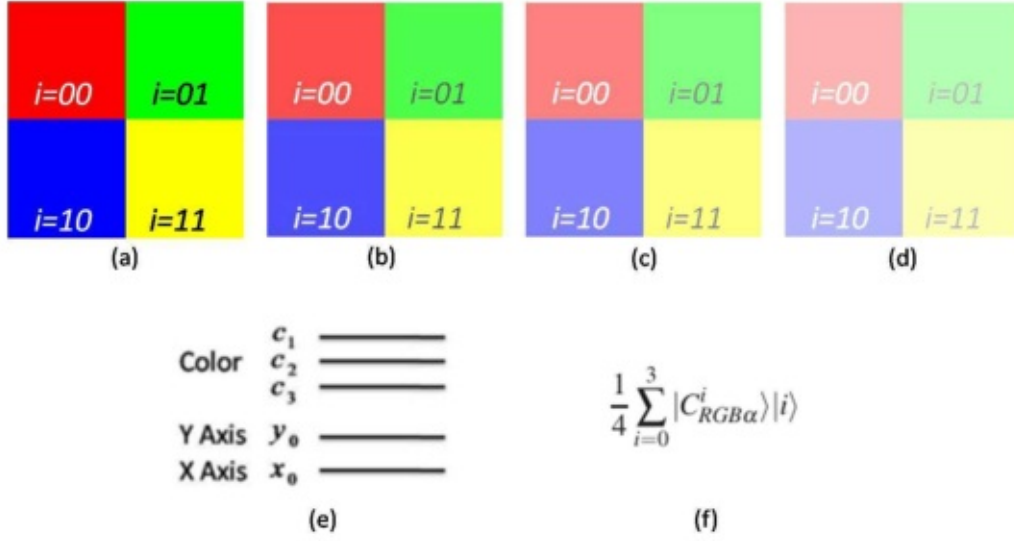
Figure 3.2: *A simple image and its MCQI state ((a) the RGB color image with $T_\alpha = 255$; (b) the RGB color image with $T_\alpha = 178$; (c) the RGB color image with $T_\alpha = 128$; (d) the RGB color image with $T_\alpha = 77$; (e) the MCQI quantum circuit to encode 4 pixels color image; (f) the MCQI quantum state).*

3.3 Image processing operators on revised MCQI quantum images based on unitary transforms

Representations of images provide the background for image processing algorithms. The algorithms use an image as input to produce another image as output by performing simple operations. Furthermore the output image is analyzed to obtain useful information. This procedure in classical computers can be applied to quantum computers by using unitary transforms as image processing operations.

In classical image processing, basic operators provide fundamental manipulations in various algorithms for processing images. These operators include changes of colors at some positions, geometric transformations, shifting color information on interested channel (Channel of Interest or *CoI* operation), etc. These basic operations are important in constructing and understanding the processing algorithms. In quantum images, however, the primary manipulations are not obvious since they should be invertible. Meanwhile, some classical operations are not invertible such as convolution operators [31] that means they are physically impossible in quantum computation.

The FRQI and MCQI representations share the same method for position information encoding (the same arrangement for position qubits), and the differences between the two representations are the color qubits (The FRQI uses 1 qubit to encode the color of an image. The MCQI, however, applies 3 qubits to carry the multi-channel color information). These characteristics bring two advantages of MCQI representation:

- all the FRQI based geometric operations (such as two-point swapping, flip and coordinate swap, etc) proposed in [28] can be transplanted to MCQI directly,

- as the multi-channel information is stored in the three color qubits, the Channel of Interest (CoI) (applying operator only on one interested channel, such as, R G B and α channels) operation and Channel Swapping operation (swapping the grayscale values between two channels), can be realized by simple quantum operations (including NOT, CNOT, and SWAP gates), which are unable to fulfill on FRQI images.

3.3.1 Channel of interest operator

The Channel of Interest (CoI) operator (shifting the grayscale value of the interested color channel(R, G, B or α channel)), CoI_X ($X \in \{R, G, B, \alpha\}$, CoI_R, CoI_G, CoI_B, and CoI_α are operators applied on R, G, B, and α channels respectively) is defined as an operator, $CoI_X = U_X \otimes I^{\otimes 2n}$, by using $U_X = C^2 R_y(2\theta)$ gate, where θ is the shifting parameter (or shifting angle). As defined in (4), by changing the angles of the coefficients of the quantum states (from $|000\rangle$ to $|111\rangle$), the grayscale value of pixels are changed. The calculation produces the result $|I(\theta)_{mc}^X\rangle$ of the application of CoI_X on $|I(\theta)_{mc}\rangle$, given as

$$
\begin{aligned}
|I(\theta)_{mc}^X\rangle &= CoI_X(|I(\theta)_{mc}\rangle), \\
&= (U_X \otimes I^{\otimes 2n}) \left(\frac{1}{2^{n+1}} \sum_{i=0}^{2^{2n}-1} |C_{RGB\alpha}^i\rangle \otimes |i\rangle \right), \\
&= \frac{1}{2^{n+1}} \sum_{i=0}^{2^{2n}-1} |C_{RGB}^{Xi}\rangle \otimes |i\rangle,
\end{aligned}
\tag{3.4}
$$

where $|C^i_{RGB\alpha}\rangle$ state carries the RGB color information defined in Eq.(3); $|C^{Xi}_{RGB\alpha}\rangle$ is the new color state after applying CoI_X operator, shown as

$$\begin{aligned}
|C^{Ri}_{RGB\alpha}\rangle &= \cos(\theta^i_R - \theta)|000\rangle + \cos\theta^i_G|001\rangle + \cos\theta^i_B|010\rangle + \cos\theta^i_\alpha|011\rangle + \\
&\quad + \sin(\theta^i_R - \theta)|100\rangle + \sin\theta^i_G|101\rangle + \sin\theta^i_B|110\rangle + \sin\theta^i_\alpha|111\rangle, \\
|C^{Gi}_{RGB\alpha}\rangle &= \cos\theta^i_R|000\rangle + \cos(\theta^i_G - \theta)|001\rangle + \cos\theta^i_B|010\rangle + \cos\theta^i_\alpha|011\rangle + \\
&\quad + \sin\theta^i_R|100\rangle + \sin(\theta^i_G - \theta)|101\rangle + \sin\theta^i_B|110\rangle + \sin\theta^i_\alpha|111\rangle, \\
|C^{Bi}_{RGB\alpha}\rangle &= \cos\theta^i_R|000\rangle + \cos\theta^i_G|001\rangle + \cos(\theta^i_B - \theta)|010\rangle + \cos\theta^i_\alpha|011\rangle + \\
&\quad + \sin\theta^i_R|100\rangle + \sin\theta^i_G|101\rangle + \sin(\theta^i_B - \theta)|110\rangle + \sin\theta^i_\alpha|111\rangle, \\
|C^{\alpha i}_{RGB\alpha}\rangle &= \cos\theta^i_R|000\rangle + \cos\theta^i_G|001\rangle + \cos\theta^i_B|010\rangle + \cos(\theta^i_\alpha - \theta)|011\rangle + \\
&\quad + \sin\theta^i_R|100\rangle + \sin\theta^i_G|101\rangle + \sin\theta^i_B|110\rangle + \sin(\theta^i_\alpha - \theta)|111\rangle.
\end{aligned}$$ (3.5)

The quantum image $|I(\theta)^X_{mc}\rangle$ has all of its colors coming from the original image $|I_{mc}(\theta)\rangle$ by shifting the θ angle on R, G, B, or α channel. The quantum circuits of U_X (U_R, U_G, U_R, and U_α) are $C^2R_y(2\theta)$ gates and shown in Figure 3.3, and the $C^2R_y(2\theta)$ can be constructed from basic gates (controlled rotation and CNOT gates) as shown in Figure 3.4.
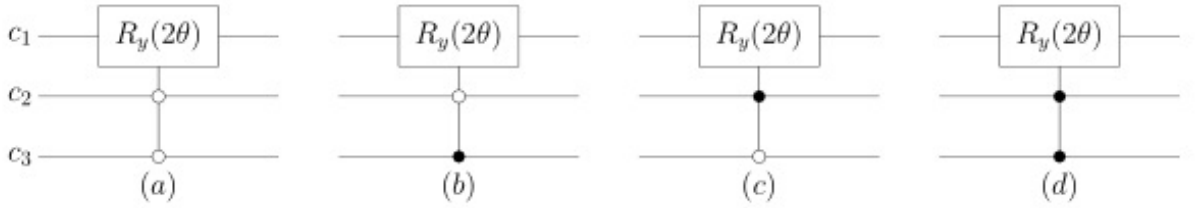
Figure 3.3: *The general quantum circuit of U_X operations ((a) U_R, (b) U_G, (c) U_B, (d) U_α)..*

From Figure 3.3 and Figure 3.4, to construct the CoI operator, at most 9 quantum basic gates are requested.

3.3.2 Channel swapping operator

The Channel Swapping (CS) operator, CS_Y ($Y \in \{RG, RB, GB\}$, CS_{RG}, CS_{RB}, and CS_{GB} are operators that swap the grayscale values between R and G, R and B, and G
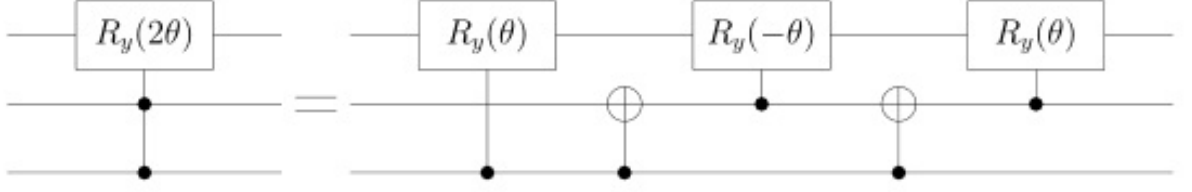
Figure 3.4: $C^2 R_y(2\theta)$ *can be constructed from basic gates ($CR_y(\theta)$, $CR_y(-\theta)$, and CNOT gates)..*

and B channels, respectively) (no operation on α channel), $CS_Y = I \otimes U_Y \otimes I^{\otimes 2n}$, by using CNOT gate or SWAP gate (CNOT and SWAP gates are two qubits gates) on c_2 and c_3 color qubits (there is no operation on c_1 color qubit). The calculation produces the result $|I(\theta)^Y_{mc}\rangle$ of the application of CS_Y on $I(\theta)_{mc}$, given as

$$
\begin{aligned}
|I(\theta)^Y_{mc}\rangle &= CS_Y(|I(\theta)_{mc}\rangle), \\
&= (I \otimes U_Y \otimes I^{\otimes 2n}) \left(\frac{1}{2^{n+1}} \sum_{i=0}^{2^{2n}-1} |C^i_{RGB\alpha}\rangle \otimes |i\rangle \right), \\
&= \frac{1}{2^{n+1}} \sum_{i=0}^{2^{2n}-1} |C^{Yi}_{RGB\alpha}\rangle \otimes |i\rangle,
\end{aligned}
\tag{3.6}
$$

where, $|C^{Yi}_{RGB\alpha}\rangle$ is the new color state after applying CS_Y operator, shown as

$$
\begin{aligned}
|C^{RGi}_{RGB\alpha}\rangle &= \cos\theta^i_G|000\rangle + \cos\theta^i_R|001\rangle + \cos\theta^i_B|010\rangle + \cos\theta^i_\alpha|011\rangle+ \\
&\quad + \sin\theta^i_G|100\rangle + \sin\theta^i_R|101\rangle + \sin\theta^i_B|110\rangle + \sin\theta^i_\alpha|111\rangle, \\
|C^{RBi}_{RGB\alpha}\rangle &= \cos\theta^i_B|000\rangle + \cos\theta^i_G|001\rangle + \cos\theta^i_R|010\rangle + \cos\theta^i_\alpha|011\rangle+ \\
&\quad + \sin\theta^i_B|100\rangle + \sin\theta^i_G|101\rangle + \sin\theta^i_R|110\rangle + \sin\theta^i_\alpha|111\rangle, \\
|C^{GBi}_{RGB\alpha}\rangle &= \cos\theta^i_R|000\rangle + \cos\theta^i_B|001\rangle + \cos\theta^i_G|010\rangle + \cos\theta^i_\alpha|011\rangle+ \\
&\quad + \sin\theta^i_R|100\rangle + \sin\theta^i_B|101\rangle + \sin\theta^i_G|110\rangle + \sin\theta^i_\alpha|111\rangle.
\end{aligned}
\tag{3.7}
$$

The quantum image $|I(\theta)^Y_{mc}\rangle$ is obtained from the original image $|I(\theta)_{mc}\rangle$ by applying CS_Y operator, and specifically, quantum circuits of U_Y (U_{RG}, U_{RB}, and U_{GB}) are shown in Figure 3.5.

From Figure 3.5, at most 3 quantum basic gates are utilized to build the CS operator.
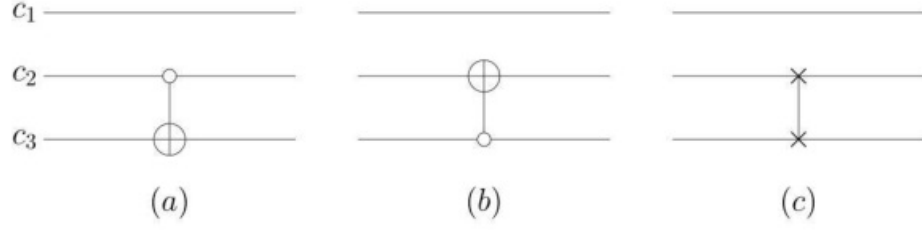
Figure 3.5: $C^2 R_y(2\theta)$ *can be constructed from basic gates (he general quantum circuit of U_Y operations ((a) U_{RG}, (b) U_{RB}, (c) U_{GB})..*

3.3.3 Color space transformation

In color image processing field, one important operation is color space transform. Different color spaces are applied for different image processing tasks. Besides RGB color space, there are many other color spaces, such as YUV color space which is widely used for analog television (PAL or NTSC), and YIQ for pattern recognition.

From classical image processing, it is easy to conclude that all the color space transformation (CST) operations are invertible. This truth provides the theoretical foundation to construct CST algorithms on quantum computer (in quantum computation, all transformations must be invertible). Specifically, most color spaces can be obtained from RGB color space by linear or nonlinear combination of R, G, and B components. For example, YUV and YIQ color space can be obtained by

$$
\begin{aligned}
Y &= 0.299R + 0.587G + 0.114B, \\
U &= -0.14713R - 0.28886G + 0.436B, \\
V &= 0.625R - 0.51499G - 0.10001B,
\end{aligned}
\tag{3.8}
$$

$$
\begin{aligned}
Y &= 0.299R + 0.587G + 0.114B, \\
I &= -0.595716R - 0.274453G - 0.31263B, \\
Q &= 0.211456R - 0.522591G + 0.311134B,
\end{aligned}
\tag{3.9}
$$

To build CST on quantum computer, the combination of R, G, and B components are request to be constructed. Considering the structure of MCQI, 2 ancilla qubits are added on the circuit for the preparation of 4 identical MCQI images which are utilized to build

the combination of R, G, and B components. The circuit with ancilla qubits to carry 4 MCQI images and the corresponding quantum state are shown in Figure 3.6.
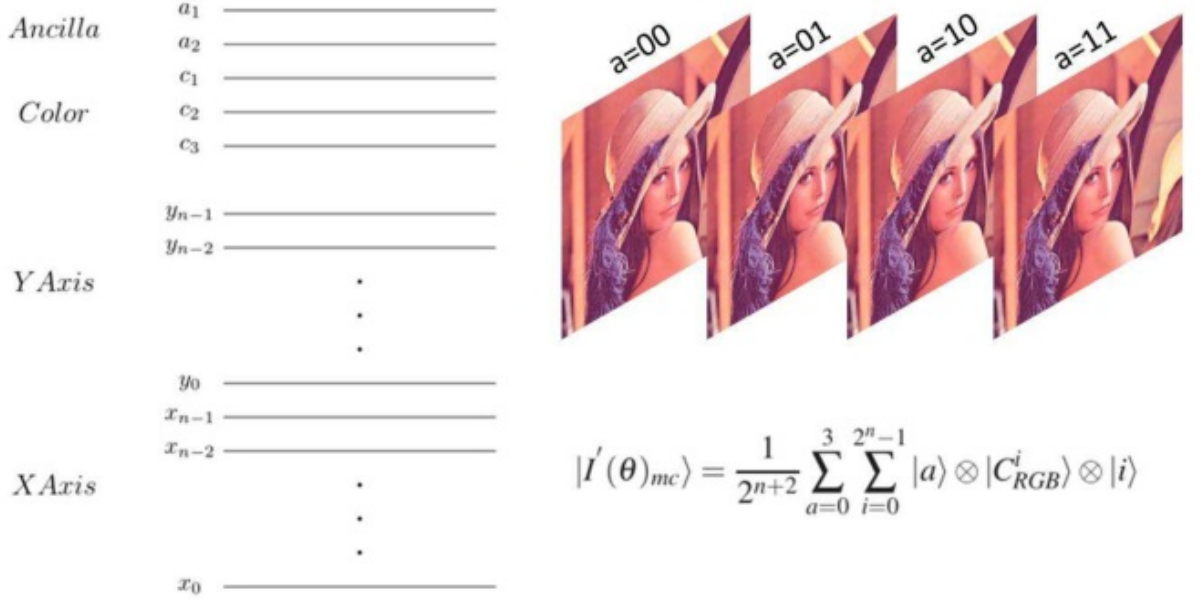
Figure 3.6: *The general quantum circuit to encoding 4 identical images by 2 ancilla qubits..*

Where $|I'(\theta)_{mc}\rangle$ is the quantum state of MCQI images which stores 4 identical images concurrently. Specifically, if the state of anccilla qubits (a_1 and a_2) are $|0\rangle$ and $|0\rangle$ (or $|00\rangle$), it indicates the first image stored in $|I'(\theta)_{mc}\rangle$ state ($|01\rangle$ indicates the second image, and so on). The $|C_{RGB}^i\rangle$ in Figure 3.6. is different from $|C_{RGB\alpha}^i\rangle$ in (3). Because in designing CST, the information of α channel is not requested to be stored in MCQI state, we revise the $|C_{RGB\alpha}^i\rangle$ to obtain $|C_{RGB}^i\rangle$, and it is defined as

$$|C_{RGB}^i\rangle = \cos\theta_R^i|000\rangle + \cos\theta_G^i|001\rangle + \cos\theta_B^i|010\rangle + \cos 0|011\rangle +$$
$$+ \sin\theta_R^i|100\rangle + \sin\theta_G^i|101\rangle + \sin\theta_B^i|110\rangle + \sin 0|111\rangle. \tag{3.10}$$

The differences between $|C_{RGB\alpha}^i\rangle$ and $|C_{RGB}^i\rangle$ are the coefficients of the states of $|011\rangle$ and $|111\rangle$. Specifically, we set the two coefficients be constants 1 ($\cos 0$) and 0 ($\sin 0$) to carry

no information. The detail information of $|I'(\theta)_{mc}\rangle$ can be expressed by

$$|I'(\theta)_{mc}\rangle = \frac{1}{2^{n+2}} \sum_{i=0}^{2^{2n}-1} \{\cos\theta_R^i|00000\rangle + \cos\theta_G^i|00001\rangle + \cos\theta_B^i|00010\rangle + \cos 0|00011\rangle +$$

$$+ \sin\theta_R^i|00100\rangle + \sin\theta_G^i|00101\rangle + \sin\theta_B^i|00110\rangle + \cos 0|00111\rangle +$$

$$+ \cos\theta_R^i|01000\rangle + \cos\theta_G^i|01001\rangle + \cos\theta_B^i|01010\rangle + \cos 0|01011\rangle +$$

$$+ \sin\theta_R^i|01100\rangle + \sin\theta_G^i|01101\rangle + \sin\theta_B^i|01110\rangle + \sin 0|01111\rangle +$$

$$+ \cos\theta_R^i|10000\rangle + \cos\theta_G^i|10001\rangle + \cos\theta_B^i|10010\rangle + \cos 0|10011\rangle +$$

$$+ \sin\theta_R^i|10100\rangle + \sin\theta_G^i|10101\rangle + \sin\theta_B^i|10110\rangle + \sin 0|10111\rangle +$$

$$+ \cos\theta_R^i|11000\rangle + \cos\theta_G^i|11001\rangle + \cos\theta_B^i|11010\rangle + \sin 0|11011\rangle +$$

$$+ \sin\theta_R^i|11100\rangle + \sin\theta_G^i|11101\rangle + \sin\theta_B^i|11110\rangle + \sin 0|11111\rangle\} \otimes |i\rangle.$$

$$(3.11)$$

By applying CS operators, we can rearrange the coefficients of $|I'(\theta)_{mc}\rangle$ to obtained a new quantum state $|I''(\theta)_{mc}\rangle$ which is more convenient for combination of R, G, and B components is defined as

$$|I''(\theta)_{mc}\rangle = \frac{1}{2^{n+2}} \sum_{i=0}^{2^{2n}-1} \{\cos\theta_R^i|00000\rangle + \cos\theta_G^i|00001\rangle + \cos\theta_B^i|00010\rangle + \cos 0|00011\rangle +$$

$$+ \cos\theta_G^i|00100\rangle + \cos\theta_B^i|00101\rangle + \cos\theta_R^i|00110\rangle + \cos 0|00111\rangle +$$

$$+ \cos\theta_B^i|01000\rangle + \cos\theta_R^i|01001\rangle + \cos\theta_G^i|01010\rangle + \cos 0|01011\rangle +$$

$$+ \sin\theta_R^i|01100\rangle + \sin\theta_G^i|01101\rangle + \sin\theta_B^i|01110\rangle + \sin 0|01111\rangle +$$

$$+ \cos\theta_R^i|10000\rangle + \cos\theta_G^i|10001\rangle + \cos\theta_B^i|10010\rangle + \cos 0|10011\rangle +$$

$$+ \sin\theta_G^i|10100\rangle + \sin\theta_B^i|10101\rangle + \sin\theta_R^i|10110\rangle + \sin 0|10111\rangle +$$

$$+ \sin\theta_B^i|11000\rangle + \sin\theta_R^i|11001\rangle + \sin\theta_G^i|11010\rangle + \sin 0|11011\rangle +$$

$$+ \sin\theta_R^i|11100\rangle + \sin\theta_G^i|11101\rangle + \sin\theta_B^i|11110\rangle + \sin 0|11111\rangle\} \otimes |i\rangle.$$

$$(3.12)$$

The rearrangement of coefficients is very important for further constructing of the circuit, and $|I''(\theta)_{mc}\rangle$ is as the input information for the 3×3 steps algorithm.

The angle θ_X^i represents the grayscale value of X channel (or component) of the ith pix-

el of an image. Hence, the task of CST on quantum computer is to build the combination of the coefficients $(\cos \theta_X^i)$ (in MCQI representation, we just consider the cos coefficients, the sin coefficients are considered as redundances) in (14), and then the combination results are requested to stored in the quantum state.

Specifically, we can rewrite the mathematics representation of MCQI image. Let $\overrightarrow{Q}$ be RGB color image with a resolution of $2^n \times 2^n$, and its 3 color components (channels) are $\overrightarrow{R}$, $\overrightarrow{G}$, and $\overrightarrow{B}$ respectively, as

$$\overrightarrow{X} = \frac{1}{2^n} \sum_{i=0}^{2^{2n}-1} \overrightarrow{X_i}, \quad X \in \{R, G, B\}, \tag{3.13}$$

where,

$$\begin{aligned} \overrightarrow{R_i} &= (\cos \theta_R^i |00000\rangle + \sin \theta_R^i |01100\rangle) \otimes |i\rangle, \\ \overrightarrow{G_i} &= (\cos \theta_G^i |00001\rangle + \sin \theta_G^i |01101\rangle) \otimes |i\rangle, \\ \overrightarrow{B_i} &= (\cos \theta_B^i |00010\rangle + \sin \theta_B^i |01110\rangle) \otimes |i\rangle. \end{aligned} \tag{3.14}$$

The grayscale value of the ith pixel of image $\overrightarrow{Q}$ are $Q_R^i = \cos \theta_R^i$, $Q_G^i = \cos \theta_G^i$ (ranging from 0 to 1)(also easy to convert the grayscale value to ranging from 0 to 255), and $Q_B^i = \cos \theta_B^i$, respectively. The destination color space image is $\overrightarrow{D}$ which also contain 3 components (channels), $\overrightarrow{D_1}$, $\overrightarrow{D_2}$, and $\overrightarrow{D_3}$. The greyscale value of the ith pixel of image $\overrightarrow{D}$ is defined as

$$D_m^i = a_{m1} \times Q_R^i + a_{m2} \times Q_G^i + a_{m3} \times Q_B^i, \quad m \in \{1, 2, 3\}. \tag{3.15}$$

To obtain the combination (D_m^i), the 3×3 steps algorithm is proposed. The first 3 steps are shown in Figure 3.7. From the procedure in Figure 3.7, we successfully construct the combination of Q_R^i, Q_G^i, and Q_B^i. Specifically, the first component D_1^i of the destination color space is obtained and stored in the state $|00000\rangle$. Where the value of a, b, c, a_{11},
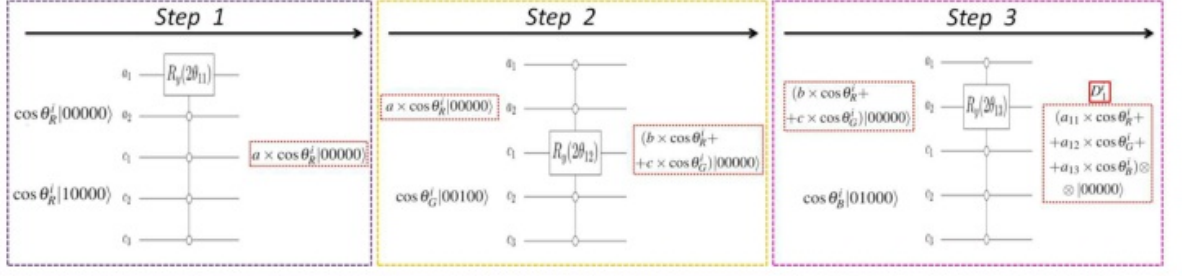
Figure 3.7: *The first three steps of 3×3 algorithm..*

a_{12}, and a_{13} are computed as

$$
\begin{aligned}
a &= \cos\theta_{11} - \sin\theta_{11}, \\
b &= \cos\theta_{12}(\cos\theta_{11} - \sin\theta_{11}), \\
c &= -\sin\theta_{12}, \\
a_{11} &= \cos\theta_{13} \times b, \\
a_{12} &= -\cos\theta_{13}\cos\theta_{13}\sin\theta_{12}, \\
a_{13} &= -\sin\theta_{13}.
\end{aligned}
\tag{3.16}
$$

The circuit in step 1 is utilized for combining the two coefficients of state $|00000\rangle$ and $|10000\rangle$ (The two coefficients are $\cos\theta_R^i$ and $\cos\theta_R^i$ (same)) to obtain the new coefficient of state $|00000\rangle$, namely, $a \times \cos\theta_R^i$; the second step in Figure 3.7 combines the coefficient of $|00000\rangle$ ($a \times \cos\theta_R^i$) and $|00100\rangle$ ($\cos\theta_G^i$) to get the new coefficient $b \times \cos\theta_R^i + c \times \cos\theta_G^i$ of state $|00000\rangle$; similar with the first and the second steps, the third step combines $b \times \cos\theta_R^i + c \times \cos\theta_G^i$ and $\cos\theta_B^i$ to obtain $a_{11} \times \cos\theta_R^i + a_{12} \times \cos\theta_G + a_{13} \times \cos\theta_B$ as the latest coefficient of $|00000\rangle$ which is the ith pixel's grayscale value of the first component (D_1^i) of image $\overrightarrow{D}$. The steps 4–6 and 7–9 are shown in Figure 3.8 to obtain the D_2^i and

D_3^i respectively. Where the value of d–i and a_{21}–a_{33} are computed as

$$d = \cos\theta_{21} - \sin\theta_{21},$$

$$e = \cos\theta_{22}(\cos\theta_{21} - \sin\theta_{21}),$$

$$f = -\sin\theta_{22},$$

$$a_{21} = -\sin\theta_{23}, \tag{3.17}$$

$$a_{22} = \cos\theta_{23} \times e,$$

$$a_{23} = -\cos\theta_{23}\cos\theta_{22}\sin\theta_{22},$$

$$g = \cos\theta_{31} - \sin\theta_{31},$$

$$h = \cos\theta_{32}(\cos\theta_{31} - \sin\theta_{31}),$$

$$l = -\sin\theta_{32},$$

$$a_{31} = -\cos\theta_{33}\cos\theta_{32}\sin\theta_{32}, \tag{3.18}$$

$$a_{32} = -\sin\theta_{33},$$

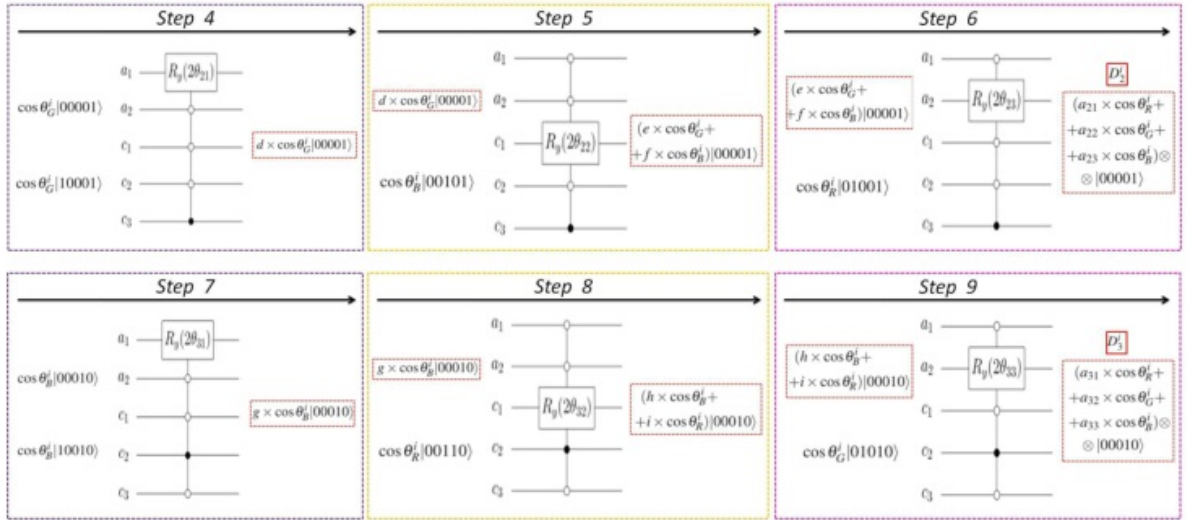$$a_{33} = \cos\theta_{33} \times h.$$

Figure 3.8: *The second and the third three steps of 3×3 algorithm..*

To sum up, through the 3×3 algorithm, 3 linear combinations of RGB components are built, and this 3 combination are the 3 components of the generated color space

transformed from original RGB color space. The whole circuit for this 3×3 algorithm is shown in Figure 3.9. The first part of Figure 3.9 is preparation procedure which
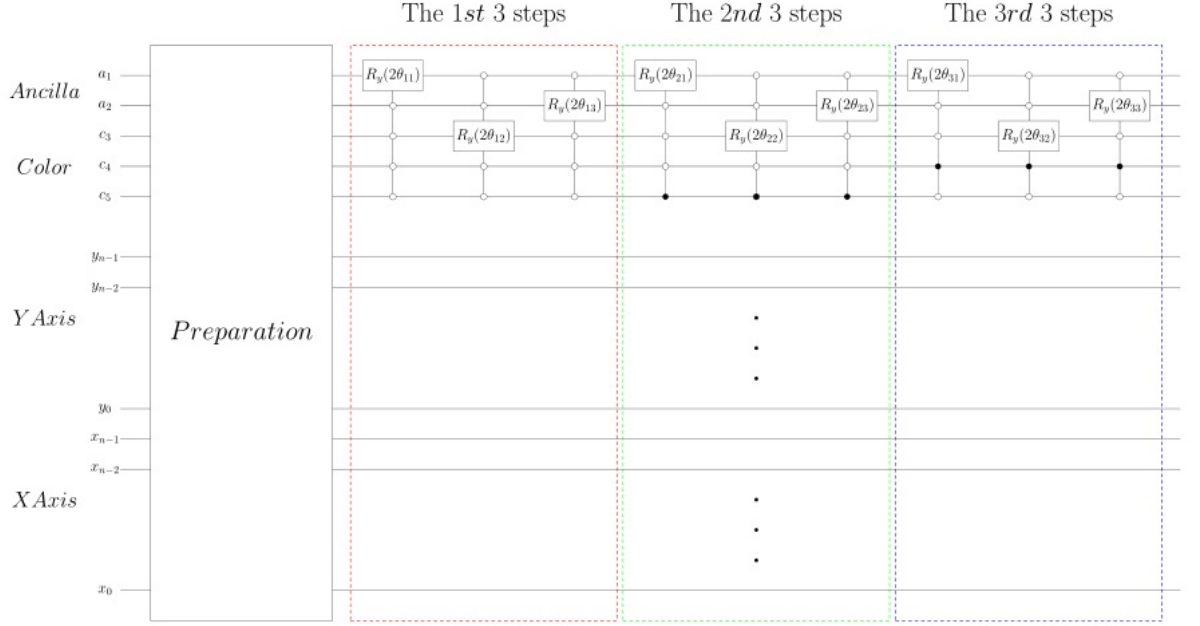
Figure 3.9: *Quantum circuit for color space transformation operation..*

contains two operations: one is converting the initial quantum state $(|0\rangle^{\otimes(2n+5)})$ to the MCQI color quantum image state (the original RGB images) (4 identical images), and the second, third, and forth parts are the quantum circuits of 3×3 algorithm. It is easy to compute that the CST operator can be constructed by 287 quantum basic gates.

3.3.4 The α blending operator

The α blending (αB) is defined as an operator, $\alpha B_{AB} = U_{AB} \otimes I^{\otimes 2n}$, to blend an image (image A) with a background (image B) to create the appearance of partial or full transparency. It is widely used in image matte, image rendering, and watermarking in classical image processing field. In this subsection, the circuit to realize this operation on quantum computer is designed.

Assuming images A and B are two same sized MCQI images with 4 components (R, G, B, and α) (A is the image to be blended, and B is the background image), to encode the 2 images in the MCQI quantum states, 1 ancilla qubit is used accompany with the

MCQI qubits (3 color qubits and 2n position qubits for $2^n \times 2^n$ image), as shown in Figure 3.10. Where C_A^i and C_B^i are the color states of image A and B respectively, which are
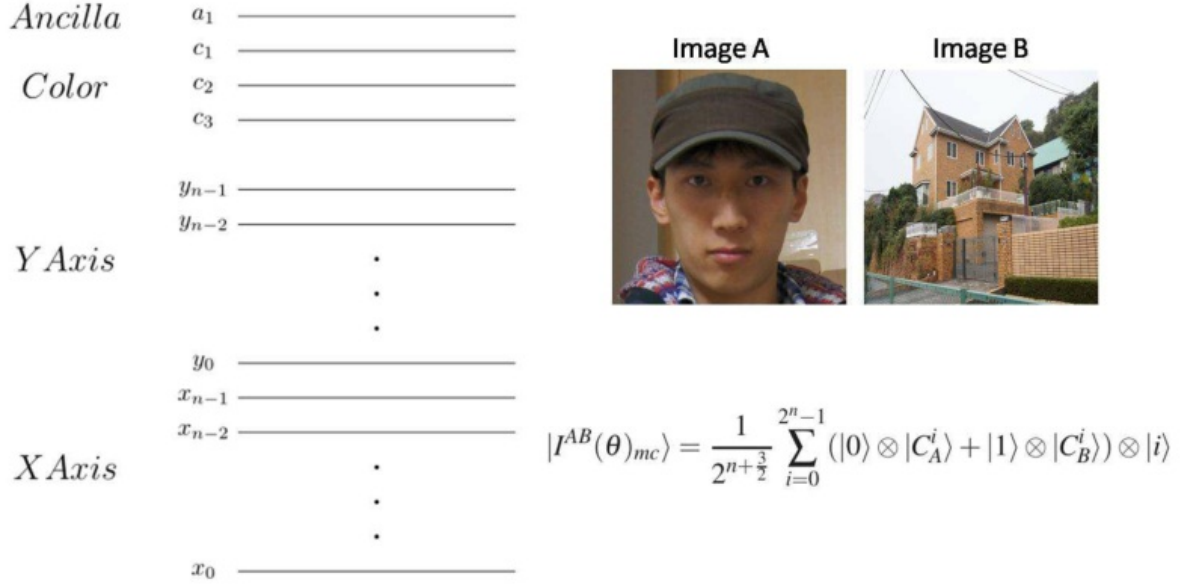
Figure 3.10: *The general quantum circuit to encoding 2 images (A and B) for further αB operation..*

defined as

$$
\begin{aligned}
|C_A^i\rangle =& \cos\theta_{AR}^i|000\rangle + \cos\theta_{AG}^i|001\rangle + \cos\theta_{AB}^i|010\rangle + \cos\theta_{A\alpha}^i|011\rangle + \\
& + \sin\theta_{AR}^i|100\rangle + \sin\theta_{AG}^i|101\rangle + \sin\theta_{AB}^i|110\rangle + \sin\theta_{A\alpha}^i|111\rangle, \\
|C_B^i\rangle =& \cos\theta_{BR}^i|000\rangle + \cos\theta_{BG}^i|001\rangle + \cos\theta_{BB}^i|010\rangle + \cos\theta_{B\alpha}^i|011\rangle + \\
& + \sin\theta_{BR}^i|100\rangle + \sin\theta_{BG}^i|101\rangle + \sin\theta_{BB}^i|110\rangle + \sin\theta_{B\alpha}^i|111\rangle.
\end{aligned}
\tag{3.19}
$$

The θ_{AX} and θ_{BX} ($X \in \{R, G, B, \alpha\}$) are angles encoding the color information of images A and B respectively (Because before blending, the two images are totally opaque, the initial value of $\theta_{A\alpha}$ and $\theta_{B\alpha}$ are 0). Using this circuit, two images are stored concurrently. And then, two C^4-rotation gates gates are applied on a_1 and color (c_1, c_2, c_3) qubits (the control operations are on a_1, c_2, c_3 and the rotation are on c_1 qubits). The computation

procedure is shown as

$$
\begin{aligned}
|I_{\alpha B}\rangle &= \alpha B_{AB}|I^{AB}(\theta)_{mc}\rangle \\
&= \frac{1}{2^{n+\frac{3}{2}}} \sum_{i=0}^{2^n-1} U_{AB}(|0\rangle \otimes |C_A^i\rangle + |1\rangle \otimes |C_B^i\rangle) \otimes I^{\otimes 2n}|i\rangle \\
&= \frac{1}{2^{n+\frac{3}{2}}} \sum_{i=0}^{2^n-1} (|0\rangle \otimes |C_A'^i\rangle + |1\rangle \otimes |C_B'^i\rangle) \otimes |i\rangle,
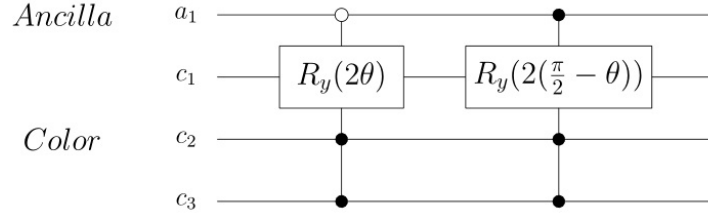\end{aligned}
\tag{3.20}
$$

Figure 3.11: *The general quantum circuit to realize the αB operator..*

By applying this 2 C^4-rotation gates in Fig. 13, the transparency value (transparency parameter) (defined in definition 1) of image A and B are, $T_\alpha^A = \cos^2 \theta$ and $T_\alpha^B = \cos^2(\frac{\pi}{2} - \theta) = \sin^2 \theta$. Hence, this satisfy the definition of α blending, and also, by changing the angles (θ) of the 2 C^4-rotation gates, the transparency values are changed.

3.3.5 The rC_I category operation

The CoI_X and CS_Y are operations in the C_I category, that change the color information of the whole image. In some image processing tasks, however, we want to focuss our interest on part region of an image and apply some operators on these specific positions. Hence the rC_I category operation is proposed in this subsection. The change in a channel of the color space at some points in an image depends on the specific positions in the image. Information about the positions is used as conditions encoded in the matrix Po of the controlled-gate rC_I to construct the processing operations. For instance, let us consider a 2×2 image and the change in color at positions $|0\rangle$, $|2\rangle$. The matrix $Po = |0\rangle\langle 0| + |2\rangle\langle 2|$ and $\bar{Po} = |1\rangle\langle 1| + |3\rangle\langle 3|$ are used to construct the controlled-gate rC_I, given as

$$
rC_I = U \otimes (|0\rangle\langle 0| + |2\rangle\langle 2|) + I \otimes (|1\rangle\langle 1| + |3\rangle\langle 3|).
\tag{3.21}
$$

The action of this particular rC_I on a general 2×2 image in MCQI form, $|I(\theta)_{mc}\rangle = \frac{1}{4}\sum_{i=0}^{3}|C_{RGB}^{i}\rangle \otimes |i\rangle$, is given by

$$rC_I|I(\theta)_{mc}\rangle = \frac{1}{4}[(U \times |C_{RGB}^{0}\rangle) \otimes |0\rangle + (U \times |C_{RGB}^{2}\rangle) \otimes |2\rangle + \\ + |C_{RGB}^{1}\rangle) \otimes |1\rangle + |C_{RGB}^{3}\rangle) \otimes |3\rangle]. \tag{3.22}$$

The calculation shows that the action of operation U for changing color has affects only on the specific positions $|0\rangle$, $|2\rangle$. U is an 1 qubit, 2 qubits, or 3 qubits operation.

3.4 Experiments on revised MCQI images

The experiments are carried out on laptop computer with Intel Core (TM) i5 Duo 2.40 GHz CPU and 4 GB RAM. The simulations are linear algebra based with complex vectors as quantum states and unitary matrices as unitary transforms using QLIB [34] (A Matlab package for quantum information). To demonstrate the feasibility of the proposed 4 MCQI based operators, 4 experiments are conducted:

- experiment on channel of interest operation,

- experiment on channel swapping operation,

- experiment on color space transformation,

- experiment on α blending operation,

- experiments on rC_I category operation.

3.4.1 Experiments on channel of interest operation

The storage and retrieval of quantum images in MCQI representation is presented in chapter 2. The experiments involved simulating the quantum images on a classical computer. These simulations use linear algebra in which the complex vectors are the quantum image states and the unitary matrices are the image processing operations. The

final step in these simulations is measurement which converts the quantum information into the classical information in form of probability distributions. Extracting and analyzing the distributions gives the information for retrieving the transformed images. Using matrix operations, however, is not practical since the size of unitary matrices increases exponentially with the number of qubits. In addition, the main information for simulation is about the images only and not about the operations. In order to increase the size of images in the program memory we focus on the main information of the MCQI representation; color and positions. Therefore, for every point in the simulation of MCQI quantum images there are two arrays, named COLOR (containing four channels) for colors $|c_k^X\rangle$ ($X \in \{R, G, B, \alpha\}$) and POS for positions $|k\rangle$. The performance of the color transformations is on the COLOR array only and the new quantum image after the transformations is obtained by combining the POS array with its corresponding COLOR array. The simulation-based experiments are carried out on laptop computer with Intel Core (TM) i5 Duo 2.40 GHz CPU and 4 GB RAM. The simulations are based on linear algebra with complex vectors as quantum states and unitary matrices as unitary transforms using QLIB package.

In this section, the experiment on the first MCQI based operator (CoI) is conducted using a human facial image shown in Figure 3.12.

Channel of interest operator aims to change the color information on only one channel (component) (R, G, B, or α). To realized this operation, the Toffoli gate is applied on the first color qubit (here Toffoli gate is considered as a special case of $C^2 R_y(2\theta)$ gate), and the controlled operations are on the second and third color qubits. The result images and quantum circuits are shown in Figure 3.13 and Figure 3.14.

3.4.2 Experiment on channel swapping operation

Channel swapping operation, CS_Y, is the operator which swaps the grayscale values between R and G, R and B, or G and B channels. The result images obtained from Fig. 14 by applying CS_Y are shown in Figure 3.15, and the realization circuit is shown in Figure 3.16.
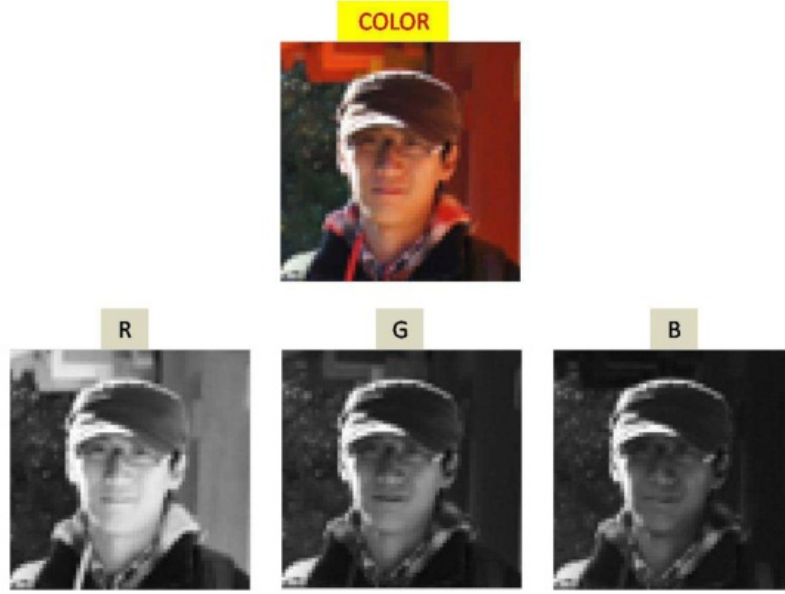
Figure 3.12: *The image used in experiment of channel of interest operator..*

3.4.3   Experiment on color space transformation

The color human facial image with 128×128 pixels is used for color space transform operation from RGB color space to YIQ color space. The original color image and its RGB components image are shown in Figure 3.17. The circuit to realize this transform is shown in Figure 3.18. The angle value of the 3×3 C^4-rotation gates can be computed as

$$\cos\theta_{13} \times \cos\theta_{12}(\cos\theta_{11} - \sin\theta_{11}) = a_{11} = 0.299,$$

$$-\cos\theta_{13}\cos\theta_{12}\sin\theta_{12} = a_{12} = -0.595716,$$

$$-\sin\theta_{13} = a_{13} = 0.211456;$$

$$-\sin\theta_{23} = a_{12} = 0.587;$$

$$\cos\theta_{23} \times \cos\theta_{22}(\cos\theta_{21} - \sin\theta_{21}) = a_{22} = -0.274453,$$

$$-\cos\theta_{23}\cos\theta_{22}\sin\theta_{22} = a_{23} = -0.522591,$$

$$-\cos\theta_{33}\cos\theta_{32}\sin\theta_{32} = a_{31} = 0.114,$$

$$-\sin\theta_{33} = a_{32} = -0.31263,$$

$$\cos\theta_{33} \times \cos\theta_{32}(\cos\theta_{31} - \sin\theta_{31}) = a_{33} = 0.311134.$$
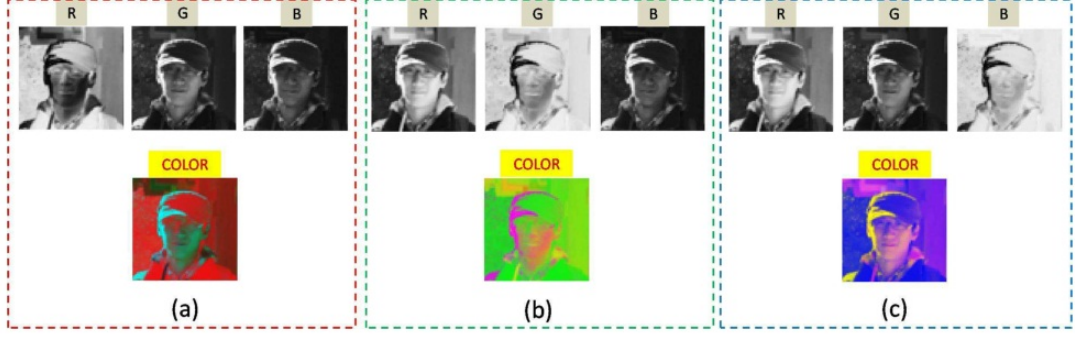
$$(3.23)$$

Figure 3.13: *The result images obtained from Figure 3.12 by applying C^2-NOT (Toffoli) gates on color qubits ((a)the result image by invert the R component of Figure 3.12, (b)the result image by invert the G component of Fig. 13, (c)the result image by invert the B component of Figure 3.12).*

3.4.4 Experiment on α blending operation

One 256×256 human facial image and a same sized Japanese style house image are used in this experiment as an original (image A) and background (image B) image respectively, as shown in Fig. 3.9.

3.4.5 Experiment on rC_I operation

In this subsection the experiments on the operators which change the color information on the part region of an image (the rC_I operation) are conducted by applying some control operations on color qubits from position qubits. The first experiment on rC_I category applies the CoI_X operator on the upper half of R component of Fig.3.12, and CS_Y operator on the lower half of Fig.3.12. Specifically, the CoI_R operator using $C^2R_y(\frac{2}{3}\pi)$ gate is applied on the upper half of the original image, and the CS_{RG} operator is conducted on the lower half. The result images and the realization circuit are shown in Fig.3.20.

Through the experiment, the specific positions can be decided by applying additional control operations on C_I operations. In the next experiment, more small regions (not only upper half or lower half shown in the first experiment in this subsection) are considered. The same image (Fig.3.12) with the sub-blocks labeled is used as original image, and we limit the size of each sub-block to 32×32, shown in Fig.3.21.

The operators of CoI_R, CoI_G, and CoI_B are applied on sub-blocks A, D, and E with
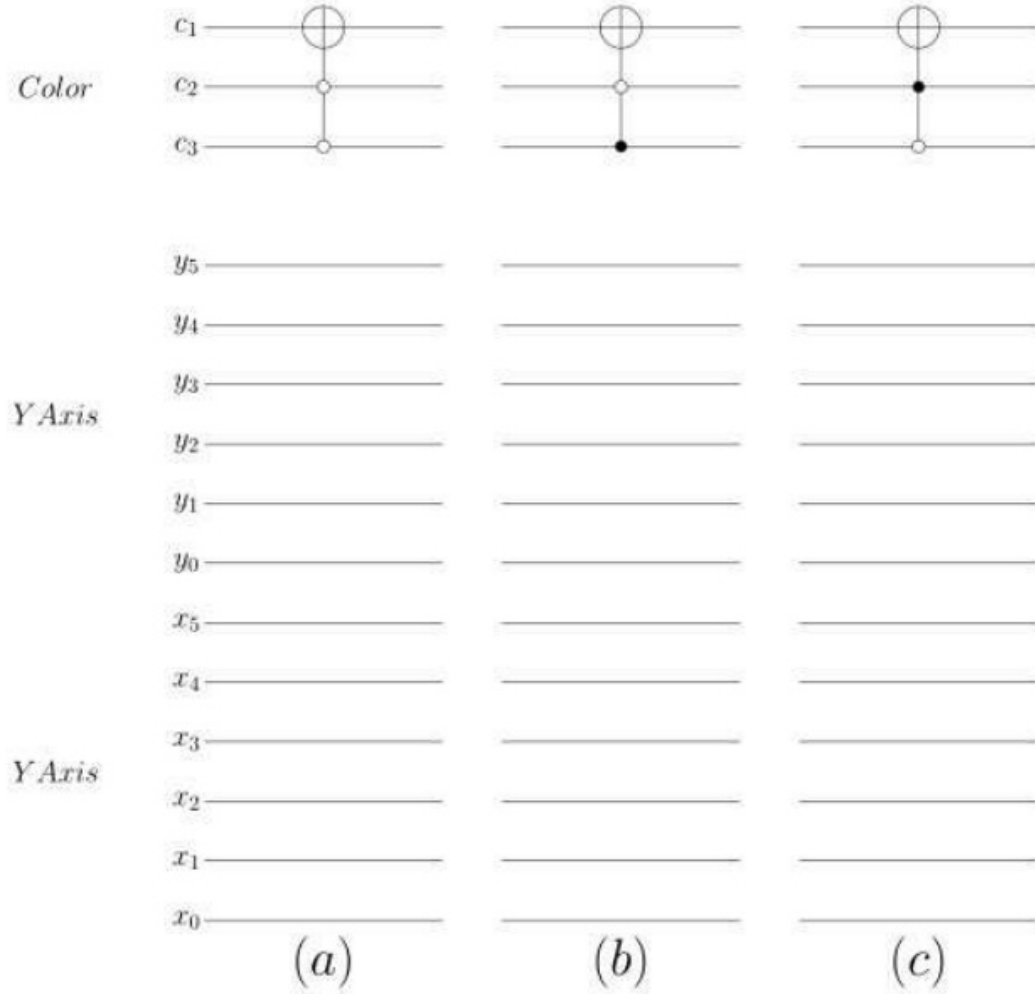
Figure 3.14: *Circuits to realize the operations of Figure 3.13 ((a) circuit of the color invert operation on R component only, (b) circuit of the color invert operation on G component only, (c) circuit of the color invert operation on B component only)..*

the shifting angle $\theta = \pi/4$ of $C^2 R_y(2\theta)$ gates. The operations of CS_{RG}, and CS_{RB} are conducted on sub-blocks B, and C respectively. The *NOT* operation is applied on sub-block F. The result image by this operation is shown in Fig.3.22, and the quantum circuit to realize this operation is shown in Fig.3.23.

3.5 Summary of Color Information Transformations on Multi-Channel Quantum Images

Color information transformations on quantum images including Channel of Interest, Channel Swapping, Color Space Transformation, and α Blending with low complexity
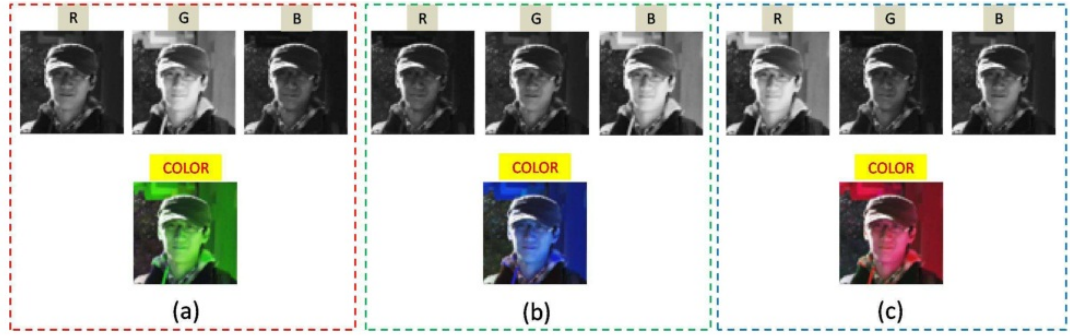
Figure 3.15: *Circuits to realize the operations of Figure 3.13.*

are proposed using basic gates like NOT, CNOT, rotation, controlled rotation and Toffoli gates. This low complexity agrees with results for similar transformations which are also fast on classical images. The proposed operations can be divided into local and global operations according to their effect on the quantum images.

Five experiments are conducted on the four color information transformations. Firstly, the simulation result shows that to construct channel of interest operator, one $C^2 R_y(2\theta)$ gate is requested (the rotation operation is applied on c_1 qubit and the 2 controlled are from c_2 and c_3 qubits), and specifically, the number of basic gate to build CoI_R, CoI_G, CoI_B, and CoI_α operators are 7, 7, 9, 5. Secondly, from the simulation, the channel swapping operation is obtained by only 3 basic quantum gates. Thirdly, the most complex operator in this paper, the color space transformation is simulated on MATLAB by constructing 9 $C^4 R_y(2\theta)$ gates (287 basic gates). Finally, the α blending operator can be considered as CoI_α, and the simulation also proves that only 5 basic gates are enough to realize this operation. These results prove that all the 4 operators are image size independent (the number of basic gate is constant), namely, $O(1)$, for an N-sized image.

In the next chapter of the thesis, the results in this chapter will be extended towards the following application. In chapter 4, using channel information transformations in other applications of quantum image processing appears very promising, for example applications in quantum image watermarking, quantum image cryptography can be done by hiding secret information in the design of quantum circuits. Combining with the quantum
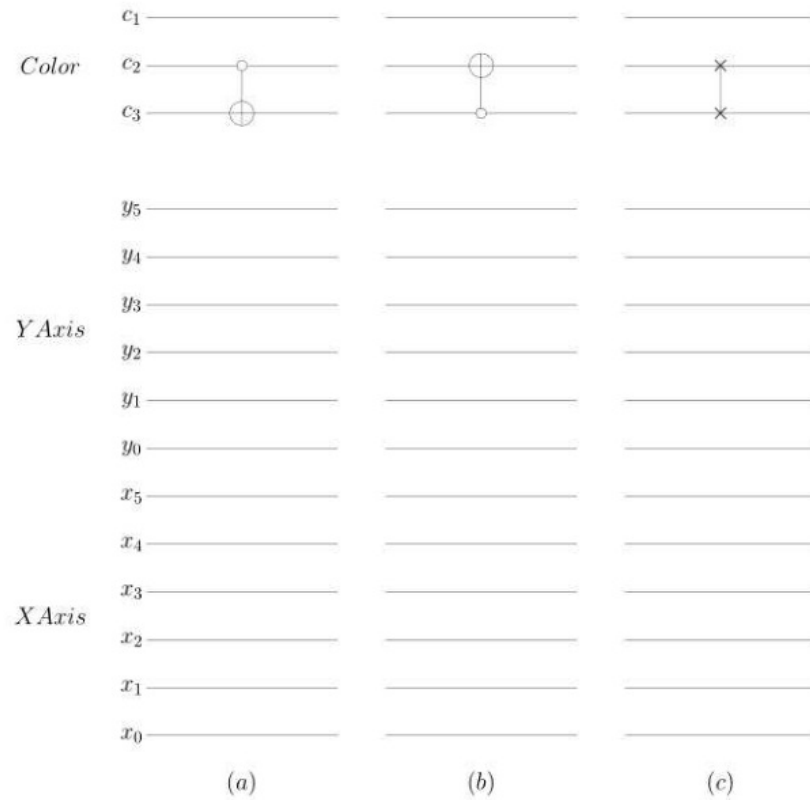
Figure 3.16: *The result images obtained from Figure 3.12 by applying CS_Y operation on color qubits ((a) the result image by applying CS_{RG} operation on Figure 3.12, (b) the result image by applying CS_{RB} operation on Figure 3.12, (c) the result image by applying CS_{GB} operation on Figure 3.12)..*

measurement operation presented in chapter 4, the channel information operations can be used as major components to build full quantum image processing applications.
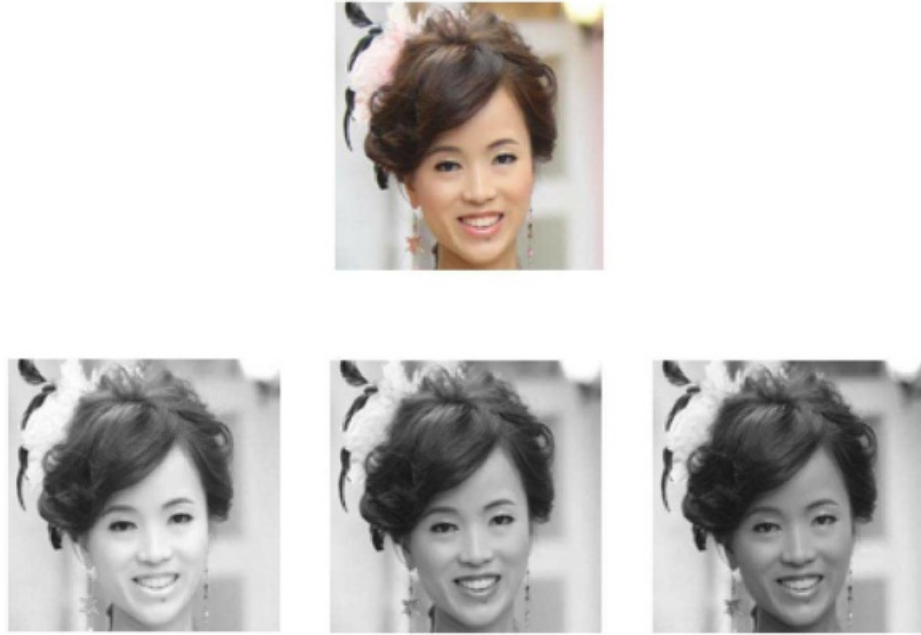
Figure 3.17: *The original color human facial image and its RGB components..*

Figure 3.18: *The obtained YIQ image..*
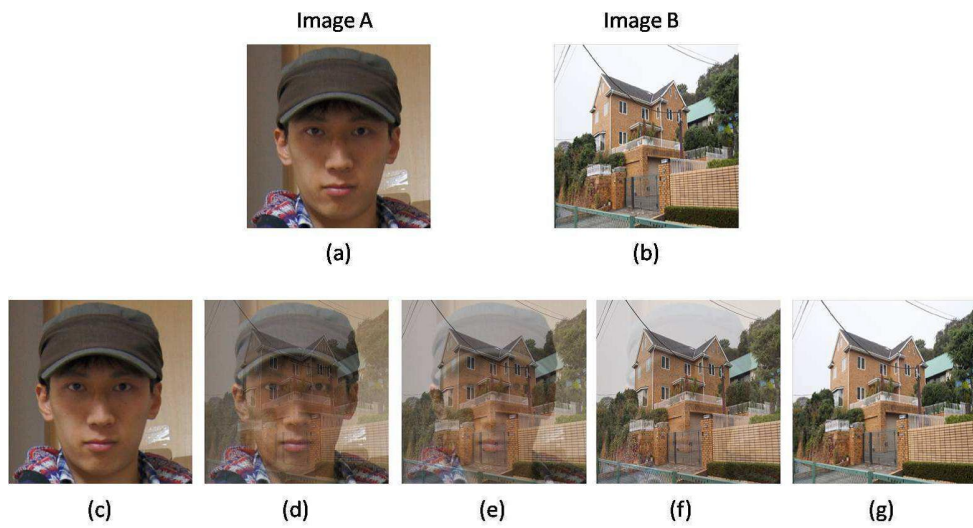
Figure 3.19: *The obtained YIQ image..*
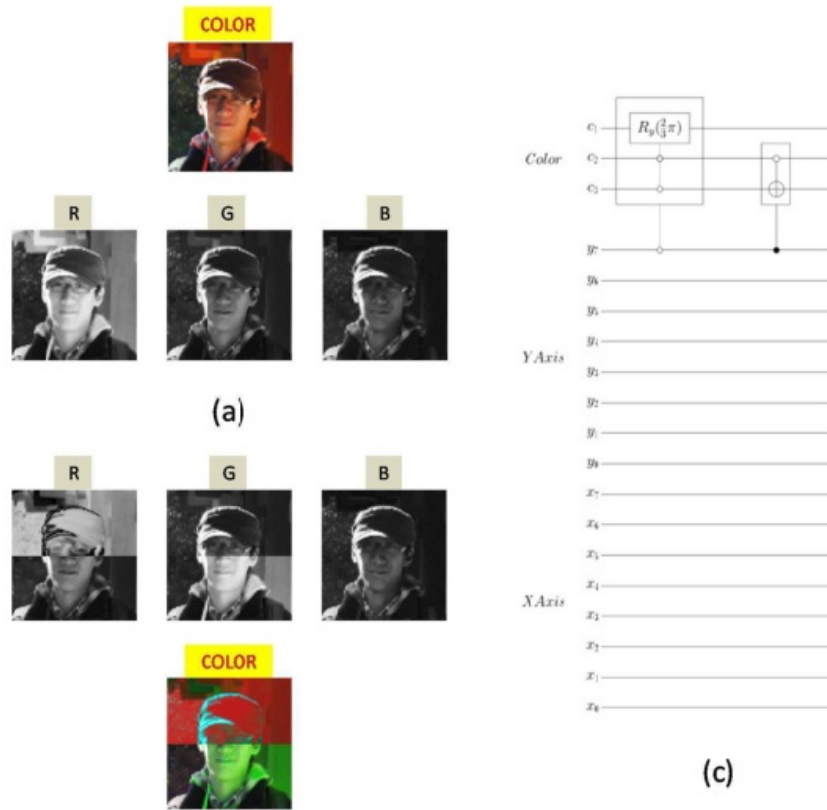
Figure 3.20: *The original 256×256 version images, the result images by applying CoI_R operator and CS_{RG} operator on the upper half and lower half of the original image, and the realization circuit..*
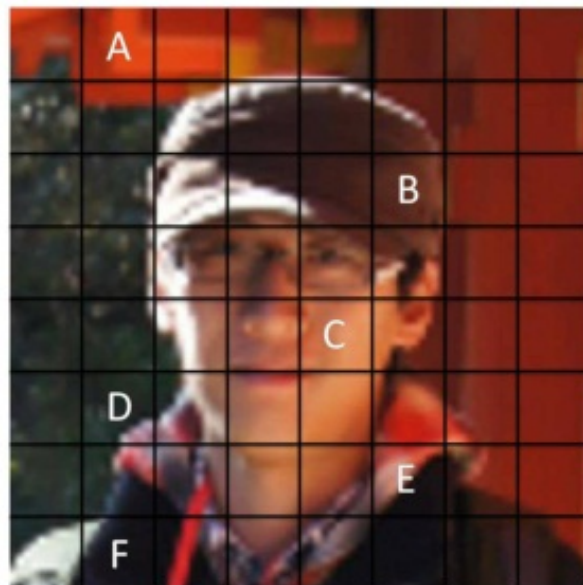
Figure 3.21: *The original image with labeled sub-blocks..*
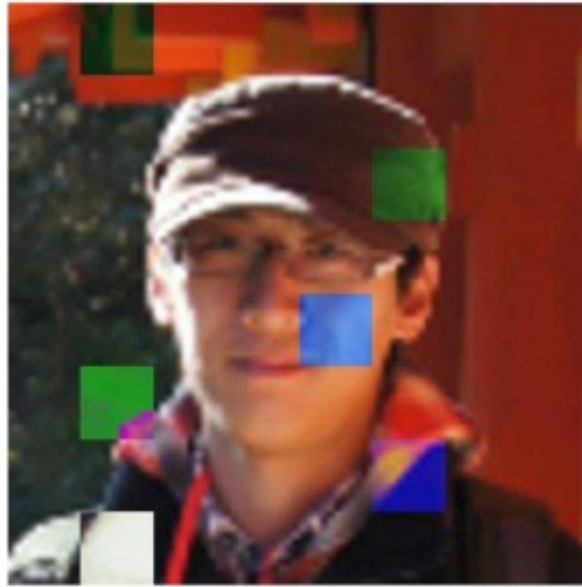
Figure 3.22: *The result image after applying CoI_X, CS_Y, and NOT operations on the sub-blocks..*
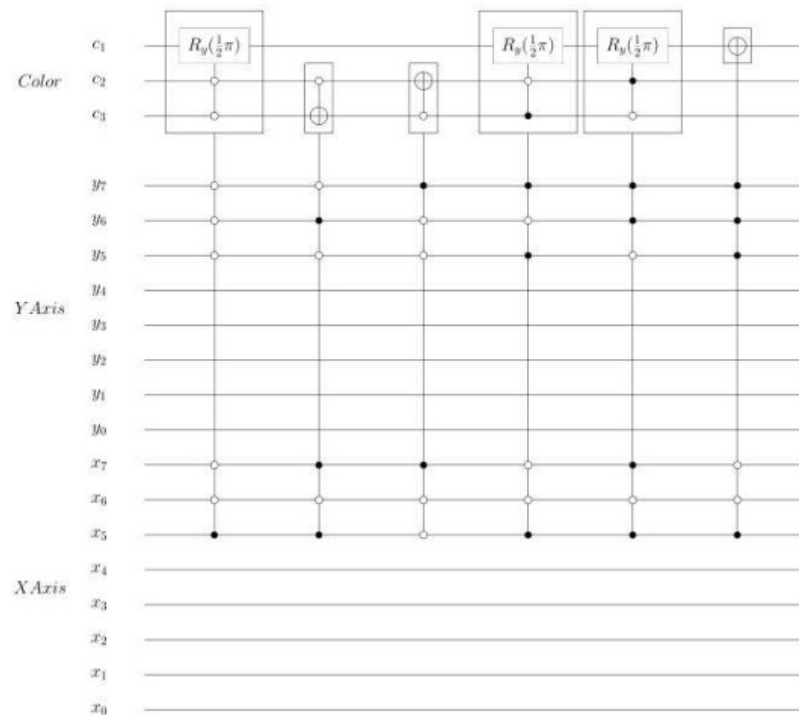
Figure 3.23: *The quantum circuit to realize the operation of Fig3.22..*

Chapter 4

Quantum measurement based double-key double-domain watermarking strategy for multi-channel quantum images

4.1 Introduction

As with classical data on classical computers, quantum data such as images will be susceptible to all kinds of abuse. Watermarking of digital image has found enormous success as a method for discouraging illicit copyright and description of material on classical computers [19] [13] [25] [39] [32]. In order to guard against their abuse extending similar techniques to quantum data appears imperative. Quantum cryptography: involving mostly the exchange of information between the famous Alice and Bob security protocol notations over a quantum channel, is considered as one of the most advanced areas of quantum computation. As a result, researchers began to investigate strategies for quantum watermarking to protect the copyright of the quantum images, which embeds the specific quantum symbolic information (such as the logo representing the image's owner) into quantum images. The watermarking and authentication of quantum images (WaQI) [20] is proposed, which is secure, keyless, and blind. Another quantum image watermarking strategy using quantum Fourier transform (QFTW) is investigate in [54], which embeds the logo information into quantum Fourier transform (QFT) coefficients.

Quantum image processing, which utilizes the characteristic of quantum parallelism [11] to speed up many processing tasks, is a subfield of quantum information processing. Because the first step in quantum image processing field involves proposals on representations to capture and store the image on quantum computers, various representations for images on quantum computer are proposed, such as qubit lattice [51], grid qubit [50], flexible representation of quantum image (FRQI) [27], and multi-channel quantum image (MCQI) [48]. Many image processing strategies exploiting these representations are also developed to process transformations that target the geometric information, GTQI [28], the color information, CTQI [29], and the multi-channel information, Channel of Interest (CoI) and Channel Swapping (CS) [48]. Because of the appearing of these representation methods, researchers begin to investigate strategies for quantum watermarking to protect the copyright of the quantum images, which embeds the specific quantum symbolic information (such as the logo representing the image's owner) into quantum images. Quantum cryptography, which involves mostly the exchange of information between the famous Alice and Bob security protocol notations over a quantum channel, is considered one of the most advanced areas of quantum computation. Watermarking of quantum images is expected to cover at least one or more of the three objectives listed in the sequel.

- Data hiding, for embedding information to make the images useful or easier to use;

- Integrity control, to verify that the image has not been modified without authorization;

- Authentication, that is to verify the true ownership of an image available in the public domain.

Before the proposal of FRQI, there is few standard for implementing watermarking on quantum image and often there may be the need for some trade-offs especially in terms of which of the objectives enumerated above should be accorded top priority. However, none of the available literature deal with all of these objectives. This stems from the fact that none of them is based on a quantum representation that encodes and stores the content of the image and watermark signal, nor for their subsequent transformation.

The watermarking and authentication of quantum images (WaQI) [20] is proposed, which is secure, keyless, and blind. Another quantum image watermarking strategy using quantum Fourier transform (QFTW) is investigate in [54], which embeds the logo information into quantum Fourier transform (QFT) coefficients.

The WaQI strategy can be used to authenticate the identity of the owner, and is computationally efficient. In this method, however, only if we know the content of watermark image, can we design the quantum circuit to authenticate the identity of the owner of the carrier images (only if we know who the owner of the carrier images is, can we extract the watermark image, and hence, authenticate the owner's identity). Hence, the WaQI can only be used to find out who the illegal user is, but can not find where the images come from. The QFTW strategy is developed to solve this insufficiency of WaQI. With a specified key, the watermark image (the logo) can be retrieved. The existence of the key makes the QFTW strategy more secure that even the illegal user can extract the watermarked information (the logo information) from the watermarked image (embedded carrier image), he/she can not understand what it means. But in this strategy, the key is fixed, and it means that if the illegal user can get the key, he/she will realize the existence of the watermarking and will obtain the information of copyright about the carrier image. And also, both the WaQI and the QFTW are the strategies that deal with greyscale quantum images only. Multi-channel (multi-component) color images, however, are often used in various color spaces, including the standard RGB color model which contains R, G, and B channels (components). Hence, a new watermarking strategy for color (multi-channel) quantum images, which can embed the color quantum information (color watermark image or color logo image) into color quantum carrier images (color images to be embedded), should be developed. And this new watermarking strategy should realize a key generation procedure (KGP) that the key can be updated in this procedure (unfixed key), which is much more secure than the fixed key method (in the fixed method, if the illegal user can obtain the key, he/she will extract copyright information, and hence, the designing of attack algorithm may become much easier).

Based on MCQI presented in chapter 2, 4 color information transformations are pro-

posed in chapter 3, and combining with the quantum measurement operation, which provide the basis to design the color quantum image watermarking strategies, a quantum measurement based double-key, double-domain multi-channel watermarking strategy for quantum images (MC-WaQI) is proposed. The proposal is adopted for the input images, watermark signals, and as the main resources to realize the watermarked images and their subsequent authentication. In this chapter, we shall assume that these MCQI input images (and watermark signals) are fault-tolerant and the congenital error inherent to the resources used to manipulate them are less than the accuracy threshold as alluded to earlier. Hence, a quantum computer with in-built error correction is assumed. The preparation of the MCQI quantum image state has been discussed thoroughly in previous chapter.

In this chapter, a quantum measurement based double-key, double-domain multi-channel watermarking strategy for quantum images (MC-WaQI) is proposed, which can be used to find the real owner. Specifically, this strategy includes three parts (three procedures):

- Preprocessing part: in MC-WaQI strategy, the copyright information is requested to be embedded into both frequency domain and spatial domain of the carrier image, hence, two logo information are requested to be generated from the original watermark image (the logo). To transform the two meaningful logo images into meaningless images, which is used to strengthen the power to resist invalid attack, two keys are generated to scrabble both the position and the color information;

- Embedding part: after preprocessing procedure, the watermark images (logo images) have been transformed into two meaningless images (noise-like), and then the two noise-like images are embedded into both the spatial (color channels) and frequency domain (the QFT coefficients of the carrier image);

- Extracting part: using the two keys generated in preprocessing part, only the embedder (owner) can extract the two watermark images (the logo images) correctly, which ensures the security.

In the first part (preprocessing part), two keys are used that one key is fixed (assign by the owner) like in [54] used to scramble the pixels' position information of the watermark image (position information key or PIK), and the other one used to protect the color information of the watermark image (color information key or CIK) is generated by the quantum measurement based key generation procedure.

The second part as the main part in the MC-WaQI strategy is the embedding part, which embeds the watermark image into spatial domain by using the alpha blending operation, and into frequency domain by making subtle change to the QFT coefficients of the carrier image. Same with other watermarking strategy, the extracting part should be only available to the owner in the MC-WaQI. And in this strategy, the owner uses PIK and CIK to recover the position information and the color information of the two watermark images. And the main contribution of this paper are four-fold:

- The utilization of MCQI representation makes MC-WaQI strategy possible to deal with color quantum images;

- The double-key (PIK and CIK) scheme produces the double protection on the watermark image, and the CIK is unfixed updated by the result image obtained through applying quantum measurement on the watermark image;

- The watermark image is embedded into both spatial domain and frequency domain, and hence, the copyright information can be extracted even under the condition of attack by the illegal user;

- The alpha blending operation is used to embed the watermark image into spatial domain of the carrier, which makes the complexity of the embedding procedure much lower.

The multi-channel information operations with their low complexity provide the foundation on which WaQI is built. The main components of these transformations consist of the inverter NOT (N), the controlled-NOT or just CNOT (C), and the Tofolli (T)gates, considered as the universal quantum gates.

4.2 Multi-channel images and their transformations

4.2.1 Resources for watermarking on quantum computation

A quantum computer is a physical machine that can accept input states, which represent a coherent superposition of many different inputs and subsequently evolve them into a corresponding superposition of outputs. Computation, i.e. a sequence of unitary transformations, affects simultaneously each element of the superposition, generating a massive parallel data processing albeit within one piece of hardware [11]. The smallest unit to facilitate such computation, the qubit, has logical properties that are inherently different from its classical counterpart, the bit. While bits and their manipulation can be described using two constants (0 and 1 or true and false) and the tools of Boolean algebra, qubits, on the other hand must be discussed in terms of vectors, matrices, and other tools of linear algebra. The state of a quantum system is described as a vector say $|u\rangle$ in a complex Hilbert space, which is called a ket in the Dirac or quantum mechanical notation. Its adjoint, $\langle u|$, is called the bra. Quantum state preparation is the first of five criteria for realising any physical quantum system. The result is a scalable physical state with well-characterized qubits. In addition, this state can be initialized in a way that isolates it from the environment. Often, a quantum state can be obtained (prepared) from its classical equivalent. A quantum state can only be manipulated using a universal set of quantum gates. In such gates, time flows from left to right with horizontal lines, called quantum wires representing separate qubits that comprise the quantum register [21]. In modeling a quantum circuit, complex transformations are broken into simpler gates (i.e. single qubit gates such as the NOT, Hadamard, or Pauli gates and controlled two-qubit gates like the controlled NOT gates) Recently, the following set of gates have found wide acceptance in the literature as the elementary or basic quantum gates arising from the universality of the set and the ease with which very complex circuits can decomposed in terms of them.

- NOT gate (N). This is a single qubit gate which inverts the content of the qubit it operates upon.

- Controlled-NOT or CNOT gate (C). It is a two qubit gate and the content of the target qubit is inverted if and only if the control qubit is 1.

- Toffoli gate (T). This is a controlled-CNOT gate, thus, making it a three qubit gate comprising two controls and a single target qubit. The target qubit is inverted if and only if both control qubits are 1s.

Together these gates are referred to as the NCT library. [4]

Finally, qubit-specific measurements are employed in order to obtain the classical readout of the new manipulated state, leading to a collapse (loss) of the hitherto quantum state. And also used as a key generator.

4.2.2 Back ground on RGB multi-channel representation for quantum images and channel information operations

To process color images on quantum computers, a new representation encoding the information of R, G, B channels should be established, and these multi-channel information are requested to be stored in quantum states simultaneously. Based on the pixel representation for images on classical computers, the multi-channel representation for quantum image (MCQI) is proposed to capture RGB channels information. This is accomplished by assigning three qubits to encode color information of images. The mathematical expression is presented as

$$|I(\theta)_{mc}\rangle = \frac{1}{2^{n+1}} \sum_{i=0}^{2^{2n}-1} |C_{RGB}^i\rangle \otimes |i\rangle. \tag{4.1}$$

The color information $|C_{RGB}^i\rangle$ encoding the R, G, B, channels information is defined as

$$\begin{aligned} |C_{RGB}^i\rangle = &\cos\theta_R^i|000\rangle + \cos\theta_G^i|001\rangle + \cos\theta_B^i|010\rangle + \\ &+ \sin\theta_R^i|100\rangle + \sin\theta_G^i|101\rangle + \sin\theta_B^i|110\rangle + \\ &+ \cos 0|011\rangle + \sin 0|111\rangle, \end{aligned} \tag{4.2}$$

where $|000\rangle$, $|001\rangle$, ..., $|111\rangle$ are 8-D computational basis; $\{\theta_R^i, \theta_G^i, \theta_B^i\} \in [0, \pi/2]$ are three angles encoding the colors of the R, G, B, channels of the *ith* pixel, respectively; $\otimes$ is the tensor product notation; $|i\rangle$ for $i = 0, 1, \ldots, 2^{2n} - 1$ are 2^{2n}-D computational basis states. Specifically, there are two parts in the MCQI quantum image: $|C_{RGB}^i\rangle$ and $|i\rangle$, which encode information about colors and their corresponding positions in the image, respectively. In Eq.(2), the coefficients of $|011\rangle$ and $|111\rangle$ are $\cos 0$ and $\sin 0$. In RGB color images, there are only three channels' information requested to be encoded (6 coefficients are enough), hence, we set the two coefficients be constant ($\cos 0$ and $\sin 0$) to carry no information (these two coefficients are discussed in [48]).

The Channel of Interest (CoI) operator (shifting the grayscale value of the interested color channel(R, G, B or α channel)), CoI_X ($X \in \{R, G, B, \alpha\}$, CoI_R, CoI_G, CoI_B, and CoI_α are operators applied on R, G, B, and α channels respectively) is defined as an operator, $CoI_X = U_X \otimes I^{\otimes 2n}$, by using $U_X = C^2 R_y(2\theta)$ gate, where θ is the shifting parameter (or shifting angle). As defined in (3.4), by changing the angles of the coefficients of the quantum states (from $|000\rangle$ to $|111\rangle$), the grayscale value of pixels are changed. The calculation produces the result $|I(\theta)_{mc}^X\rangle$ of the application of CoI_X on $|I(\theta)_{mc}\rangle$, given as

$$|I(\theta)_{mc}^X\rangle = CoI_X(|I(\theta)_{mc}\rangle),$$

$$= (U_X \otimes I^{\otimes 2n}) \left(\frac{1}{2^{n+1}} \sum_{i=0}^{2^{2n}-1} |C_{RGB\alpha}^i\rangle \otimes |i\rangle \right), \tag{4.3}$$

$$= \frac{1}{2^{n+1}} \sum_{i=0}^{2^{2n}-1} |C_{RGB}^{Xi}\rangle \otimes |i\rangle,$$

where $|C_{RGB\alpha}^i\rangle$ state carries the RGB color information defined in Eq.(4.3); $|C_{RGB\alpha}^{Xi}\rangle$ is

the new color state after applying CoI_X operator, shown as

$$
\begin{aligned}
|C_{RGB\alpha}^{Ri}\rangle = {} & \cos(\theta_R^i - \theta)|000\rangle + \cos\theta_G^i|001\rangle + \cos\theta_B^i|010\rangle + \cos\theta_\alpha^i|011\rangle + \\
& + \sin(\theta_R^i - \theta)|100\rangle + \sin\theta_G^i|101\rangle + \sin\theta_B^i|110\rangle + \sin\theta_\alpha^i|111\rangle, \\
|C_{RGB\alpha}^{Gi}\rangle = {} & \cos\theta_R^i|000\rangle + \cos(\theta_G^i - \theta)|001\rangle + \cos\theta_B^i|010\rangle + \cos\theta_\alpha^i|011\rangle + \\
& + \sin\theta_R^i|100\rangle + \sin(\theta_G^i - \theta)|101\rangle + \sin\theta_B^i|110\rangle + \sin\theta_\alpha^i|111\rangle, \\
|C_{RGB\alpha}^{Bi}\rangle = {} & \cos\theta_R^i|000\rangle + \cos\theta_G^i|001\rangle + \cos(\theta_B^i - \theta)|010\rangle + \cos\theta_\alpha^i|011\rangle + \\
& + \sin\theta_R^i|100\rangle + \sin\theta_G^i|101\rangle + \sin(\theta_B^i - \theta)|110\rangle + \sin\theta_\alpha^i|111\rangle, \\
|C_{RGB\alpha}^{\alpha i}\rangle = {} & \cos\theta_R^i|000\rangle + \cos\theta_G^i|001\rangle + \cos\theta_B^i|010\rangle + \cos(\theta_\alpha^i - \theta)|011\rangle + \\
& + \sin\theta_R^i|100\rangle + \sin\theta_G^i|101\rangle + \sin\theta_B^i|110\rangle + \sin(\theta_\alpha^i - \theta)|111\rangle.
\end{aligned}
\tag{4.4}
$$

The Channel Swapping (CS) operator, CS_Y ($Y \in \{RG, RB, GB\}$, CS_{RG}, CS_{RB}, and CS_{GB} are operators that swap the grayscale values between R and G, R and B, and G and B channels, respectively) (no operation on α channel), $CS_Y = I \otimes U_Y \otimes I^{\otimes 2n}$, by using CNOT gate or SWAP gate (CNOT and SWAP gates are two qubits gates) on c_2 and c_3 color qubits (there is no operation on c_1 color qubit). The calculation produces the result $|I(\theta)_{mc}^Y\rangle$ of the application of CS_Y on $I(\theta)_{mc}$, given as

$$
\begin{aligned}
|I(\theta)_{mc}^Y\rangle &= CS_Y(|I(\theta)_{mc}\rangle), \\
&= (I \otimes U_Y \otimes I^{\otimes 2n}) \left(\frac{1}{2^{n+1}} \sum_{i=0}^{2^{2n}-1} |C_{RGB\alpha}^i\rangle \otimes |i\rangle \right), \\
&= \frac{1}{2^{n+1}} \sum_{i=0}^{2^{2n}-1} |C_{RGB\alpha}^{Yi}\rangle \otimes |i\rangle,
\end{aligned}
\tag{4.5}
$$

where, $|C^{Yi}_{RGB\alpha}\rangle$ is the new color state after applying CS_Y operator, shown as

$$\begin{aligned}
|C^{RGi}_{RGB\alpha}\rangle &= \cos\theta^i_G|000\rangle + \cos\theta^i_R|001\rangle + \cos\theta^i_B|010\rangle + \cos\theta^i_\alpha|011\rangle + \\
&\quad + \sin\theta^i_G|100\rangle + \sin\theta^i_R|101\rangle + \sin\theta^i_B|110\rangle + \sin\theta^i_\alpha|111\rangle, \\
|C^{RBi}_{RGB\alpha}\rangle &= \cos\theta^i_B|000\rangle + \cos\theta^i_G|001\rangle + \cos\theta^i_R|010\rangle + \cos\theta^i_\alpha|011\rangle + \\
&\quad + \sin\theta^i_B|100\rangle + \sin\theta^i_G|101\rangle + \sin\theta^i_R|110\rangle + \sin\theta^i_\alpha|111\rangle, \\
|C^{GBi}_{RGB\alpha}\rangle &= \cos\theta^i_R|000\rangle + \cos\theta^i_B|001\rangle + \cos\theta^i_G|010\rangle + \cos\theta^i_\alpha|011\rangle + \\
&\quad + \sin\theta^i_R|100\rangle + \sin\theta^i_B|101\rangle + \sin\theta^i_G|110\rangle + \sin\theta^i_\alpha|111\rangle.
\end{aligned} \tag{4.6}$$

The CoI_X and CS_Y are operations in the C_I category, that change the color information of the whole image. In some image processing tasks, however, we want to focuss our interest on part region of an image and apply some operators on these specific positions. Hence the rC_I category operation is proposed in this subsection. The change in a channel of the color space at some points in an image depends on the specific positions in the image. Information about the positions is used as conditions encoded in the matrix Po of the controlled-gate rC_I to construct the processing operations. For instance, let us consider a 2×2 image and the change in color at positions $|0\rangle$, $|2\rangle$. The matrix $Po = |0\rangle\langle0| + |2\rangle\langle2|$ and $\bar{P}o = |1\rangle\langle1| + |3\rangle\langle3|$ are used to construct the controlled-gate rC_I, given as

$$rC_I = U \otimes (|0\rangle\langle0| + |2\rangle\langle2|) + I \otimes (|1\rangle\langle1| + |3\rangle\langle3|). \tag{4.7}$$

The action of this particular rC_I on a general 2×2 image in MCQI form, $|I(\theta)_{mc}\rangle = \frac{1}{4}\sum_{i=0}^{3}|C^i_{RGB}\rangle \otimes |i\rangle$, is given by

$$\begin{aligned}
rC_I|I(\theta)_{mc}\rangle = &\frac{1}{4}[(U \times |C^0_{RGB}\rangle) \otimes |0\rangle + (U \times |C^2_{RGB}\rangle) \otimes |2\rangle + \\
&+ |C^1_{RGB}\rangle) \otimes |1\rangle + |C^3_{RGB}\rangle) \otimes |3\rangle].
\end{aligned} \tag{4.8}$$

The calculation shows that the action of operation U for changing color has affects only on the specific positions $|0\rangle$, $|2\rangle$. U is an 1 qubit, 2 qubits, or 3 qubits operation.

4.3 Double-key, double-domain watermarking strategy

The general framework for the proposed double-key, double-domain watermarking strategy for multi-channel quantum images (MC-WaQI) is presented in Figure 4.1. From this figure we can see that the scheme is delineated into two broad divisions - the first, comprising of all the data available to the copyright owner, i.e. the publisher of the watermarked image, and the other comprising the information published (by the copyright owner) for use by the public. Therefore, it is obvious that the pre-processing, preparation, and watermark embedding tasks are handled by the copyright owner who alone access to these data. Specifically, the MC-WaQI can be separated into the following algorithms (or steps) including:

- (0) preparation procedure for MCQI images [48];

- (1) two logo information (image $|FW\rangle$ and image $|SW\rangle$) are prepared;

- (2) apply measurement operation on image $|W^2\rangle$ to obtain image M;

- (3) use image M to generate the color information key (CIK);

- (4) apply CIK on 4 sub-blocks of image $|SW\rangle$ to protect the color information of image $|W^1\rangle$ (image $|SW'\rangle$ is obtained);

- (5) resize image $|FW\rangle$ to obtain image $|FW'\rangle$;

- (6) image scrabbling by applying position information key (PIK) on image $|FW'\rangle$ and $|SW'\rangle$ (image $|FW''\rangle$ and $|SW''\rangle$ are obtained);

- (7) resize image $|FW''\rangle$ to get image $|FW'''\rangle$;

- (8) watermark images embedding procedure step 1 (embed image $|FW''\rangle$ into the QFT coefficients of carrier image (image $|I\rangle$) to get image $|I'\rangle$);

- (9) watermark images embedding procedure step 2 (embed image $|SW'''\rangle$ into the spatial domain of image $|I'\rangle$ to generate image $|I''\rangle$);
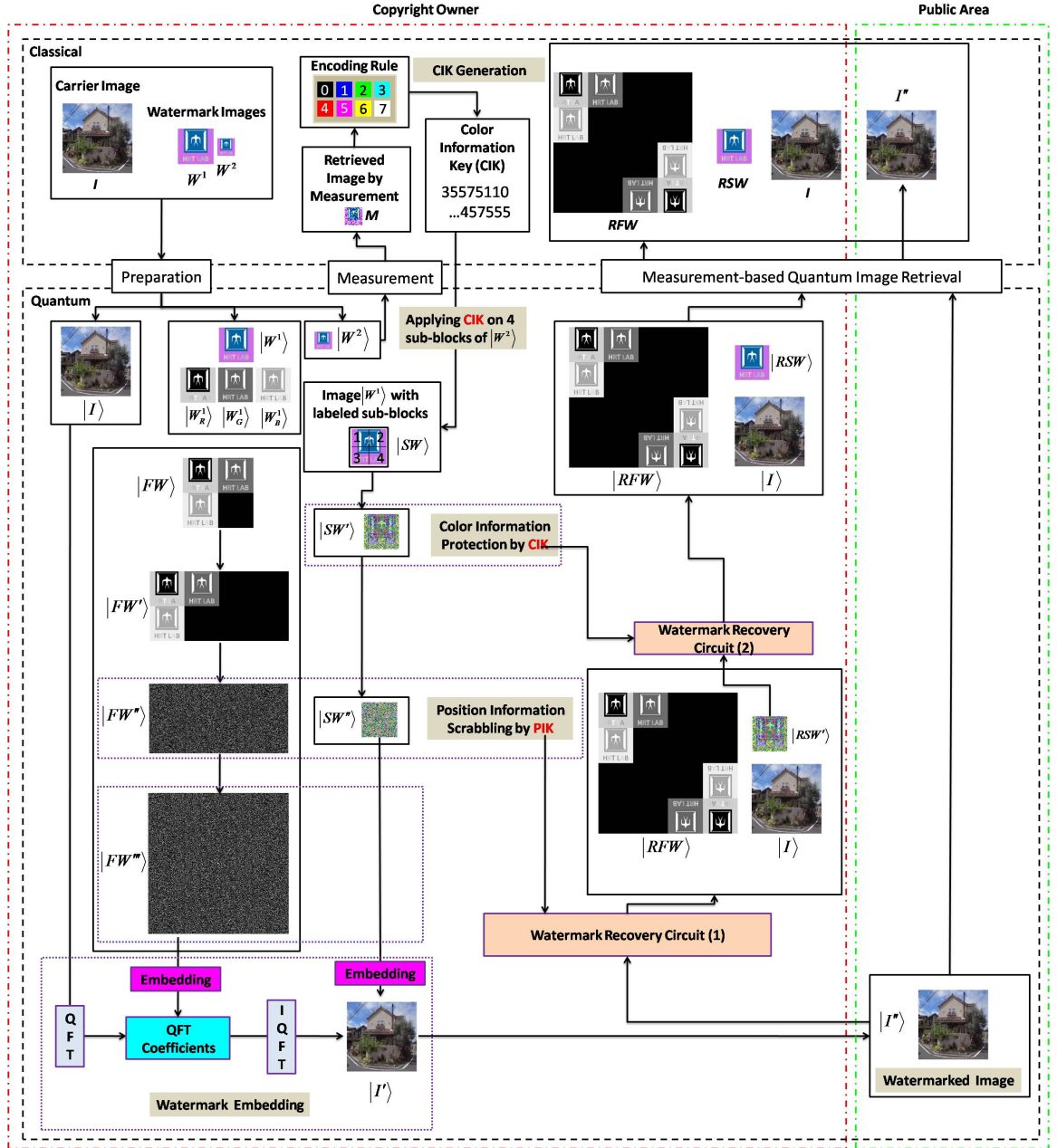
- (10) watermark image's extracting procedure.

Figure 4.1: *General schematic for MC-WaQI..*

Quantum computers are usually initialized in well-prepared states [27]. As a result, the preparation process that transforms quantum computers from the initialized state (assuming $|00...0\rangle$) to the desired quantum image state is necessary. Hence, the first procedure (step (0) in the above) is the operation that turns quantum computers from the initialized state to MCQI state (this procedure has already been discussed in [48] [27], hence, is not introduced in this paper). The steps (0) to (7) belong to the preprocessing

part of MC-WaQI strategy; steps (8) and (9) are watermark embedding part; step (10) is the watermark extracting part.

The motivation for the watermark embedding-circuit generation algorithm stems from the fact that, quantum states such as our MCQI images and watermark signals, can only be manipulated using appropriate quantum circuits.

The notations used in this chapter is defined as:

- I: the classical carrier image;

- W^1: the watermark image used to generate two logo information;

- W^2: the watermark image used to generate the color information protection key;

- $|I\rangle$: the quantum version of carrier image;

- $|W^1\rangle$: the quantum version of W^1;

- $|W^2\rangle$: the quantum version of W^2;

- $|W_R^1\rangle$: R component of image $|W^1\rangle$;

- $|W_G^1\rangle$: G component of image $|W^1\rangle$;

- $|W_B^1\rangle$: B component of image $|W^1\rangle$;

- $|SW\rangle$: image $|W^1\rangle$ with labeled sub-blocks;

- M: retrieved image by applying measurement on image $|W^2\rangle$;

- $|FW\rangle$: image generated by combining image $|W_R^1\rangle$, $|W_G^1\rangle$, $|W_B^1\rangle$, and a same sized black image;

- $|FW'\rangle$: resized image $|FW\rangle$;

- $|FW''\rangle$: image by applying position scramble key on image $|FW'\rangle$;

- $|FW'''\rangle$: resized image $|FW''\rangle$;

- $|SW'\rangle$: image by applying color information protection key on image $|SW\rangle$;

- $|SW''\rangle$: image by applying position scramble key on image $|SW'\rangle$;

- $|I'\rangle$: frequency domain embedded image;

- $|I''\rangle$: double domain embedded image;

- $|RFW\rangle$: recovery logo information image 1;

- $|RSW\rangle$: recovery logo information image 2;

- RFW: classical version of recovery logo information image 1;

- RSW: classical version of recovery logo information image 2;

- I'': classical version of double domain embedded image;

- CIK: color information protection key;

- PIK: position information scramble key.

4.3.1 Preparation procedure for MCQI images

In this watermarking strategy, three images are prepared. The first image is the carrier, and the other two images are logo information, as shown in Figure.4.2.
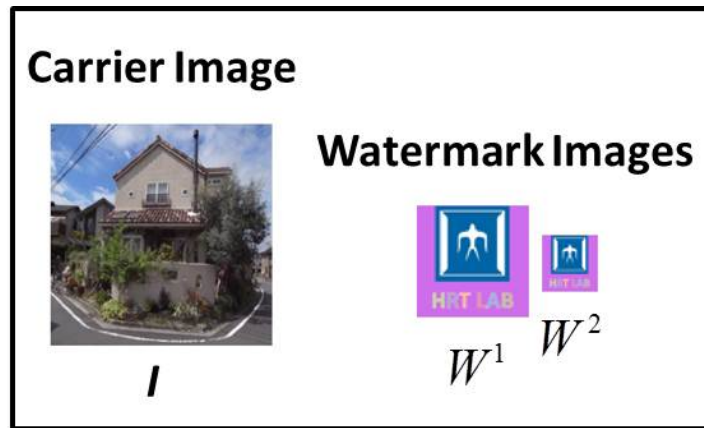
Figure 4.2: *Three classical images to be prepared..*

Image I is the carrier to be embedded. Usually, it is belong to a image database which is requested to be protected. Image W^1 is the logo image or watermark image, which

is used to generated the quantum signals embedded into carrier image. The image W^2 is half sized logo image used to generate the color information protection key. All the three images are prepared to be quantum images. The preparation procedure includes two part: Hadamard operation $\mathcal{P}$ and Rotation operation $\mathcal{R}$. Given 3 vectors of angles $\theta_X = (\theta_X^0, \theta_X^1, \ldots, \theta_X^{2^{2n}-1})$, $X \in \{R, G, B\}$, where 2n is the number of qubits carrying the position information. Assume the initialized state is $|0\rangle^{\otimes 2n+3}$ (3 is the number of qubit to encode color information) there is a unitary transformation $\mathcal{P}$ that turns the quantum computers to the MCQI state, $|I_{mc}(\theta)\rangle$ composed by Hadamard and controlled rotation transformations.

After the preparation procedure, we can get three quantum images $|I\rangle$, $|W^1\rangle$, and $|W^2\rangle$ as shown in Figure.4.3. From Fig.4.3, the image $|W^1\rangle$ is separated into 3 channels,
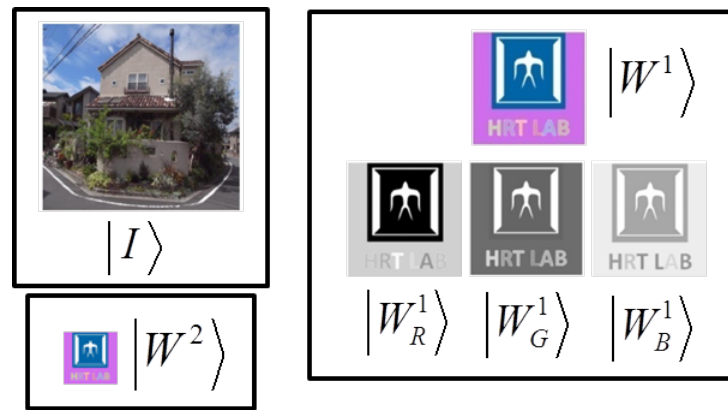

Figure 4.3: *Carrier image and two logo images..*

$|W_R^1\rangle$, $|W_G^1\rangle$, and $|W_B^1\rangle$. Image $|W^2\rangle$ is used to generate the CIK by measurement.

4.3.2 Measurement based CIK generation procedure

In [54], a position key is use to scrabble the watermark image. This key is proved efficient to protect the geometric information of an image. But, the key is fixed, which is assigned by the copyright owner, and if the illegal user can get this key, the watermarking strategy will fail to protect the copyright. The CIK, however, is an unfixed key, which is generated by applying quantum measurement on watermark image. A measurement applied on a superposition $\alpha|0\rangle + \beta|1\rangle$ will lead to the collapse of this superposition, and

will obtain the 0 result with probability of α^2, or the 1 result with probability of β^2, where $\alpha^2 + \beta^2 = 1$. Hence, using this characteristic (collapse of superposition), we apply a measurement on the watermark image to obtain a post-measurement image (image M) (classical image), which is then used to generate the CIK. Putting measurement on a single pixel is shown in Fig.4.4. Based on this property (state collapse), we can get 8 possible
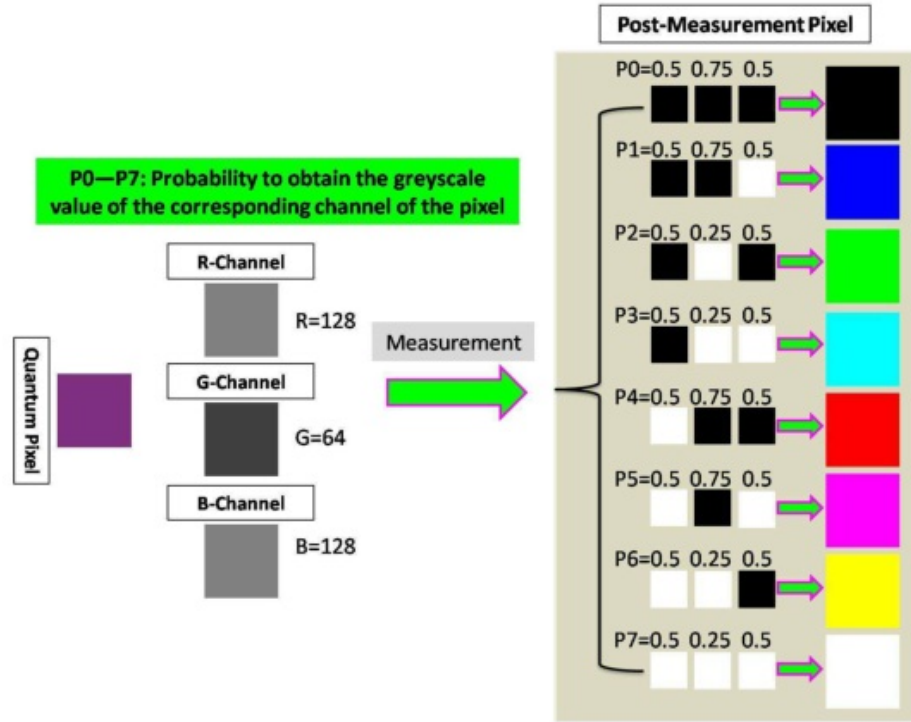

Figure 4.4: *Measurement operation on a single pixel..*

colors in Fig.4.4. Then we make this discussion further. We applying the measurement operation on the whole image to generate the CIK, as shown in Fig.4.5. The whole CIK generation procedure is shown in Fig.4.6.

This procedure includes three parts:

- (1) applying measurement operation to image $|SW^2\rangle$;

- (2) obtaining classical image M;

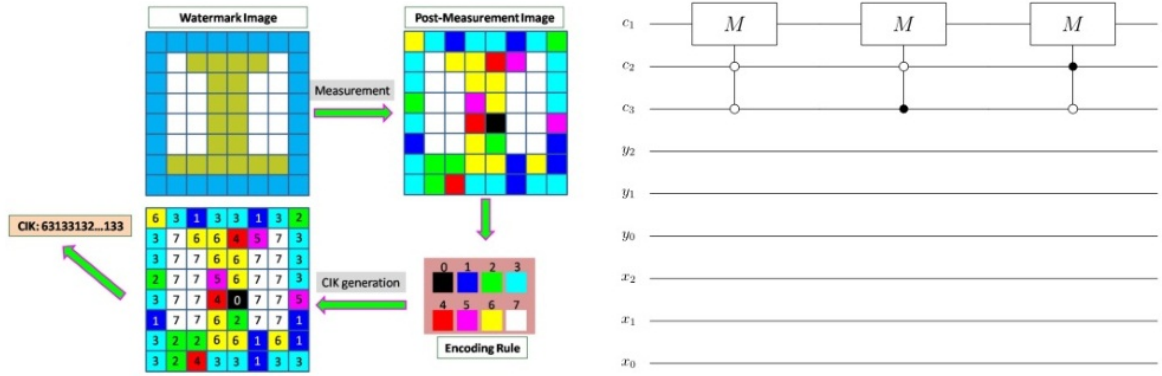- (3) according to the color information of M and the encoding rules to generate the CIK.

Figure 4.5: *Measurement operation on logo image..*

4.3.3 Images $|SW\rangle$ and $|FW\rangle$ generation

Because there are two logo images need to be generated which are embedded into both spatial and frequency domains. As shown in Fig.4.3, we used logo image $|W^1\rangle$ and its R G B components to realize this task. The details are shown in Fig.4.7. Image $|FW\rangle$ is generated by combining the R G B components of $|W^1\rangle$ and plus one same sized black image. Image $|SW\rangle$ is $|W^1\rangle$ with sub-block labels. The image $|FW\rangle$ is grayscale image which will be embedded into the frequency domain and image $|SW\rangle$ is color image embedded into spatial domain of the carrier image (image $|I\rangle$).

4.3.4 CIK and PIK protection

In order to strengthen the protection ability, we apply the Color Information protection Key (CIK) on four sub-blocks of image $|SW\rangle$. The details are shown in Fig.4.8. In this color protection procedure, there are four steps:

- (1) applying measurement to the image $|W^2\rangle$ to obtain CIK;

- (2) applying CIK to image $|SW\rangle$ to obtain image $|SW'\rangle$.

Because the CIK is generated by measurement, this key is an unfixed key. Even though the potential illegal can obtain this key one time, the content of the key will change after the next measurement. And from Fig.4.8, although the CIK can protect the color information of the logo information, we can still get some original information from
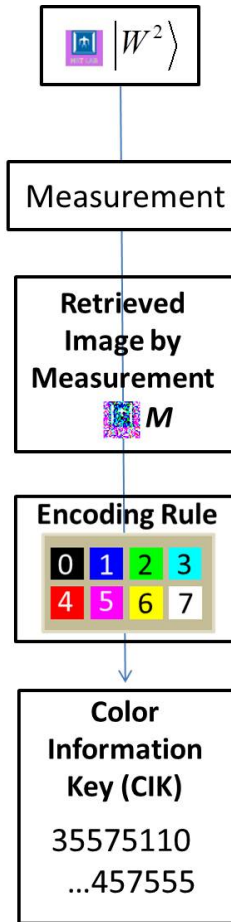
Figure 4.6: *Whole CIK generation procedure..*

image $|SW'\rangle$. Hence, another key should be used to scramble the pixels' position of image $|SW'\rangle$ and image $|FW\rangle$ as shown in Fig.4.9. In this procedure, there are three steps:

- (1) double size $|FW\rangle$ to obtain $|FW'\rangle$;

- (2) applying PIK to $|FW'\rangle$ and $|SW'\rangle$ to obtain $|FW''\rangle$ and $|SW''\rangle$;

- (3) double size image $|FW''\rangle$ to obtain $|FW'''\rangle$.

First, because the size of Fourier coefficients of the carrier image are four sized than image $|FW\rangle$, we double size it in the first step. Second, then we apply PIK to scramble the image $|FW'\rangle$ and $|SW'\rangle$. Finally, double size image $|FW''\rangle$ to obtain $|FW'''\rangle$ to guarantee the logo information symmetry (If the logo information is not symmetry, the coefficients of the embedded image will become not real numbers).
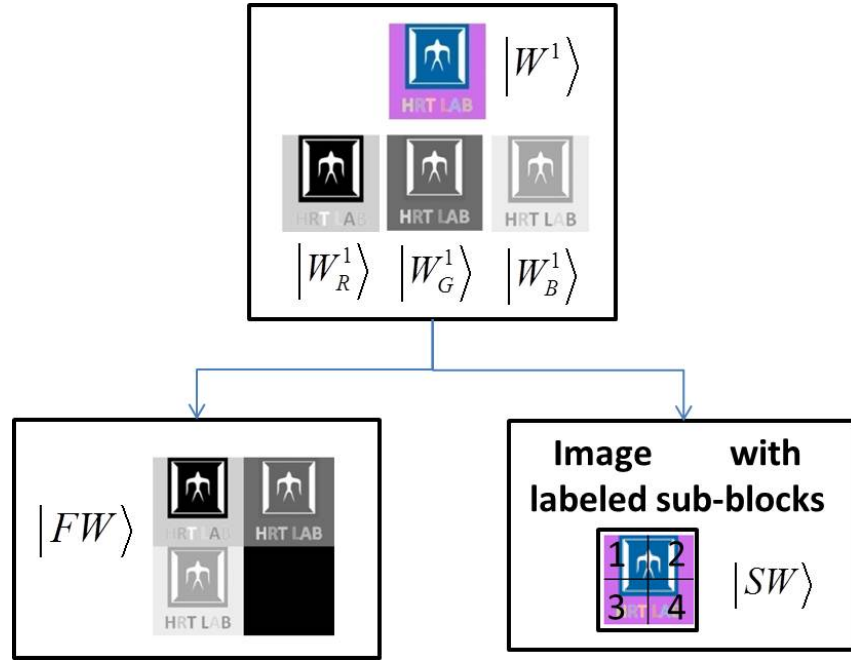
Figure 4.7: *Image $|FW\rangle$ and image $|SW\rangle$ generation procedure..*

4.3.5 The embedding procedure

This is the last step of the embedding procedure. A color image consists of many pixels and each pixel's color information can be separated into three channels. According to the MCQI, a quantum image can be rewritten as

$$|I(\theta)_{mc}\rangle = \sum_{i=0}^{N-1}(X_R^i|0\rangle + X_G^i|1\rangle + X_B^i|2\rangle + X_O|3\rangle)|i\rangle, \tag{4.9}$$

where, i is the position information (the ith pixel of the image), N is the pixels' number in the image, and X_R^i, X_G^i, and X_B^i are color channel information (X_O is other channel, which is not discussed in this paper (we let it is $cos\theta0|3\rangle + sin\theta0|3\rangle$ to carry no information), and in [48], it represents the α channel) (greyscale value of the ith pixel of R, G, and B channels, respectively). Because the watermark image will be embedded into both frequency domain (QFT coefficients) and spatial domain (color channels), we separate the embedding procedure into two part to discuss.

Firstly, frequency domain is discussed. Considering the property of QFT, to guarantee that the pixels' value of the embedded carrier image (image $|I'\rangle$) are still real, the revised value of the QFT coefficients should be symmetrical [54]. Suppose the size of carrier
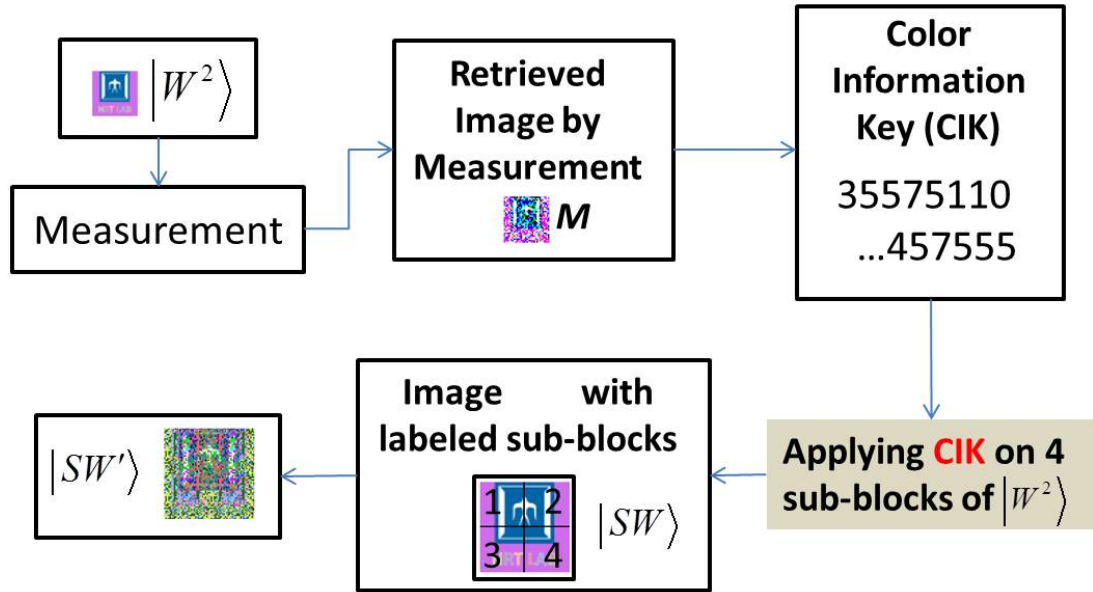
Figure 4.8: *Applying the Color Information protection Key (CIK) on two sub-blocks of image* $|SW\rangle$.

image is $m \times n$, the revised value of the QFT coefficients should meet this conditions:

$CE_X(i,j) = CE_X(m-1-i, n-1-j)$ (3 channels in MCQI image, $X \in \{R,G,B\}$), where $CE_X(i,j)$ is the revised value of QFT coefficients of X channel of the carrier image, and hence, the watermark image to be embedded into the carrier image should also be symmetrical ($Wa_X(i,j) = Wa_X(m-1-i, n-1-j)$), and also the image $|I\rangle$ and image $|FW'''\rangle$ should be uniform-sized, which is the reason why we resized the image $|FW\rangle$. Then we embed image $|FW'''\rangle$ into the Fourier coefficients of image $|I\rangle$, and $|SW''\rangle$ into image $|I\rangle$ as shown in Fig.4.10. First, applying quantum Fourier transform on image $|I\rangle$, then embed the image $|FW'''\rangle$ into Fourier coefficients. Second, apply reverse Fourier transform to obtain image $|I'\rangle$ then embed image $|SW''\rangle$ into image $|I'\rangle$ to obtain image $|I''\rangle$. The image $|I''\rangle$ is the embedded image.

4.3.6 The recovery procedure

The recovery procedure is easy to design if we can obtain the correct CIK and PIK as shown in Fig.4.11. And it is clearly that user without CIK and PIK can not recover the logo information, which guarantee the security of the proposal.
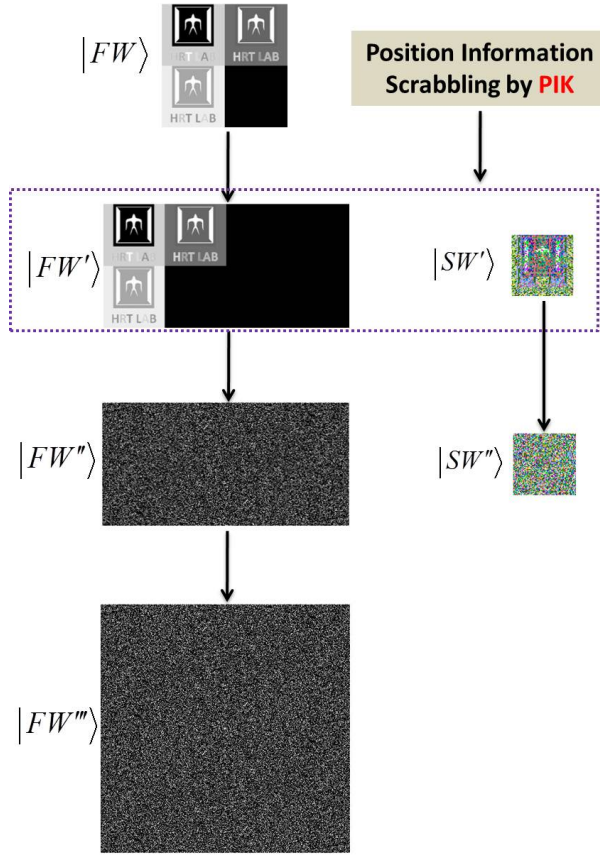
Figure 4.9: *Position information scrabble by using PIK..*

4.4 Simulation based experiments and analysis

The experiments are carried out on laptop computer with Intel Core (TM) i5 Duo 2.40 GHz CPU and 4 GB RAM. The simulations are based on linear algebra with complex vectors as quantum states and unitary matrices as unitary transforms using QLIB [34] (A Matlab package for quantum information). Fifteen Japanese house images are used as carrier image and a university logo image is the watermark image as shown in Fig. 4.12 and Fig.4.13. To evaluate the quality of the embedded images, average RGB peak-signal to-noise ratio (RGB-PSNR) [33] [3] [10] is used, which is defined as

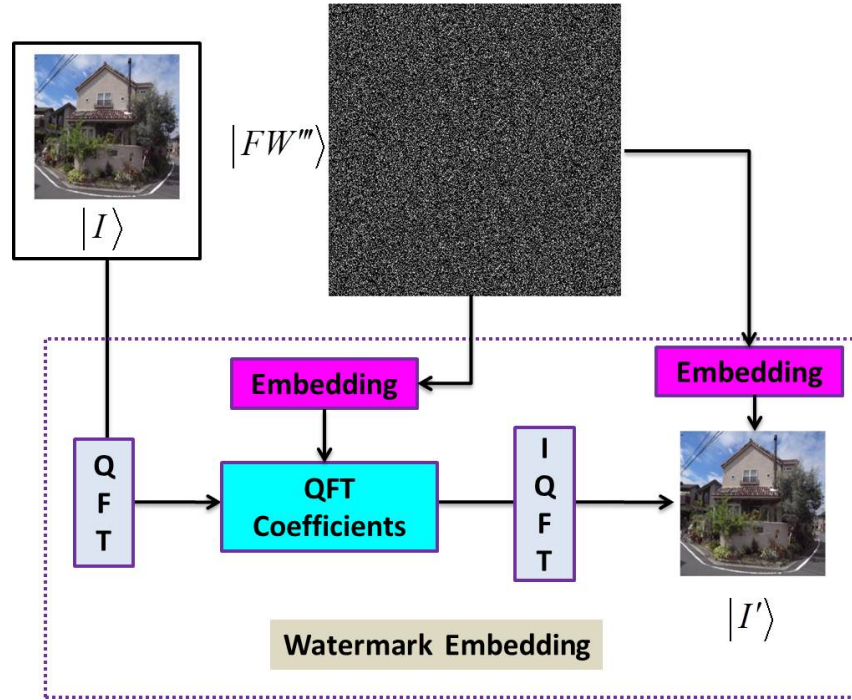$$PSNR_{RGB} = (PSNR_R + PSNR_G + PSNR_B)/3, \qquad (4.10)$$

Figure 4.10: *Logo information embedding procedure..*

where

$$PSNR_X = 20log_{10}\left(\frac{255}{\sqrt{MSE}}\right), X \in \{R, G, B\},$$

$$MSE = \frac{1}{mn}\sum_{i=0}^{m-1}\sum_{j=0}^{n-1}[I'(i,j) - I(i,j)]^2.$$

(4.11)

Here, MSE is mean squared error between the carrier image $I(i,j)$ and the embedded image $I'(i,j)$. $m \times n$ are the number of pixels of the image. The size of the carrier images in the experiments are all resized to 256 by 256. And the size of the logo is 128 by 128. The average RGB PSNR between the embedded images and the carrier images are shown as in table 4.1. From table 4.1, the average RGB-PSNR for all the 15 images is about 53dB, which is about 8 dB better than QFTW [54], and 3 dB better than WaQI [20]. And also, both QFTW and WaQI can not deal with the color quantum images (only can be applied to grayscale quantum images). The PIK rules used in this experiment is shown in Fig.4.14 (This rules can be changed in different experiments).
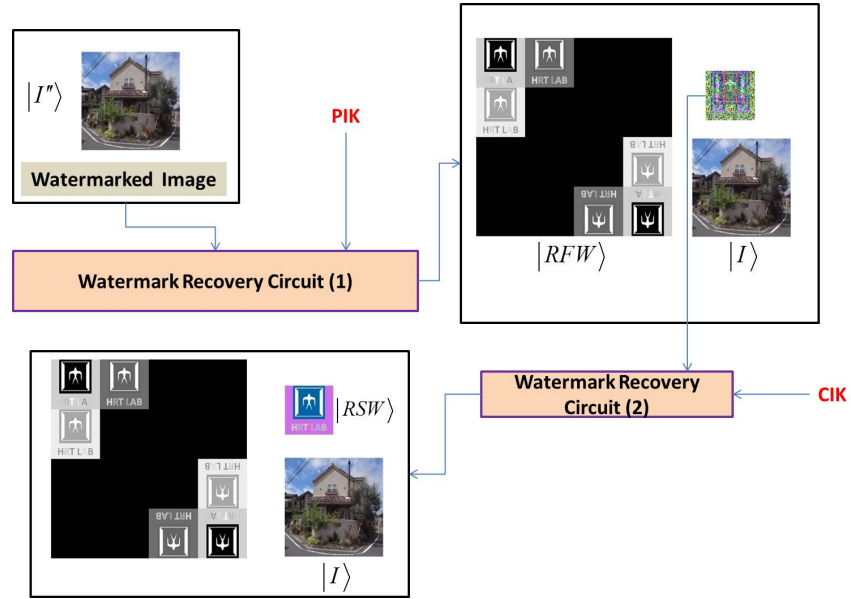
Figure 4.11: *Recovery procedure of the proposed strategy.*

4.5 Perspective for quantum image watermarking

Research in the field of quantum image watermarking started with proposals of the concept of quantum image. Aiming to protect the copyright of quantum image database, many watermarking strategies were proposed. In our strategy, we focus on the color information transformations. Through changing the images' color, we can hide the secrete data into the carrier images. However, the information in an image are two parts: color information and geometric information. Hence, if a watermarking strategy can focus on the both part, it will enforce the protection ability of this strategy. Hence, to design the circuit for geometric transformations on quantum images is very important for quantum image watermarking field. Luckily, because the data structure of the position information of MCQI is similar with FRQI, we can borrow the geometric transformations designing methods from FRQI. Specifically, geometric transformations are the operations which are performed based on the geometric information of images, i.e., information about position of every point in the image. Therefore, these transformations, G_I, on MCQI quantum images can be defined as

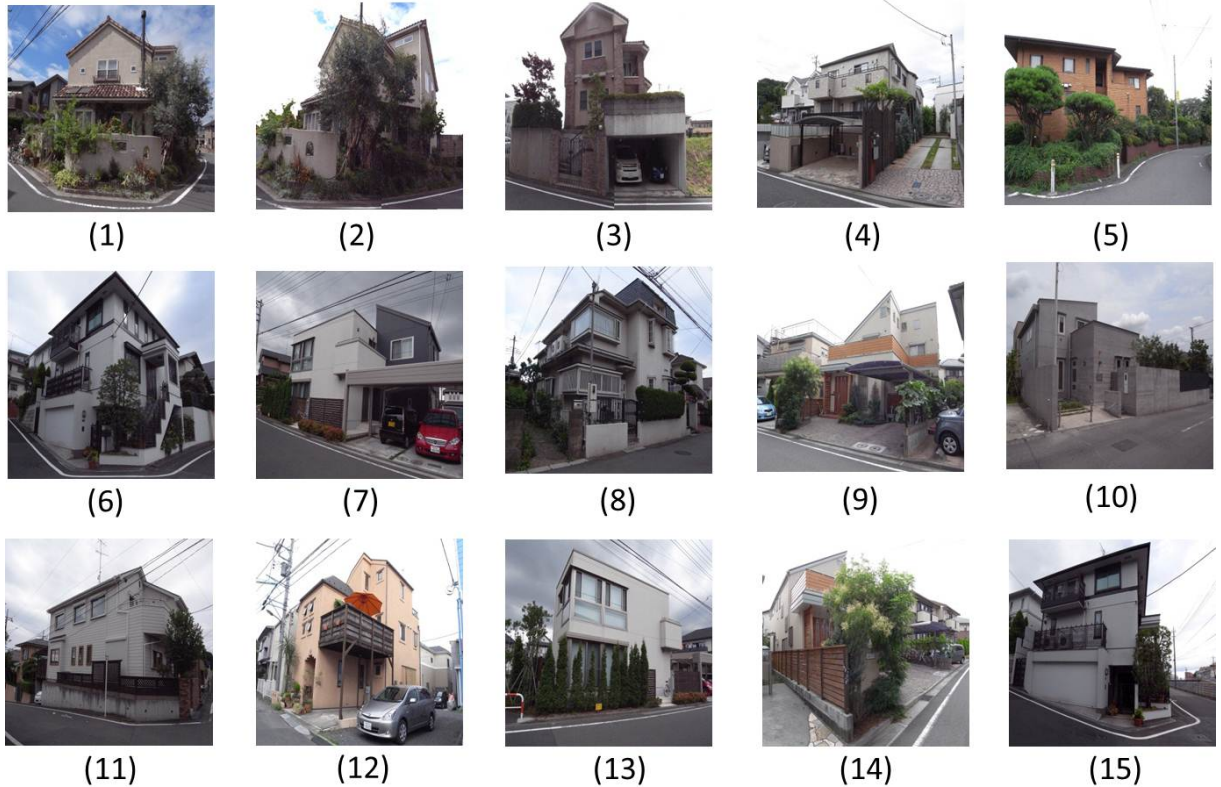$$G_I(|I(\theta)\rangle) = \frac{1}{2^{n+1}} \sum_{k=0}^{2^{2n}-1} |c_k\rangle \otimes G(|k\rangle), \tag{4.12}$$

(1) (2) (3) (4) (5)

(6) (7) (8) (9) (10)

(11) (12) (13) (14) (15)

Figure 4.12: *Carrier images used in this experiment.*

Figure 4.13: *Logo image to be embedded into carrier images.*

where, $G(|k\rangle$ for $k = 0, 1, ..., 2^{2n} - 1$ are the unitary transformations performing geometric exchanges based on the vertical and horizontal locations. The performance of the geometric transformations on quantum images, G_I, is based on the function, G, on the computational basis vectors. The general structure of circuits for geometric transformations on FRQI images is shown in Fig.4.15. The structure of the set of all geometric transformations on MCQI images can be studied from the algebraic theory view point. Each geometric transformation can be considered as a permutation of positions. Therefore, all geometric transformations on MCQI images form a group under the operation
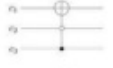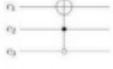
Figure 4.14: *PIK rules used in this experiment.*

of cascading two geometric transformations. After setting the isomorphism between the group of all geometric transformations and a subgroup of permutations, the group theory can be applied to classify these geometric transformations. The classification is based on the content of the set of generators, or the gate library, used in the corresponding circuits. There are three gate libraries related to NOT, CNOT and Toffoli gates as follows

- the library, N, contains only NOT gate.

- the library, NC, contains NOT and CNOT gates.

- the library, NCT, contains NOT, CNOT, and Toffoli gates.

The circuits which contain only NOT gates perform the bit translations as follows

$$f(x) = x \oplus b, b \in \mathcal{Z}_n^2, \tag{4.13}$$

Table 4.1: *Average RGB PSNRs of the retrieved images.*

Carrier images	Logo image	Average RGB PSNR (dB)
Fig.4.12(1)	Fig.4.13	50.0341
Fig.4.12(2)	Fig.4.13	45.3376
Fig.4.12(3)	Fig.4.13	58.2286
Fig.4.12(4)	Fig.4.13	55.1435
Fig.4.12(5)	Fig.4.13	58.5801
Fig.4.12(6)	Fig.4.13	51.3692
Fig.4.12(7)	Fig.4.13	52.9246
Fig.4.12(8)	Fig.4.13	54.1216
Fig.4.12(9)	Fig.4.13	55.0982
Fig.4.12(10)	Fig.4.13	58.9326
Fig.4.12(11)	Fig.4.13	51.9072
Fig.4.12(12)	Fig.4.13	52.0371
Fig.4.12(13)	Fig.4.13	54.2134
Fig.4.12(14)	Fig.4.13	45.2942
Fig.4.12(15)	Fig.4.13	58.9471

The circuits which contain only CNOT gates perform the linear transformations as follows

$$f(x \oplus y) = f(x) \oplus f(y), x, y \in \mathcal{Z}_n^2, \tag{4.14}$$

If we put a linear transformation, f, after a bit translation indicated by b then we produce an affine transformation g

$$g(x) = f(x \oplus b) = f(x) \oplus f(b), x, b \in \mathcal{Z}_n^2. \tag{4.15}$$

These circuits comprise of CNOT and NOT to perform affine transformations. Using the library NCT, we can generate all geometric transformations on FRQI images. The following three parameters are usually used to analyze the complexity of quantum circuits, C,

- the number of basic gates, —C—, used in the circuit,

- the width, W(C), of the circuit or the number of qubits involved in the circuit,

- the depth, D(C), of the circuit or the minimum number of layers that the circuit can be partitioned into.

$$|I(\theta)\rangle \qquad G(|I(\theta)\rangle)$$

Color

y_{n-1}

y_{n-2}

Y Axis

y_0

G

x_{n-1}

x_{n-2}

X Axis

x_0
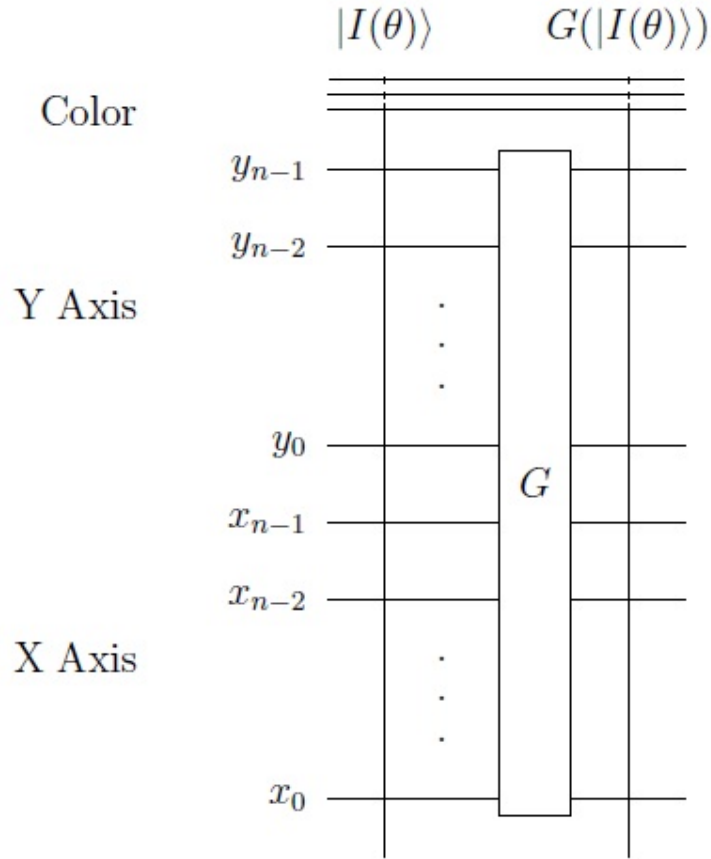
Figure 4.15: *General circuit design for geometric transformations on quantum images..*

Here, we will provide some basic geometric transformations proposed in[28].

The two-point swapping operation on FRQI quantum images between two positions i, j is the operation, S_I, which when applied on $I(\theta)$ produces the output of the following form

$$S_I(I(\theta)) = \frac{1}{2^{n+1}} \sum_{k=0}^{2^{2n}-1} |c_k\rangle \otimes S(|k\rangle), \qquad (4.16)$$

where $S(|k\rangle) = |k\rangle$, $K \neq i, j$ and $S(|i\rangle) = |j\rangle$, $S(|j\rangle) = |i\rangle$, i.e.,

$$S = |i\rangle\langle j| + |j\rangle\langle i| + \sum_{k \neq i,j} |k\rangle\langle k|. \qquad (4.17)$$

Fig.4.15 shows an example of two-point swapping operation in which the operation swaps the points $|110\rangle|110\rangle$ and $|011\rangle|010\rangle$.
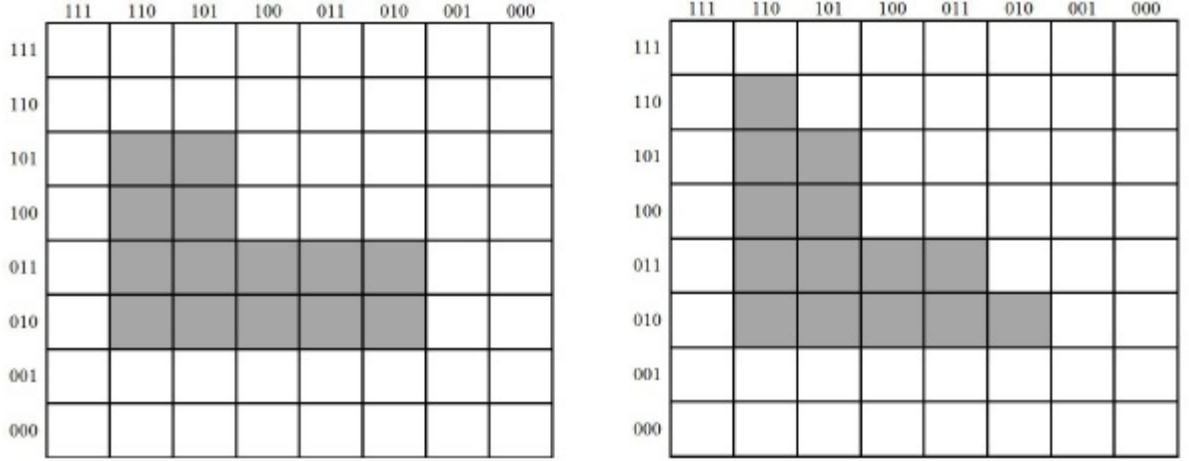
Figure 4.16: *An example of two-point swapping operation..*

The flipping operations on MCQI quantum images along the X and Y axes are the operation F_I^X F_I^Y which when applied on $I(\theta)$ produces the outputs of the following form;

$$F_I^X = \frac{1}{2^{n+1}} \sum_{k=0}^{2^{2n}-1} |c_k\rangle \otimes F^X(|k\rangle), \qquad (4.18)$$

$$F_I^Y = \frac{1}{2^{n+1}} \sum_{k=0}^{2^{2n}-1} |c_k\rangle \otimes F^Y(|k\rangle), \qquad (4.19)$$

where $|k\rangle = |y\rangle|x\rangle$ and

$$F^Y(|y\rangle|x\rangle) = |\overline{y}\rangle|x\rangle, \qquad (4.20)$$

$$F^X(|y\rangle|x\rangle) = |y\rangle|\overline{x}\rangle, \qquad (4.21)$$

$$|x\rangle = |x_{n-1}x_{n-2}...x_0\rangle$$

,

$$|y\rangle = |y_{n-1}y_{n-2}...y_0\rangle$$

,

$$|\overline{x}\rangle = |\overline{x}_{n-1}\overline{x}_{n-2}...\overline{x}_0\rangle$$

,

$$|\overline{y}\rangle = |\overline{y}_{n-1}\overline{y}_{n-2}...\overline{y}_0\rangle$$

87

,

$$\overline{x}_i = 1 - x_i, \overline{y}_i = 1 - y_i$$

,

$$i = 0, 1, ..., n - 1$$

. Examples of image flipping along X and Y axis are shown in Fig.4.16 and Fig.4.17.
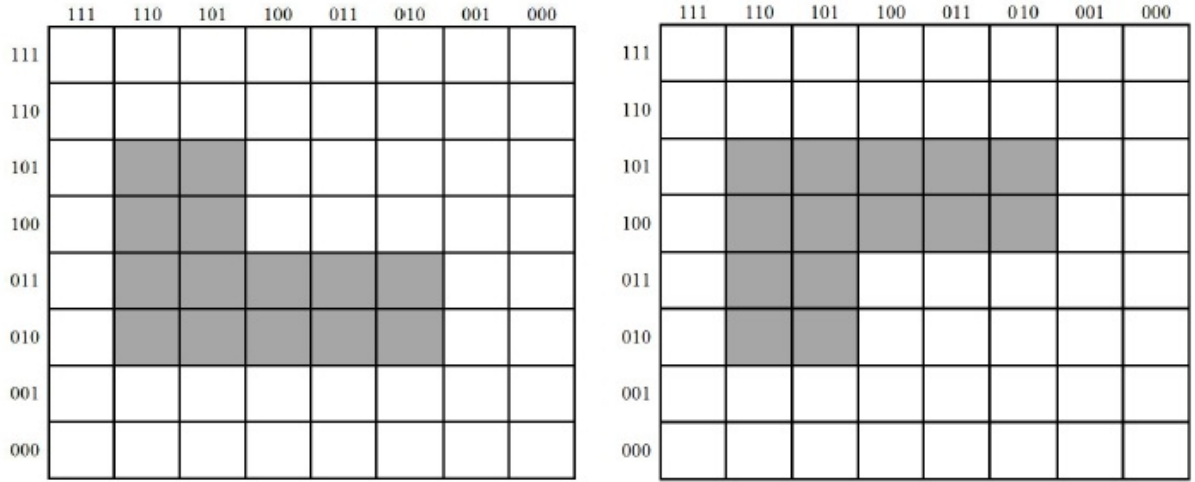
Figure 4.17: *An example of image flipping along X axis..*
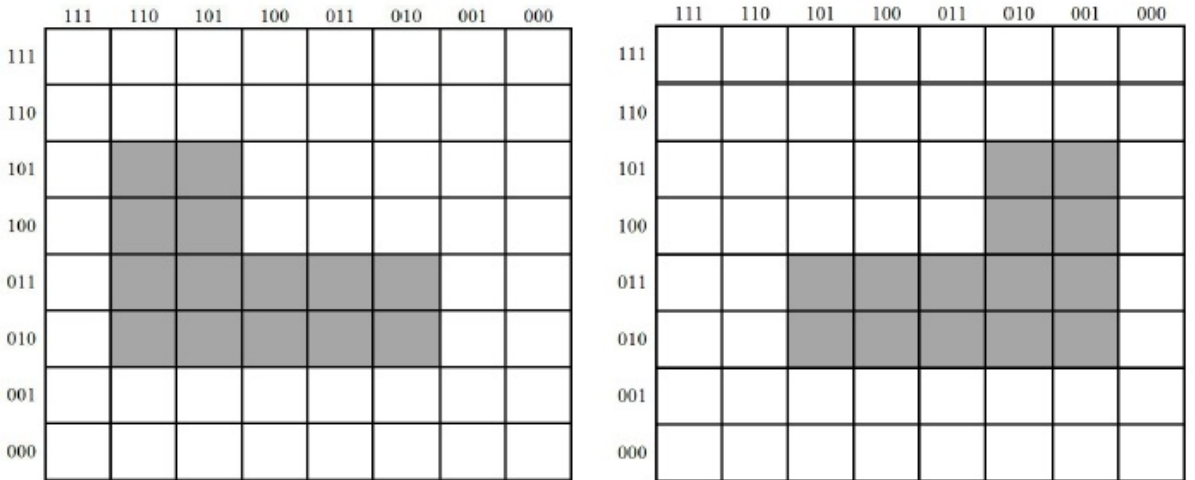
Figure 4.18: *An example of image flipping along Y axis..*

In the above introduction, we give two concepts of geometric transformations on quantum images. We can also design other transformations by carefully design the circuit. The designing of the geometric transformations is important, but can not apply them on image

watermarking directly. Because, sometimes, we do not want to change all the geometric information of one image, and we just focus our interest on some specific pixels. Therefore, the designing of the restricted version of geometric information transformations is very important. After some geometric transformations are well understood, it is often that the designers of new operations would want to use smaller versions of the transformations as the main components in the larger operations. Therefore, a major strategy is the application of a transformation to a sub-block in an image.

Luckily, the data structure allows us to design the restricted version of geometric transformations [21]. Therefore, we expect that we can design the new watermarking strategy using both color information operations and geometric information transformations, which can enforce the power of protection on our image, or movie or other quantum data. Also, the existence of α channel provide a potential possibility which allows the background image to embed into the original image. An example of α blending is shown in Fig.4.19.

Figure 4.19: *Examples of α blending images ((a) The original image; (b) the back ground image; (c) the blended image with $T_\alpha = 178$); (d) the blended image with $T_\alpha = 128$; (d) the blended image with $T_\alpha = 77$.*

4.6 Summary of Quantum measurement based double-key double-domain watermarking strategy for multi-channel quantum images

A watermarking strategy for quantum images based on quantum measurement, quantum Fourier transform, and multi-channel operations is proposed. Th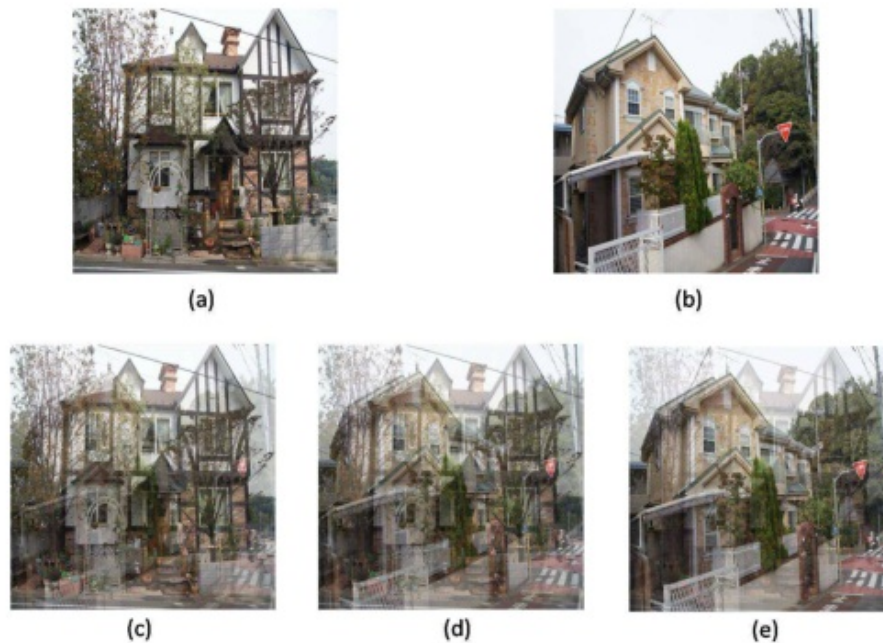e purpose of the double-key double-domain watermarking strategy is to insert an invisible watermark signal onto a quantum image in order to produce a watermarked version of the same size as the original image. The channel of interest, channel swapping operations are used as the main resources to transform a specific pixel or group of pixels within an image combining with quantum measurement operation. The resulting watermarked image shows no trace of the watermark signal, thereby, making the proposed scheme invisible. The proposal was evaluated using simulation experiments on a classical computer. These simulation-based experiments demonstrated the feasibility of the proposed strategy in addition to outperforming some select digital watermarking methods in terms of their overall watermark capacity and the visible quality of the watermarked images, such as 8dB better than QFTW and 3 dB better than WaQI.

In our strategy, all the resources used for image watermarking are multi-channel information operations. The geometric operations on quantum images [28], however, are also the important resources. Hence, in this section, we will discuss this issue. The difference between MCQI and FRQI is the color qubit/qubits. In FRQI representation, only 1 qubit is used to encode the color information, hence FRQI can only carry the color information as a single channel. MCQI, however, assigns three qubits to do this job, and provide a new data structure, which the multi-channel information are encoded in this representation simultaneously. Both FRQI and MCQI include two parts, the color qubit part and the position qubit part. The color qubit part is different as discussed above. The position qubit part, however, is same. Therefore, all the FRQI based geometric operations can be transplanted into MCQI directly.

For the future work of this field, the watermarking resources should be extended.

Not only considering the color information operations, but also considering the geometric transformations. Fast geometric transformations such as the two-point swapping, flip, co-ordinate swapping, orthogonal rotations and their variants for quantum images, specifically those based on the FRQI representation, are proposed in [28] using the basic quantum gates, NOT, CNOT and Toffoli gates. For an N-sized image, the detailed analysis of quantum circuits show that the complexity is $O(log^2N)$ for two-point swapping and $O(logN)$ for the other operations. The two-point swapping operation is powerful since it can be built by arbitrary geometric transformations, but it is slower than the others. This fact is in contrast to their performance in classical versions but it agrees with the parallelism characteristic of quantum computation. In terms of their effect on images, the local transformations are slower than global ones among quantum image processing operations. The orthogonal rotations are the first examples of applying a succession of quantum transformations to create new applications on quantum image processing. All these GTQI operations can be used to design quantum image watermarking strategy combining with the operation proposed in this thesis. The GTQI operations, however, are aiming to change the geometric information on the whole images. The restrict version of GTQI maybe much more suitable for image watermarking task [21].

Furthermore, One of the problems in the watermarking scheme is the issue on how to decide places in an image to applied restricted geometric transformations. In order to improve the whole scheme, the contents of each sub-block should be analyzed more detail. The visual complexity of images should also be considered, which can be used to improve the pre-processing step in the watermarking scheme. Using the visual complexity, some important and useful control parameters can be estimated in many real applications of image processing, such as image compression, image watermarking, and image retrieval.

Another extension to the proposed scheme is its remodeling to fit in with customized applications to safeguard other quantum data such as video sound, etc from illicit tampering. Before then, representations to encode some of these data such as sound on the quantum computing framework must be broached. In the meantime, as a consequence of often bad correlation between the values obtained and the actual visual quality of the wa-

termarked images, the use of the PSNR as an evaluation metric for evaluating the fidelity of watermarked data on the quantum computing paradigm is being reviewed. The proposal advances available literature geared towards safeguarding quantum resources from unauthorise reproduction and confirmation of their proprietorship in cases of dispute leading to commercial applications of quantum information.

Chapter 5

Conclusion

The speed of our computers increased double every 18 months. In order to continue this trend, electronic transistors inside our computers are becoming smaller and smaller. At a certain level of this process, quantum mechanics has to be used to explain the behavior of the system. This is the observation made by Richard Feynman. Since the pioneering work, quantum effects are considered in the development of future computing hardware. Although the field of quantum computation has already been built 30 years before, the connection between earlier theoretical works with practical applications is still in a very early state. The main motivation of this research are three-fold:

- building the connection between quantum computation and the image processing application;

- developing the quantum computation based color transformation;

- by using color transformation to solve real image processing tasks.

Quantum computation and quantum information is a very exciting field in terms of storing, processing, and transmitting information in a new way based on principle of quantum mechanics. Images and image processing applications are popular in our daily life both. From a general viewpoint, images do not depend on computation devices but on their representation in the devices. When ones store images in a representation, processing transformations have to use the representation in order to change the images' content.

From the above motivations, the research started with the fundamental of image processing on quantum computation, quantum image representation. A new proposal of multi-channel representation for quantum images (MCQI) was proposed in chapter 2 to allow unitary transformations to apply on quantum images. And it also solve the problem that other quantum image representations consider the color of an image as a single channel, which is proved not convenient in the image processing field.

Considering the data structure of MCQI representation, all the FRQI based image processing operations can be used directly. Furthermore, various transformations, which focus on changing information about channels (components) of a color image, named Channel of Interest (CoI), Channel Swapping (CS), Color Space Transformation (CST), and α Blending (αB) operators were proposed based on the FRQI representation of the images as presented in chapter 3. The transformations serve as foundation blocks to build quantum image processing. Their complexity in terms of the number of basic quantum gates was analyzed.

Quantum measurement based double-key double-domain watermarking strategy for multi-channel quantum images were proposed in chapter 4, which is based on the MCQI representation and the transformations of channels' information. In this framework, the main contributions are three-fold:

- Solve the problem of color quantum image watermarking;

- Provide a new key generation procedure based on quantum measurement;

- The PSNR of the watermarked images are better than the chosen methods.

As discussed in the thesis, the applications of quantum image processing depend on the three components, the MCQI representation, the channel information operations, and the design strategies. New applications can be discovered by new contributions in each of the three components. Therefore, the research can be extended to the following directions.

- Considering the data structure of MCQI, it can be used for capturing more images. This idea can be applied to color qubit to improve the resolution of information about color stored in MCQI representation;

- The αB operator maybe used for making special effect for quantum movies;

- The CST operator provides a possibility to solve the pattern recognition tasks.

Bibliography

[1] T. Acharya. Integrated color interpolation and color space conversion algorithm from 8-bit bayer pattern rgb color space to 12-bit ycrcb color space, May 21 2002. US Patent 6,392,699.

[2] T. Acharya. Median computation-based integrated color interpolation and color space conversion methodology from 8-bit bayer pattern rgb color space to 24-bit cie xyz color space, Apr. 2 2002. US Patent 6,366,692.

[3] A. Al-Nu aimi and R. Qahwaji. Robust self embedding watermarking technique in the dwt domain for digital colored images. *Journal of Digital Information Management*, 5(4):211, 2007.

[4] A. Barenco, C. Bennett, R. Cleve, D. DiVincenzo, N. Margolus, P. Shor, T. Sleator, J. Smolin, and H. Weinfurter. Elementary gates for quantum computation. *Physical Review A*, 52(5):3457, 1995.

[5] G. Beach, C. Lomont, and C. Cohen. Quantum image processing (quip). In *Applied Imagery Pattern Recognition Workshop, 2003. Proceedings. 32nd*, pages 39–44. IEEE, 2003.

[6] J. I. Cirac and P. Zoller. A scalable quantum computer with ions in an array of microtraps. *Nature*, 404(6778):579–581, 2000.

[7] D. G. Cory, R. Laflamme, E. Knill, L. Viola, T. Havel, N. Boulant, G. Boutis, E. Fortunato, S. Lloyd, R. Martinez, et al. Nmr based quantum information processing: Achievements and prospects. *Fortschritte der Physik*, 48(9-11):875–907, 2000.

[8] E. Davies. Information and quantum measurement. *Information Theory, IEEE Transactions on*, 24(5):596–599, 1978.

[9] D. Deutsch. Quantum theory, the church-turing principle and the universal quantum computer. *Proceedings of the Royal Society of London. A. Mathematical and Physical Sciences*, 400(1818):97–117, 1985.

[10] F. Di Martino, V. Loia, and S. Sessa. Direct and inverse fuzzy transforms for coding/decoding color images in yuv space. *Journal of Uncertain Systems*, 3(1):11–30, 2009.

[11] R. Feynman. Simulating physics with computers. *International journal of theoretical physics*, 21(6):467–488, 1982.

[12] A. Fijany and C. Williams. Quantum wavelet transforms: Fast algorithms and complete circuits. *Quantum Computing and Quantum Communications*, pages 10–33, 1999.

[13] X. Gao, C. Deng, X. Li, and D. Tao. Geometric distortion insensitive image watermarking in affine covariant regions. *Systems, Man, and Cybernetics, Part C: Applications and Reviews, IEEE Transactions on*, 40(3):278–286, 2010.

[14] A. M. Gleason. Measures on the closed subspaces of a hilbert space. *J. Math. Mech*, 6(6):885–893, 1957.

[15] L. Grover. Fast quantum mechanical algorithms, Nov. 13 2001. US Patent 6,317,766.

[16] P. R. Halmos and P. P. R. Halmos. *A Hilbert space problem book*, volume 19. Springer Verlag, 1982.

[17] P. Hillman, J. Hannah, and D. Renshaw. Alpha channel estimation in high resolution images and image sequences. In *Computer Vision and Pattern Recognition, 2001. CVPR 2001. Proceedings of the 2001 IEEE Computer Society Conference on*, volume 1, pages I–1063. IEEE, 2001.

[18] A. S. Holevo. Information-theoretical aspects of quantum measurement. *Problemy Peredachi Informatsii*, 9(2):31–42, 1973.

[19] H.-C. Huang and W.-C. Fang. Metadata-based image watermarking for copyright protection. *Simulation Modelling Practice and Theory*, 18(4):436–445, 2010.

[20] A. Iliyasu, P. Le, F. Dong, and K. Hirota. Watermarking and authentication of quantum images based on restricted geometric transformations. *Information Sciences*, 2011.

[21] A. Iliyasu, Q. Le Phuc, F. Dong, and K. Hirota. A framework for representing and producing movies on quantum computers. *International Journal of Quantum Information*, 9(6):1459–1497, 2011.

[22] H. R. Kang. *Computational color technology*. Spie Press Bellingham, 2006.

[23] A. Klappenecker and M. Rotteler. Discrete cosine transforms on quantum computers. In *Image and Signal Processing and Analysis, 2001. ISPA 2001. Proceedings of the 2nd International Symposium on*, pages 464–468. IEEE, 2001.

[24] E. Knill, R. Laflamme, R. Martinez, and C.-H. Tseng. An algorithmic benchmark for quantum information processing. *Nature*, 404(6776):368–370, 2000.

[25] C.-C. Lai and C.-C. Tsai. Digital image watermarking using discrete wavelet transform and singular value decomposition. *Instrumentation and Measurement, IEEE Transactions on*, 59(11):3060–3063, 2010.

[26] B. Lanyon, M. Barbieri, M. Almeida, and A. White. Experimental quantum computing without entanglement. *Physical review letters*, 101(20):200501, 2008.

[27] P. Le, F. Dong, and K. Hirota. A flexible representation of quantum images for polynomial preparation, image compression, and processing operations. *Quantum Information Processing*, 10(1):63–84, 2011.

[28] P. Le, A. Iliyasu, F. Dong, and K. Hirota. Fast geometric transformations on quantum images. *IAENG International Journal of Applied Mathematics. v40 i3*, pages 113–123, 2010.

[29] P. Le, A. Iliyasu, F. Dong, and K. Hirota. Efficient color transformations on quantum images. *Journal ref: Journal of Advanced Computational Intelligence and Intelligent Informatics*, 15(6):698–706, 2011.

[30] H.-K. Lo. Classical-communication cost in distributed quantum-information processing: A generalization of quantum-communication complexity. *Physical Review A*, 62(1):012313, 2000.

[31] C. Lomont. Quantum convolution and quantum correlation algorithms are physically impossible. *Arxiv preprint quant-ph/0309070*, 2003.

[32] L. Luo, Z. Chen, M. Chen, X. Zeng, and Z. Xiong. Reversible image watermarking using interpolation technique. *Information Forensics and Security, IEEE Transactions on*, 5(1):187–193, 2010.

[33] F. Luthon, B. Beaumesnil, and N. Dubois. Lux color transform for mosaic image rendering. In *Automation Quality and Testing Robotics (AQTR), 2010 IEEE International Conference on*, volume 3, pages 1–6. IEEE, 2010.

[34] S. Machnes. Qlib-a matlab package for quantum information theory calculations with applications. *Arxiv preprint arXiv:0708.0478*, 2007.

[35] N. D. Mermin. Quantum computer science. *Quantum Computer Science, by N. David Mermin, Cambridge, UK: Cambridge University Press, 2007*, 1, 2007.

[36] U. Mutze. Quantum image dynamics–an entertainment application of separated quantum dynamics. `http://genie1.ma.utexas.edu/mp_arc/c/08/08-199.pdf`, 2008.

[37] M. Nagy and S. Akl. Quantum computation and quantum information? *The International Journal of Parallel, Emergent and Distributed Systems*, 21(1):1–59, 2006.

[38] M. A. Nielsen and I. L. Chuang. *Quantum computation and quantum information*. Cambridge university press, 2010.

[39] H. Nyeem, W. Boles, and C. Boyd. On the robustness and security of digital image watermarking. In *Informatics, Electronics & Vision (ICIEV), 2012 International Conference on*, pages 1136–1141. IEEE, 2012.

[40] K. Plataniotis and A. Venetsanopoulos. *Color image processing and applications*. Springer Verlag Wien, 2000.

[41] C. R. Putnam. *Commutation properties of Hilbert space operators and related topics*. Springer Berlin, 1967.

[42] R. Raussendorf and H. J. Briegel. A one-way quantum computer. *Physical Review Letters*, 86(22):5188–5191, 2001.

[43] P. V. Sander, D. Gosselin, and J. L. Mitchell. Real-time skin rendering on graphics hardware. In *the proceedings of SIGGRAPH*, 2004.

[44] P. Shor. Algorithms for quantum computation: discrete logarithms and factoring. In *Foundations of Computer Science, 1994 Proceedings., 35th Annual Symposium on*, pages 124–134. IEEE, 1994.

[45] S. K. Singh, D. Chauhan, M. Vatsa, and R. Singh. A robust skin color based face detection algorithm. *Tamkang Journal of Science and Engineering*, 6(4):227–234, 2003.

[46] A. Steane. Quantum computing. *Reports on Progress in Physics*, 61(2):117, 1998.

[47] M. Stokes, M. Anderson, S. Chandrasekar, and R. Motta. A standard default color space for the internet-srgb. *Microsoft and Hewlett-Packard Joint Report*, 1996.

[48] B. Sun, P. Le, A. Iliyasu, F. Yan, J. Garcia, F. Dong, and K. Hirota. A multi-channel representation for images on quantum computers using the rgbα color space. In *Intelligent Signal Processing (WISP), 2011 IEEE 7th International Symposium on*, pages 1–6. IEEE, 2011.

[49] C. Tseng and T. Hwang. Quantum circuit design of 8×8 discrete cosine transform using its fast computation flow graph. In *Circuits and Systems, 2005. ISCAS 2005. IEEE International Symposium on*, pages 828–831. IEEE, 2005.

[50] S. Venegas-Andraca and J. Ball. Processing images in entangled quantum systems. *Quantum Information Processing*, 9(1):1–11, 2010.

[51] S. Venegas-Andraca and S. Bose. Storing, processing and retrieving an image using quantum mechanics. In *Proceedings of the SPIE Conference Quantum Information and Computation*, pages 137–147, 2003.

[52] H. Wiseman. Quantum trajectories and quantum measurement theory. *Quantum and Semiclassical Optics: Journal of the European Optical Society Part B*, 8(1):205, 1996.

[53] H. M. Wiseman and G. J. Milburn. Quantum measurement and control. *Quantum Measurement and Control, by Howard M. Wiseman, Gerard J. Milburn, Cambridge, UK: Cambridge University Press, 2009*, 1, 2009.

[54] W. Zhang, F. Gao, B. Liu, Q. Wen, and H. Chen. A watermark strategy for quantum images based on quantum fourier transform. *Quantum Information Processing*, pages 1–11, 2012.

Related Publications

- Journal Papers

  J1 Bo Sun, Abdullah M. Iliyasu, Le, Fei Yan, Fangyan Dong, and Kaoru Hirota, *"A Multi-Channel Representation for Quantum Images using RGB Color Space"*, Journal of Advanced Intelligence and Intelligent Informatics, Vol.17 No.3, 2013. (Published)

  J2 Bo Sun, Abdullah M. Iliyasu, Phuc Q. Le, Fei Yan, J. Adrian Sanchez Garcia, Fangyan Dong, and Kaoru Hirota, *Color Information Transformations on Multi-Channel Quantum Images*, Entropy. (submitted)

  J3 Bo Sun, Abdullah M. Iliyasu, Phuc Q. Le, Fei Yan, J. Adrian Sanchez Garcia, Fangyan Dong, and Kaoru Hirota, *Strategies for Color Quantum Image Watermarking*, Entropy. (in preparation)

- International Conference Papers

  C1 Bo Sun, Phuc Q. Le, Abdullah M. Iliyasu, Fei Yan, J. Adrian Sanchez Garcia, Fangyan Dong, and Kaoru Hirota, *A Multi-Channel Representation for Images on Quantum Computers using RGBa Color Space*, IEEE 7th International Symposium on Intelligent Signal Processing (WISP), PP. 160-165, 2011. (Published)

  C2 Bo Sun, Phuc Q. Le, Abdullah M. Iliyasu, Fei Yan, J. Adrian Sanchez Garcia, Fangyan Dong, and Kaoru Hirota, *Quantum Computation based Color Information Transformation on Multi-Channel Images*, (Accepted)